

ACTA INNOVATIONS

ISSN 2300-5599

Publisher:
Research and Innovation Centre
Pro-Akademia

no. 46
January 2023

WWW.ACTAINNOVATIONS.EU

Acta Innovations

quarterly

no. 46

Konstantynów Łódzki, Poland, March 2023

ISSN 2300-5599

Original version: online journal

Online open access: www.proakademia.eu/en/acta-innovations

Articles published in this journal are peer-reviewed

Publisher:

**Research and Innovation Centre Pro-Akademia
9/11 Innowacyjna Street
95-050 Konstantynów Łódzki
Poland**

Editor in Chief:

Rafał Marcin Łukasik, Prof.

© Copyright by Research and Innovation Centre Pro-Akademia, Konstantynów Łódzki 2023

ACTA INNOVATIONS

no. 46

March 2023

Content

Li-Min Chuang, Yu-Po Lee, Yu-Ju Chang

THE CRITICAL TRAIT OF DIGITAL ENTREPRENEUR: MIXED METHODS RESEARCH.....5

Pavlo Pokataiev, Anastasiia Liezina, Anhelina Andriushchenko, Helena Petukhova

THE ROLE OF BIOTECHNOLOGY IN THE DEVELOPMENT OF THE BIOECONOMY.....18

Marcoaurélio Almenara Rodrigues, André M. da Costa Lopes, Rafal M. Lukasik

CHEMICAL HYDROLYSIS OF HEMICELLULOSE FROM SUGARCANE BAGASSE
A COMPARISON BETWEEN THE CLASSICAL SULFURIC ACID METHOD WITH THE ACIDIC IONIC LIQUID 1-ETHYL-
3-METHYLIMIDAZOLIUM HYDROGEN SULFATE.....34

Aswani Kumar Gera, Rajesh Kumar Burra

EVALUATION OF DESIGN AND INSERTION ANALYSIS OF A CONICAL SHAPED POLYMERIC BASED MICRONEEDLE
FOR TRANSDERMAL DRUG DELIVERY APPLICATIONS.....53

Laince Pierre Moulebe, Abdelwahed Touati, Eric Akpoviroro Obar, Nabila Rabbah

SIMULATION AND DESIGN OF AN ENERGY ACCUMULATOR AROUND THE HYDROGEN ENERGY
VECTOR.....65

Jan Fabián, Tomáš Binar, Pavel Šafl

PHOTOVOLTAIC SYSTEM DESIGN FOR STRATEGIC INFRASTRUCTURE AND MOBILE COMMAND
CENTRE.....79

Saja A. Alattar, Khalid A. Sukkar, May A. Alsaffar


THE ROLE OF TiO_2 NPS CATALYST AND PACKING MATERIAL IN REMOVAL OF PHENOL FROM WASTEWATER
USING AN OZONIZED BUBBLE COLUMN REACTOR.....90

THE CRITICAL TRAIT OF DIGITAL ENTREPRENEUR: MIXED METHODS RESEARCH

Li-Min Chuang

The Department of International Business, Chang Jung Christian University, Tainan, Taiwan

liming@mail.cjcu.edu.tw

 <https://orcid.org/0000-0001-6997-8486>

Yu-Po Lee*

The Ph.D. Program in Business and Operations Management, College of Management

Chang Jung Christian University, Tainan, Taiwan, 109d00107@mail.cjcu.edu.tw

 <https://orcid.org/0000-0002-2365-2373>

Yu-Ju Chang

Kaohsiung Veterans General Hospital Tainan Branch, Tainan, Taiwan

aau88os107@yahoo.com.tw

Article history: Received 25 July 2022, Received in revised form 25 July 2022, Accepted 12 August 2022, Available online 12 August 2022

Abstract

Pioneers of the digital era have invented a different business model and expanded the existence of the digital economy, and the digital entrepreneurship is the beginning of this digital revolution. To explore the key characteristics of digital entrepreneurs, this study is divided into two stages. The first stage conducted a literature review and case study to construct the characteristic elements of the entrepreneurship into a model of digital entrepreneurs. In the second stage, the relative weights of the key characteristics of digital entrepreneurs are understood through an analysis of the AHP questionnaire results. The results show that autonomy and self-discipline are keys among the main dimensions of the key characteristics of digital entrepreneurs' entrepreneurship; the secondary dimension of "action power" is key in the main dimension of "autonomy and self-discipline"; the secondary dimension of "business networks" is key in the main dimension of "social capital"; the secondary dimension of "insight" is key in the main dimension of "innovation and breakthrough"; the secondary dimension of "communication ability" is key in the main dimension of "leadership communication".

Keywords

digital entrepreneurship; digital economy; entrepreneurship; entrepreneurs; analytic hierarchy process (AHP).

Introduction

The psychological and behavioral characteristics of entrepreneurs are very important for the success of entrepreneurship, as well as undeniable key factors to overcome difficulties in the process of entrepreneurship. To cope with the unpredictable market competition, entrepreneurs must take different plans and decisions at different stages, and exert their personality traits, which is also the focus of many scholars when studying entrepreneurship. While extensive literature has discussed the key characteristics of entrepreneurial success, few have studied the issue from the perspective of entrepreneurs in the digital industry. However, as the environment changes, successful entrepreneurship has become difficult, and there are many entrepreneurs, but few succeed. In addition to the capital injection, how to continue and stabilize entrepreneurship and development in this field is a major issue. Therefore, this study explores the key entrepreneurial characteristics of entrepreneurs in the digital industry. The research motivations of this study are, as follows:

- for an organization to be successful, there must be a successful founder, who always plays an important role in the organization, and the entrepreneurship is an important factor for determining the success of the enterprise. From the performance of the founders of some successful enterprises, it is easy to see that they are the key figures in the success and development of the business.
- many scholars in Taiwan have carried out research on topics related to the characteristics of entrepreneurs, such as analyzing the relationship between entrepreneurs' personal characteristics and social networks, taking Chinese entrepreneurs as the research object, taking middle-level executives in the high-tech industry as the research object, taking the application of agricultural industrialization in Taiwan as the direction, studying the relationship between five personality traits

- and the characteristics of social entrepreneurs, and exploring the impacts of the characteristics of entrepreneurs, as well as their previous knowledge and external environments, on entrepreneurial intention, and conducted a comparative analysis of different countries, such as Taiwan and Vietnam, which is the first motivation of this study. Some scholars focused their research on topics related to digital entrepreneurship, such as analysis of the entrepreneurial ecosystem in the digital economy era driven by the entrepreneurship boom, how to stimulate the development of innovation and entrepreneurship through the digital economy, and taking the development of innovation and entrepreneurship in Taiwan under the digital economy as the topic to analyze the innovation and entrepreneurship opportunities in Taiwan under the trend of digital transformation. However, there is currently no relevant literature that studied the key characteristics of successful entrepreneurship by integrating the digital industry and the characteristics of entrepreneurs or has directly taken entrepreneurs operating in the digital industry as the object. Previous studies on entrepreneurs have not discussed the connotation of digital entrepreneurs, which is the second motivation of this study.

Based on the above research background and motivations, there is a lack of literature on digital entrepreneurs, and most focused on industry or technology, thus, this study could not directly obtain the theoretical basis and the weight of key characteristics through literature review. Therefore, case empirical methods must be adopted for further discussion. This study aims to conceptualize the definition of digital entrepreneurs, and it is expected that future research will focus on the model and framework of the digital entrepreneurship and further study the entrepreneurial ability of digital entrepreneurs. Due to the impact of the digital entrepreneurship - oriented competitive market, traditional industries and emerging entrepreneurs must change their old thinking and actively seek new business models. Inspired by the research background and motivations of this study, the analysis framework of the entrepreneurship of entrepreneurs in the digital industry is constructed to explore and determine the key characteristics. Therefore, the research objectives of this study are, as follows:

- to discuss and analyze the entrepreneurship of successful entrepreneurs in the existing digital industry through literature review.
- to explore the characteristics, significance, dimensions, and indicators of the entrepreneurship of entrepreneurs in the digital industry.
- to construct an analysis framework for the key characteristics of digital entrepreneurs.
- to invite experts in related fields to conduct an empirical analysis on the AHP level according to the above analysis framework of the key characteristics of digital entrepreneurs.
- to propose suggestions as a reference for future research directions according to the construction process and empirical results.

Literature Review

Digital entrepreneurs: Digital entrepreneurship is a mechanism of the innovation system, which often occurs in the formation of new enterprises or the transformation of current enterprises [1]. The characteristics of digital technology, such as editable, re-combinable, re-programmable, and generative nature, affect entrepreneurship in many aspects [2–5]. Digital entrepreneurship is to use the characteristics of digital technology to create new values for enterprises and become the driving force for innovation [6–10]. Digital entrepreneurs are usually defined as those who pursue business or economy based on opportunities to use digital technology. Entrepreneurs who participate in digital entrepreneurship are described as digital entrepreneurs, and the resulting economic and social values of venture enterprises, companies, or communities are known as digital enterprises [11]. Despite the widespread use of the term "the digital entrepreneurship" by many experts, scholars, and government policy makers, and despite growing interest in understanding the digital entrepreneurship, its concept and definition remain elusive, and there is little related literature to provide empirical evidence. With the rapid developments of digital technology, the resulting digital economy has created unprecedented economic benefits for many countries, and it is believed that this is due to the development of the entrepreneurship, and people begin to pay attention to the empirical research of entrepreneurship and experience. Table 1 sorts the definitions of digital entrepreneurship from other literature. In short, digital entrepreneurship includes "selling digital products or services across electronic networks" [12]. In addition to the different definitions of the digital entrepreneurship phenomenon in Table 1, the term "digital entrepreneurship" is used differently in all articles, including digital entrepreneurship, digital innovation, digital industry, and digital commerce. Therefore, the proper nouns used in the corresponding articles are used in Table 1. Exploration of the digital entrepreneurship: The digital entrepreneurship is an important driving force in innovation systems, as it changes the structure, objectives, and network mechanism of the entire relevant business system, which affects the various levels and scales of innovation systems and brings unprecedented changes to innovation

systems. While digital technology provides new business opportunities, it is also quite destructive to the original business model [3]. In order to study the mixed concept of the digital entrepreneurship, Sataalkina and Steiner conducted a systematic literature review of innovation transformation systems, and confirmed the key categories of digital entrepreneurship, as well as the differences from other fields, by studying 52 core papers [9]. A total of three key core elements of entrepreneurship were developed from the analysis results, including:

- entrepreneurs: including behavior, competence, and mindset patterns, as well as the results and consequences of individual entrepreneurial activities.
- entrepreneurial process: including digital-related activity strategies and operational activities in the organizational management process, as well as digital entrepreneurial companies.
- related ecosystem: including the impacts of external infrastructure and institutions on the development of digital entrepreneurs .

Table 1. Summary of Definitions of Digital Entrepreneurship in Previous Studies. *Source: [13].*

Literature	Definition of digital entrepreneurship
[11]	Digital entrepreneurship: pursue new venture opportunities presented by new media and internet technologies
[12]	[Digital entrepreneurship is] the creation of a venture to produce and generate revenue from digital goods across electronic networks
[14]	Digital entrepreneurship may be defined as entrepreneurship in which some or all of the entrepreneurial venture takes place digitally instead of in more traditional formats
[15]	Digital entrepreneurship is a subcategory of entrepreneurship in which some or all of what would be physical in a traditional organization has been digitized
[16]	Digital entrepreneurship is defined as the reconciliation of traditional entrepreneurship with the new way of creating and doing business in the digital era
[17]	Entrepreneurship [...] is [...] defined as occupying niches, monetizing business opportunities, as well as being innovative, radical and risk-taking
[18]	Digital entrepreneurship [...] includes any agent that is engaged in any sort of venture be it commercial, social, government, or corporate that uses digital technologies. [...] In other words, they are performing activities that need digital engagement but may not in themselves be digital, for example, an Uber taxi driver

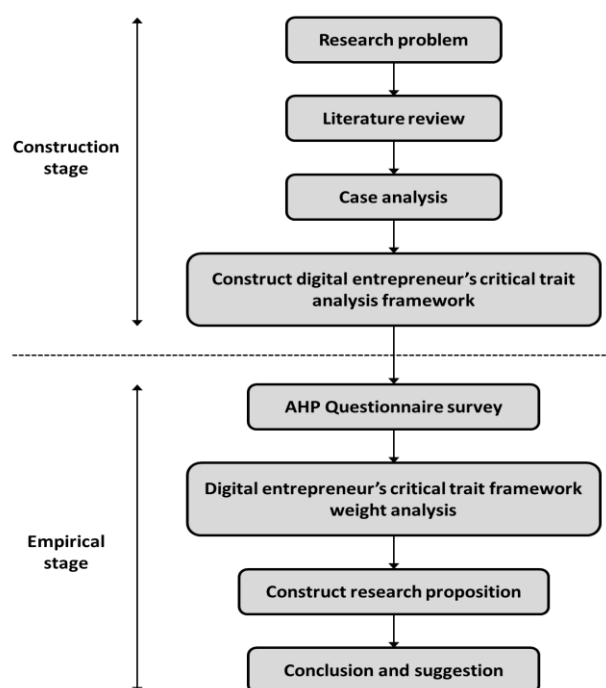


Figure 1. The research flow chart. *Source: Author.*

Methods

Construction of the Model of Key Characteristics of Digital Entrepreneurs

Construct an analysis framework for key characteristics of digital entrepreneurs: In order to construct the research model of the key characteristics of digital entrepreneurs' entrepreneurship, this study developed 4 main dimensions and 12 secondary dimensions as the theoretical basis and took internationally well-known digital entrepreneurs as the research objects to explore the key characteristics of their entrepreneurship and revise the structural model of this study.

Case analysis of digital entrepreneurs.

This study referred to the following 37 materials (6 papers, 4 journal articles, 23 books, and 4 websites), and conducted content analysis according to Table 1. In terms of qualitative research, this study mainly conducted an analysis of actual content, in order to identify the psychological and behavioral characteristics of entrepreneurs when they faced people, events, and objects during their childhood, growth background, study process, and work experience, as well as the characteristics of each behavioral motivation in their entrepreneurial process. The key characteristics of digital entrepreneurs were identified from the literature, relevant materials, and quotations and speeches of entrepreneurs, which were summarized into 15 key characteristics, as shown in Table 2. Each entrepreneur has their own key characteristics for success, and while they also have differences, they all have willpower full action power and strong intention, and innovation ability. Regarding the key characteristics, Item 1 is "taking the initiative to challenge, taking responsibility, and having strong willpower to persist". Entrepreneurs with such characteristics have full action power; for example, Zhengfei Ren has the spirit of a wolf pack, perseverance, fearlessness, and group struggle. He said that, in addition to hard work, what we learned over the past 20 years is that we should be struggle-based and customer-centered, and we need to be able to persist for a long time. Jeff Bezos believes that someone who wants to succeed in entrepreneurship must persist to the point that others find it unconscionable. Jack Ma believes in his own judgment and sticks to it.

In terms of Item 2, "having the spirit of adventure without fear of failure", entrepreneurs take the initiative to accept challenges, have the courage to take risks without fear of failure, and possess the willpower to persist. An enterprise that has grown to global renown was not always stable, instead, it passed countless difficulties through its perseverance and persistence. Zhengfei Ren stated that we learn through failure. Jeff Bezos believes that, in order to have no regret in the future, we should try even if we fail, and failure is a necessary element for innovation. Jack Ma said that failure is the greatest wealth of life. About 18 months into its start-up, the Alibaba Group was on the verge of bankruptcy, then an order from an American customer allowed the company to turn a profit, thus, the spirit of unrelenting effort resulted in the active expansion of the business.

In terms of Item 3, "be enthusiastic about charity", with the success of entrepreneurship, entrepreneurs must also do their best to fulfill their social responsibilities in charity and public welfare. In 2016, Huateng Ma ranked first in the Hurun China Philanthropy List, with a total donation of RMB 13.9 billion. The Jack Ma Foundation and the Alibaba Public Welfare Foundation donated medical supplies and large amounts of cash to support the research and development of COVID-2019 vaccines during the COVID-2019 epidemic. The "Bezos Earth Fund" was established, which will donate USD 10 billion to fight climate change, charitable funds were established to assist homeless families, and pre-schools for young children were established in low-income communities. In terms of Item 4, "attaching importance to the responsibility and obligation of individuals and enterprises to society"; for example, Mark Elliot Zuckerberg, a vegetarian, is grateful for everything. Sergey Brin invests in the development of alternative energy technologies, in order to make the environment sustainable and to seek a wider range of renewable energy sources. Regarding employees, Brin is willing to give, meaning "free" has become part of the corporate culture, and he even allows employees to bring their children and pets to work. Jack Ma says that public welfare is about managing one's own humanity. Robin Li shared the truth of helping others to achieve oneself. In terms of Item 5, "family network", some entrepreneurs had access to relevant environments since childhood, and some parents had relevant knowledge to share or arranged for them to learn relevant skills. For example, when Steve Jobs was a teenager, his adoptive father gave him the opportunity to learn about devices and machinery, including disassembly, as he was a dealer of second-hand goods, and specialized in installing, refitting, and selling second-hand cars. Later, Steve Jobs believed that he liked sophisticated devices because he was deeply influenced by his family when he was young. Mark Elliot Zuckerberg started writing programs from middle school age, and his father hired software developers as his tutors.

In terms of Item 6, "relevant expertise or academic background"; for example, Zhengfei Ren joined the People's

Liberation Army after graduation to develop communication technology and started his own business in his middle age after retiring from military service. Steve Chen was very fond of mathematics and science in high school, and later majored in computer science at the University of Illinois, and he joined the PayPal Team in his senior year. As the research objects of this study, except for Jack Ma, who did not have family network support, expertise, or educational background, all other entrepreneurs examined in this study had relevant technical or educational backgrounds.

In terms of Item 7, "social network relationship", some entrepreneurs need to raise money to start a company for the first time or seek financial assistance in time of crisis. Several of the digital entrepreneurs examined in this study did not have bountiful funds at the beginning and even started their businesses in humble garages. For a company to succeed, it is difficult to achieve its ambitious goals completely on its own, and sometimes, it needs to rely on business network relationships, such as external investment and the involvement of partners. In 1999, Huateng Ma launched real-time communication software "OICQ", and obtained investment capital of USD 2.2 million from International Data Group and Richard Li's Yingke Digital Technology to establish Tencent. In 1998, Larry Page and Sergey Brin obtained investment funds from Andy Bechtolsheim, the co-founder of Sun Microsystems, and founded Google without sufficient funds in a friend's garage in Menlo Park, California. Faced with an initial funding shortfall, Jack Ma persuaded the SoftBank fund to invest in the Alibaba Group in only six minutes, which was its first venture capital.

In terms of Item 8, "ability to foresee the future and high sensitivity to environmental changes ", successful entrepreneurs have a better ability to foresee the future, have a head start in an unpredictable market, and are highly sensitive to changing circumstances. For example, Zhengfei Ren has always been able to anticipate forward-looking opportunities ahead of competitors, thus, no matter how the environment changes, it can grow in each wave of change and turn into a world-shaking technology kingdom. Through foresight, Jeff Bezos saw Apple's music store sweeping the world in 2003 and concluded that in the future, only companies would need to be like Apple dominating the music market to survive in the new digital age. Consequently, he launched the Kindle e-book reader in 2007. People who see the future before others do can seize opportunities faster than others.

In terms of Item 9, "ability to innovate and create", except for Huateng Ma, who later attracted a lot of criticism, the ability of all entrepreneurs in this area is evident around the world, and they have this ability from the very beginning. The performance of innovation and creativity is an important part of a company's sustainable operation and one of the important factors for leading competitors to create differentiation. Positive innovative products can bring profitability for an existing enterprise, obtain new customers to create new markets, and create a good overall image of the enterprise. For example, when Steve Jobs presented a new Apple product at the company's new product presentation, the audience would always burst into cheers, and when he explained new features, the audience applauded constantly, which shows the importance of innovation to a company. Jeff Bezos said innovation or death, and Jack Ma also thinks that innovation should be considered as the cause of entrepreneurs. In terms of Item 10, "a strong desire to create something that will change the world", entrepreneurs have a strong intention to change the world according to their own predictions. For example, Zhengfei Ren's sayings show that he is ambitious, and he looks at the layout of the world, rather than just the gains and losses of one city or another. For Mark Elliot Zuckerberg, making the world more open is his primary goal now and in the future, he considers innovation and layout, and makes Facebook indispensable to the world. Sergey Brin wants to make the entire world's information universally searchable. Larry Page wants to collect the world's information and make it available to the public so that everyone can benefit from it.

In terms of Items 11 and 12, "ability to communicate with customers and employees", Steve Jobs attached great importance to human capital, maintained communication with employees, clearly conveyed the company's implementation goals, put customers first, and maintained good communication with customers. Sergey Brin maintains a good communication channel with employees and allows them to express their opinions, especially when they come up with innovative ideas, which they can express at any time. Zhengfei Ren maintains communication with customers, is highly sensitive to business issues, and learns the needs of customers in the fastest way.

In terms of Items 13 and 14, "having planning ability and decision-making ability", every entrepreneur's success depends on their decision-making and planning abilities. Steve Jobs had his own methods for company planning and decision-making, and he put customers first, attached importance to customer capital, and planned

the company's innovation goals based on customers' needs. Although Ren-fei Wang has a commanding style, he is goal-oriented in planning and decision-making, with high ambitions and full execution abilities. Jeff Bezos emphasizes patience in business, and most of Amazon's investment plans are over seven years and focus on long-term growth rather than short-term profits.

In terms of Item 15, "taking customer needs as guidance to plan company innovation goals", the leadership style of Steve Jobs presented charisma to convince himself and others that his ideas were right, meaning he had unique charm during presentations and extraordinary influence on the whole team; he made the impossible possible and motivated the team to achieve their goals. Jack Ma has an optimistic attitude, saying that we should know how to warm our right hand with our left hand.

Summary of the psychological and spiritual characteristics of digital entrepreneurs

This study summarizes the previous case analysis of internationally well-known digital entrepreneurs, as shown in Table 2:

Table 2. Summary of psychological and spiritual characteristics of entrepreneurs. *Source: Author.*

Item	1	2	3	4	5	6	7	8	9	10	11	12	13	14	15
	Taking the initiative to challenge, taking responsibility, and having strong willpower to persist	Having the spirit of adventure without fear of failure	Enthusiastic about charity	Attaching importance to the responsibility and obligation of individuals and enterprises to society	Family network	Relevant expertise or academic background	Social network relationship	Ability to foresee the future and high sensitivity to environmental changes	Ability to innovate and create	A strong desire to create something that will change the world	Communicate with customers and maintain business operation sensitivity	Communicate well with employees to make them clearly understand leaders' goal orientation	Taking customer needs as the guidance, planning company innovation goals	Having planning ability and decision making ability	Leading and motivating others with a unique personal style
Jack Ma	✓	✓	✓	✓			✓	✓	✓	✓				✓	✓
Jeff Bezos	✓	✓	✓	✓	✓	✓		✓	✓	✓			✓	✓	✓
Mark Zuckerberg	✓			✓	✓	✓		✓	✓	✓					
Larry Page	✓				✓	✓	✓	✓	✓	✓					
Sergey Brin	✓		✓	✓		✓	✓	✓	✓	✓		✓		✓	✓
Steve Chen	✓					✓	✓		✓	✓					
Huateng Ma	✓		✓			✓	✓	✓	✓	✓					
Steve Jobs	✓	✓	✓	✓	✓	✓	✓	✓	✓	✓	✓	✓	✓	✓	✓
Robin Li	✓	✓	✓			✓	✓	✓	✓	✓					
Zhengfei Ren	✓	✓				✓		✓	✓	✓	✓		✓	✓	✓

Identifying and defining the dimensions of the key characteristics in this study.

According to the aspects and dimensions in Table 2, the psychological and behavioral characteristics of entrepreneurs were summarized again to determine the homogeneity among the items in the four dimensions, and the 12 secondary dimensions were sorted according to the homogeneity. This study adjusted the theoretical basis framework according to the 12 simplified dimensions, and the AHP questionnaire was

designed based on this framework to conduct empirical research on the psychological and behavioral characteristics of digital entrepreneurs in Taiwan. The 12 dimensions of the psychological and behavioral characteristics of digital entrepreneurs are respectively defined and explained, as shown in Table 3, Research Framework: The four dimensions of the key characteristics of entrepreneurs' entrepreneurship, as developed by relevant literature, were used as the main dimensions of this study, while the secondary dimensions of the entrepreneurship of entrepreneurs in the digital industry were sorted according to the above-mentioned literature, which were used as the theoretical basis, to design the components of the hierarchical framework of this study, as shown in Figure 2. Research object and AHP questionnaire design: This study adopted a qualitative research method and extended the theory developed through literature review to identify the key characteristics of entrepreneurship from the data. The AHP questionnaire was designed to further understand the key characteristics of digital entrepreneurs' entrepreneurship, and then, the characteristic elements were analyzed according to the results of the questionnaire, to construct the measurement model of the key characteristics of digital entrepreneurs. This study was carried out in stages. In the first stage, the hierarchical structure of the primary and second criteria was preliminarily established. To determine the hierarchical structure again, the preliminary hierarchical structure produced in the first stage was revised. Then, to determine the main dimensions and the secondary dimensions in the hierarchical structure, the decision support software, Expert Choice 2000, was used to calculate weights.

Taking internationally renowned digital entrepreneurs as the research object.

During data collection in the process of research and exploration, it was found that the digital industry has not been a new industry in recent years. World-renowned digital entrepreneurs, such as Jeff Bezos, Mark Elliot Zuckerberg, Jack Ma, and Bill Gates, have successfully created enterprise kingdoms. Many scholars have further studied how these enterprises succeed, and some scholars have also studied how CEOs in this industry lead enterprises to success. However, no scholars have directly taken the key characteristics of CEOs in the digital industry as the research direction, thus, this study could not obtain relevant information through literature review. Therefore, this study extracted relevant information from many books and network information as objectively as possible and identified the key characteristics of digital entrepreneurs' entrepreneurship, which were used as the secondary dimensions of the theoretical basis for constructing the dimension model of the key characteristics of entrepreneurs in the digital industry.

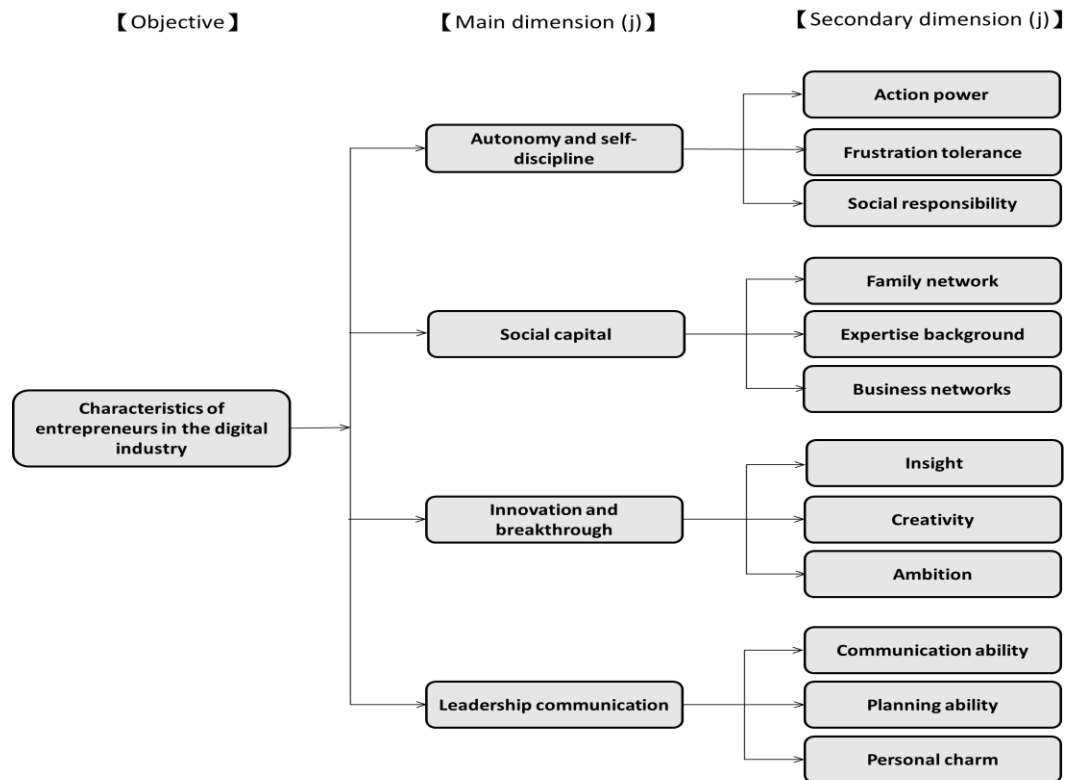
AHP questionnaire distribution

This study selected entrepreneurs in related digital industries in Taiwan as the respondents, such as e-commerce, blockchains, and the Internet of Things. While these industries are spread across different areas of northern, central, and southern Taiwan with different environmental backgrounds, it does not affect their success or failure, which proves that digital business opportunities are endless. This study distributed a total of 10 AHP questionnaires, which were delivered to the respondents at the appointed time and explained in person the entrepreneurship of entrepreneurs in the digital industry.

Empirical Analysis

To confirm the rationality of the AHP questionnaire, this study initially verified the consistency index and ratio of the recovered questionnaires. If the verification value was within the reasonable range, the relative weights of the main evaluation criteria and the evaluation index would be calculated to obtain the empirical analysis results. Consistency verification: The rate of consistency verification is acceptable when $C.R. \leq 0.1$, and the hierarchy consistency has rationality; on the contrary, there is a problem in the connection of the hierarchy, and the hierarchy for the evaluation must be reformulated; another scholar, Saaty, put forward the same argument in 1980, arguing that the acceptable range of C.I. values must be judged within $C.I. \leq 0.1$. This study distributed a total of 10 AHP questionnaires, and 10 were recovered. According to the calculation results of this verification, the 10 AHP questionnaires are all valid. Calculation of relative weights: For each "main evaluation criteria" and "evaluation index", the relative weights were calculated after consistency verification in this study (Table 4, Figure 3). After integrating the relative importance of each hierarchy, the weight ratio of each evaluation index at the second hierarchy was further summarized.

The implications of each weight index were discussed according to the calculation results of relative weights.

Figure 2. Research Framework. *Source: Author.*Table 3. Definition and Description of Key Characteristics of Digital Entrepreneurs. *Source: Author.*

Dimension	Characteristic	Definition
Autonomy and self-discipline	Action power	The ability to continuously learn, think, and develop habits and motivations that lead to successful outcomes. The practical ability to adhere to the implementation of strategic intentions and achieve predetermined goals.
	Frustration tolerance	A person's ability to avoid misconduct in the face of setbacks, the ability to withstand a blow.
	Social responsibility	Paying attention to the obligations and responsibilities of individuals and enterprises to society.
Social capital	Family network	A strong family connection, with the same values, so that knowledge and information transmission will be more efficient. Encourage entrepreneurship through linkages.
	Expertise background	Having relevant skills, education, and work experience.
	Business networks	Access to information and financial sources or other resources through business networks.
Innovation and breakthrough	Insight	One's ability to observe things from many perspectives and grasp the core of a variety of issues.
	Creativity	The ability of divergent thinking, generating new ideas, discovering, and creating new things.
	Ambition	Being aggressive and motivated to succeed. Knowing one's unique purpose in the world and believing they can make the world different.
Leadership communication	Communication ability	The process by which information, thoughts, and emotions are transmitted between specific individuals or groups of people to reach a common agreement for a set goal.
	Planning ability	Forecasting future events that are likely to affect the achievement of a goal.
	Personal charm	Having a unique personal style that attracts, inspires, or enlightens others.

Results and discussion

After systematic analysis, the relative weights of the "main evaluation criteria" and "evaluation index" are shown in Table 4, and the relative weights of the main and secondary dimensions of the key characteristics of digital entrepreneurs in Table 4 are sorted, as shown in Figure 3.

This study used Expert Choice as the application software for analysis. After hierarchical analysis, the relative weights of the main dimensions and the secondary dimensions were obtained, as shown in Figure 3. The obtained values are analyzed and discussed, as follows: "The dimension of autonomy and self-discipline" and its secondary dimensions. According to Table 4, the questionnaire respondents in this study consider "the dimension of autonomy and self-discipline" (relative weight=0.353) to be the most important among the main evaluation criteria of the first hierarchy, which accounts for the highest proportion among all the main criteria. Correspondingly, it indicates that digital entrepreneurs in Taiwan agree that it is very important to constantly think and learn, adhere to the implementation and completion of the predetermined goals, and withstand the challenges of setbacks and failures to achieve success in the process of entrepreneurship. Entrepreneurs themselves attach great importance to the social obligations and responsibilities of the individuals and enterprises they operate. According to the secondary dimensions in Table 4, "action power" (relative weight=0.167) is the most important, followed by "frustration tolerance" (relative weight=0.119) and "social responsibility" (relative weight=0.067), which indicates that the respondents consider action power to be the most important factor among the key characteristics of entrepreneurs; any lofty goals and ideals need to be put into action to be achieved. For digital entrepreneurs in Taiwan, taking practical action, making all plans according to the goals set by themselves, and consistently putting them into practice, are the foundation of the entrepreneurship and an important indicator to lead organizations to success.

Table 4. Relative Weights of "Main Evaluation Criteria". *Source: Author.*

Relative weight of "main evaluation criteria"			
First hierarchy (Main evaluation dimension)	Relative weight	C.R. value	Ranking
Autonomy and self-discipline	0.353	0.01	1
Social capital	0.093		4
Innovation and breakthrough	0.253		3
Leadership communication	0.300		2
Relative weight of "evaluation index"			
Second hierarchy (Evaluation index)	Relative weight	C.R. value	Ranking
Action power	0.167	0.01	1
Frustration tolerance	0.119		3
Social responsibility	0.067		7
Family network	0.017		12
Expertise background	0.036		11
Business networks	0.040		10
Insight	0.112		4
Creativity	0.057		9
Ambition	0.085		6
Communication ability	0.143		2
Planning ability	0.97		5
Personal charm	0.061		8

"The dimension of leadership communication" and its secondary dimensions

According to Table 4, the questionnaire respondents consider "the dimension of leadership communication" (relative weight=0.300) to be the second most important item among the main evaluation criteria of the first hierarchy, which indicates that entrepreneurs can always effectively convey information related to their goals and plans and can make good use of communication skills when facing problems with customers, employees, partners, and shareholders. In terms of planning and execution, they can play an effective role in implementing strategies and achieving predetermined goals. Entrepreneurs who think this dimension is important may also have extraordinary leadership characteristics; for example, Steve Jobs was forced to leave Apple due to his

eccentric personality. However, whenever a new product launch meeting was held, his persistence and unique personal charm always won applause from the audience. According to the secondary dimensions in Table 4, "communication ability" (relative weight=0.143) is the most important, followed by "planning ability" (relative weight=0.097) and "personal charm" (relative weight=0.061), which indicates that the respondents consider communication ability as the most important key characteristic factor of entrepreneurs in the dimension of leadership communication.

"The dimension of innovation and breakthrough" and its secondary dimensions.

According to Table 4, the secondary dimensions of "the dimension of innovation and breakthrough" (relative weight=0.253) rank third among the main evaluation criteria of the first hierarchy, meaning is less important than the dimensions of autonomy, self-discipline, and leadership communication ability for digital entrepreneurs in Taiwan. The performance of innovation and creativity is an important part of a company's sustainable operations and one of the important factors for leading competitors to create differentiation. However, for Taiwan's entrepreneurs with a relatively conservative national style, in addition to the spirit of autonomy and self-discipline, they attach more importance to corporate ethics and social responsibilities and obligations, giving play to their leadership communication characteristics in the enterprise, and adhering to the belief of achieving goals, which are more important than innovation and breakthrough. It can be seen that digital entrepreneurs in Taiwan generally have higher self-requirements than other main evaluation criteria indices. According to the secondary dimensions in Table 4, "insight" (relative weight=0.112) is the most important, followed by "creativity" (relative weight=0.057) and "ambition" (relative weight=0.085), which indicates that the respondents consider insight to be the most important key characteristic of entrepreneurs in the dimension of innovation and breakthrough. It can be seen that a successful digital entrepreneur must be able to foresee the future and understand the changing environment in order to gain an advantage in an unpredictable market.

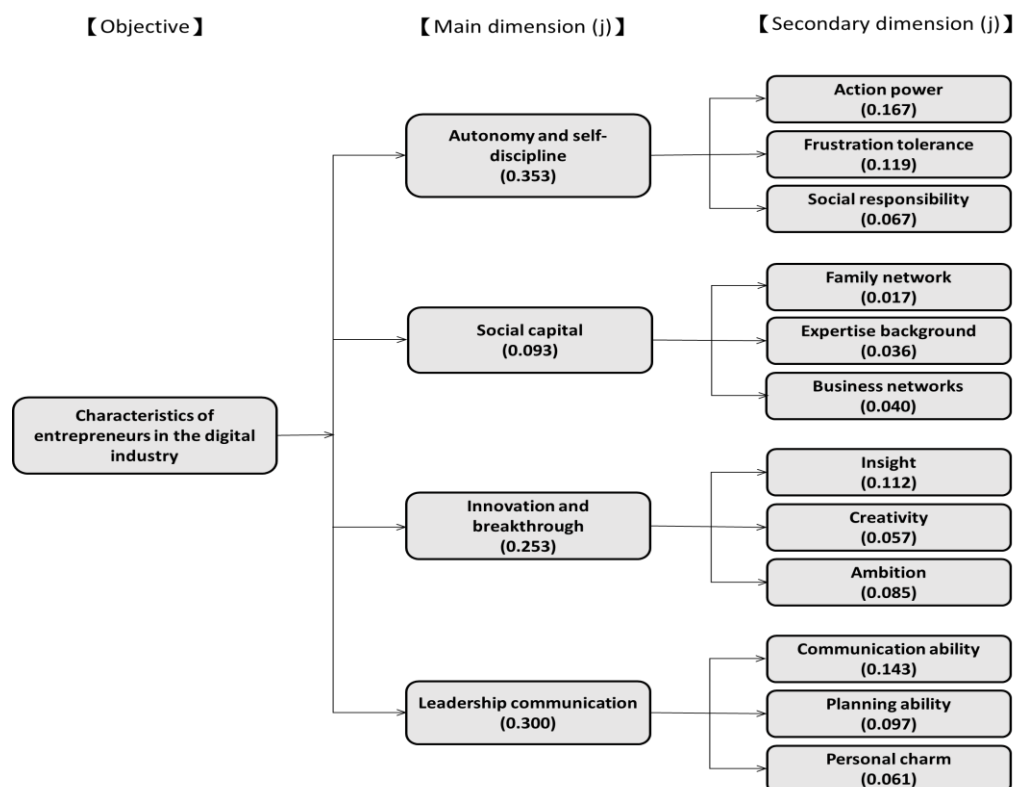


Figure 3. Relative Weights of Research on Key Characteristics of Digital Entrepreneurs. *Source: Author.*

"The dimension of social capital" and its evaluation indices.

According to Table 4, "the dimension of social capital" (relative weight=0.093) ranks last among the main evaluation criteria of the first hierarchy, which does not mean that the relevant secondary dimensions of the dimension of social capital are not important to digital entrepreneurs, but that the respondents of this questionnaire are domestic digital entrepreneurs, most of whom live in the family network without relevant

learning or access environment, meaning only a few entrepreneurs had relevant skills, expertise, or education before starting a business. This study defines social networks as being able to make good use of connections and access funds to enhance success opportunities. The enterprises run by the questionnaire respondents of this study are not as large-scale as those run by world-renowned digital entrepreneurs, such as Larry Page, Sergey Brin, and Mark Zuckerberg, which required massive capital injections as they grew. In addition, some domestic entrepreneurs themselves have richer family resources to provide financial assistance; therefore, the relative weight of this dimension is relatively low. According to the secondary dimensions in Table 4, "business networks" (relative weight=0.040) is the most important, followed by "expertise background" (relative weight=0.036) and "family network" (relative weight=0.017), which indicates that the respondents consider business networks as the most important key characteristic of entrepreneurs in the dimension of social capital. With limited resources, enterprises have to rely on business network relationships to seek capital investment or partners due to rising costs or investment failures in the development process and pressure from the competitive environment.

Impact

More and more people are interested in the term digital entrepreneurs, which has also aroused the attention of countries and government units to initiate relevant support measures, such as policy promotion. Many experts and scholars have also begun to explore how international digital entrepreneurship giants created such a prosperous era, as such changes have created incredible wealth and brought great growth to countries. Most importantly, it has changed the pattern of people relying on brick-and-mortar stores. From the discussion of domestic literature, it can be seen that entrepreneurs in different industries have different psychological and behavioral characteristics. In order to construct the evaluation framework, this study applied the analytic hierarchy process, which is flexible and easily understood hierarchical analysis method, to collect the opinions of experts and scholars through literature review of the digital industry, the characteristics of entrepreneurs, and in-depth interviews.

Conclusions

This study took "entrepreneurs in the digital industry" as the research object to explore their "key characteristics of successful entrepreneurship". This study integrated the relevant literature of the digital industry and the key personality traits of entrepreneurs as the theoretical basis and used the analytic hierarchy process to analyze and study the AHP questionnaire results of contemporary digital entrepreneurs. According to the research results, conclusions and suggestions are put forward as references for subsequent researchers.

Research conclusions and propositions

Based on the analysis results, this study developed the following propositions:

- Proposition 1: among the dimensions of the key characteristics of digital entrepreneurs, the dimension of autonomy and self-discipline" is more important than the dimensions of "leadership communication", "innovation and breakthrough", and "social capital".
- Proposition 2: among the dimensions of the key characteristics of digital entrepreneurs, the characteristic of "action power" is key in the dimension of "autonomy and self-discipline".
- Proposition 3: among the dimensions of the key characteristics of digital entrepreneurs, the characteristic of "business networks" in the dimension of "social capital" is the key.
- Proposition 4: among the dimensions of the key characteristics of digital entrepreneurs, the characteristic of "insight" in the dimension of "innovation and breakthrough" is the key.
- Proposition 5: among the dimensions of the key characteristics of digital entrepreneurs, the characteristic of "communication ability" in the dimension of "leadership communication" is the key.

Suggestions for future studies

This study also briefly summarized some suggestions for entrepreneurs who intend to start up digital industries, and a reference for related studies in the future:

- a. Select the research object to make the research and analysis more accurate
In the first stage of this study, the key psychological and behavioral characteristics of current internationally renowned digital entrepreneurs were analyzed and summarized to establish a measurement model of the key characteristics of digital entrepreneurs. Then, by applying the analytic hierarchy process questionnaire, current digital entrepreneurs in Taiwan were taken as the object of analysis. According to the data, while it is not difficult to find that the characteristics of both domestic and foreign digital entrepreneurs are inseparable from the research dimension of this study, there are still differences in the important and key characteristics; for example, among the globally famous digital

entrepreneurs, with the exception of Jack Ma, who had no relevant background in technology or education, other entrepreneurs all had relevant technical backgrounds or had studied related disciplines. Compared with foreign entrepreneurs, there are few domestic entrepreneurs who had relevant technical backgrounds or education before starting their own business. Obviously, many domestic entrepreneurs are connected to family networks or have parents who were entrepreneurs themselves. The research results show that, due to the different entrepreneurial scales and cultural backgrounds, although entrepreneurs meet the four main criteria, there are some differences in the secondary criteria. Therefore, in order to make the research value more accurate, it is suggested that follow-up research on related topics can select research objects according to their own research direction.

b. Pursue the root of the problem by exploring a single dimension

According to the questionnaire results, entrepreneurs had different results in filling out the questionnaire due to different personal characteristics. Whether in the digital industry or other industries, we know from previous literature that the beginning is the hardest for some entrepreneurs; some entrepreneurs will be tested repeatedly and suffer setbacks frequently in the entrepreneurial process, while it goes smoothly for other entrepreneurs. Moreover, the market and scale developed by enterprises will vary according to the different ideas and ambitions of entrepreneurs. As leaders with different temperaments show different personal leadership characteristics, the values created by their enterprises will also be different. As each of the different dimensions has a different reference value, it is suggested to choose a single dimension according to different cultural backgrounds to determine the root of a problem, which will give each research value a practical reference value.

Conflict of interest

There are no conflicts to declare.

Acknowledgments

This research has not been supported by any external funding.


References

- [1] European Commission, Digital Transformation of European Industry and Enterprises - A report of the Strategic Policy Forum on Digital Entrepreneurship, (2015). <https://digital-europe-website-v1.s3.fr-par.scw.cloud/uploads/2019/01/Final report Strategic Policy Forum.pdf>.
- [2] K. Lyytinen, Y. Yoo, R.J. Boland, Digital product innovation within four classes of innovation networks, *Inf. Syst. J.* 26 (2016) 47–75. <https://doi.org/10.1111/isj.12093>.
- [3] S. Nambisan, Digital Entrepreneurship: Toward a Digital Technology Perspective of Entrepreneurship, *Entrep. Theory Pract.* 41 (2017) 1029–1055. <https://doi.org/10.1111/etap.12254>.
- [4] S. Nambisan, K. Lyytinen, A. Majchrzak, M. Song, Digital Innovation Management: Reinventing Innovation Management Research in a Digital World, *MIS Q.* 41 (2017) 223–238. <https://doi.org/10.25300/misq/2017/41:1.03>.
- [5] H. Zaheer, Y. Breyer, J. Dumay, Digital entrepreneurship: An interdisciplinary structured literature review and research agenda, *Technol. Forecast. Soc. Change.* 148 (2019) 119735. <https://doi.org/10.1016/j.techfore.2019.119735>.
- [6] M. Ardolino, M. Rapaccini, N. Sacconi, P. Gaiardelli, G. Crespi, C. Ruggeri, The role of digital technologies for the service transformation of industrial companies, *Int. J. Prod. Res.* 56 (2018) 2116–2132. <https://doi.org/10.1080/00207543.2017.1324224>.
- [7] B. Hinings, T. Gegenhuber, R. Greenwood, Digital innovation and transformation: An institutional perspective, *Inf. Organ.* 28 (2018) 52–61. <https://doi.org/10.1016/j.infoandorg.2018.02.004>.
- [8] M. Luz Martín-Peña, E. Díaz-Garrido, J.M. Sánchez-López, The digitalization and servitization of manufacturing: A review on digital business models, *Strateg. Chang.* 27 (2018) 91–99. <https://doi.org/10.1002/jsc.2184>.
- [9] L. Satalkina, G. Steiner, Digital entrepreneurship and its role in innovation systems: A systematic literature review as a basis for future research avenues for sustainable transitions, *Sustain.* 12 (2020) 2764. <https://doi.org/10.3390/su12072764>. <https://doi.org/10.1016/j.indmarman.2016.06.013>
- [10] F. Vendrell-Herrero, O.F. Bustanza, G. Parry, N. Georgantzis, Servitization, digitization and supply chain interdependency, *Ind. Mark. Manag.* 60 (2017) 69–81..
- [11] E. Davidson, E. Vaast, Digital Entrepreneurship and Its Sociomaterial Enactment, in: 2010 43rd Hawaii Int. Conf. Syst. Sci., IEEE, 2010: pp. 1–10. <https://doi.org/10.1109/HICSS.2010.150>.

- [12] Guthrie, The digital factory: a hands-on learning projectdigital entrepreneurship, *J. Entrep. Educ.* 17 (2014) 115–133.
- [13] S. Kraus, C. Palmer, N. Kailer, F.L. Kallinger, J. Spitzer, Digital entrepreneurship, *Int. J. Entrep. Behav. Res. ahead-of-p* (2018) 353–375. <https://doi.org/10.1108/IJEBr-06-2018-0425>.
- [14] N. Hair, L.R. Wetsch, C.E. Hull, V. Perotti, Y.T.C. Hung, Market orientation in digital entrepreneurship: Advantages and challenges in a web 2.0 networked world, *Int. J. Innov. Technol. Manag.* 9 (2012) 1250045. <https://doi.org/10.1142/S0219877012500459>.
- [15] C.E. Hull, Y.T.C. Hung, N. Hair, V. Perotti, R. Demartino, Taking advantage of digital opportunities: A typology of digital entrepreneurship, *Int. J. Netw. Virtual Organ.* 4 (2007) 290–303. <https://doi.org/10.1504/IJNVO.2007.015166>.
- [16] T. Le Dinh, M.C. Vu, A. Ayayi, Towards a living lab for promoting the digital entrepreneurship process, *Int. J. Entrep.* 22 (2018) 1–17.
- [17] C. Richter, S. Kraus, A. Brem, S. Durst, C. Giselbrecht, Digital entrepreneurship: Innovative business models for the sharing economy, *Creat. Innov. Manag.* 26 (2017) 300–310. <https://doi.org/10.1111/caim.12227>.
- [18] F. Sussan, Z.J. Acs, The digital entrepreneurial ecosystem, *Small Bus. Econ.* 49 (2017) 55–73. <https://doi.org/10.1007/s11187-017-9867-5>.

THE ROLE OF BIOTECHNOLOGY IN THE DEVELOPMENT OF THE BIOECONOMY


Pavlo Pokataiev

First Vice-Rector Classical Private University
70-b Zhukovsky Str., Zaporizhzhia, 69002, Ukraine, katya373@i.ua
 <https://orcid.org/0000-0003-3806-2197>

Anastasiia Liezina

Department of Economics and Entrepreneurship
SHEE «Kyiv National Economic University named after Vadym Hetman»
54/1 Peremogy ave., Kyiv, 03057, Ukraine, lezya86@gmail.com
 <https://orcid.org/0000-0003-0516-6598>

Anhelina Andriushchenko

Department of Biochemistry Taras Shevchenko National University of Kyiv
60 Vladimirska Str., Kyiv, 01601, Ukraine, anelina.andr@gmail.com
 <https://orcid.org/0000-0003-4174-2740>

Helena Petukhova

Department of Mathematical Modeling and Statistics
SHEE «Kyiv National Economic University named after Vadym Hetman»
54/1 Peremogy ave., Kyiv, 03057 Ukraine, elena291961@ukr.net
 <https://orcid.org/0000-0003-2105-7666>

Article history: Received 13 August 2022, Received in revised form 30 September 2022, Accepted 3 October 2022, Available online 3 October 2022

This work has been published free of charge as a support of the publisher to the Ukrainian authors facing difficulties caused by the Russian war

Abstract

This paper analyzes the steps of the strategic development and use of innovations in the field of biotechnology in the largest and most developed countries of the world. Support for applied recommendations for state-level fundamental provisions regarding initiatives to develop the capacity of the biotechnology sector and increase the level of an international, strategic and competitive industry is presented. The authors conducted a study and evaluated the further promising use of innovations in biotechnology on the example of the EU-15 and EU-13 countries. A regularity was revealed that the biotechnology of the EU countries (EU-15) is developed at a high national and international level. The overall results of our work have helped to define further strategic directions and presented potential prospects for innovation in the field of biotechnology, which will subsequently lead to increased investment in this area. Using the graphical method, a dynamic model of trade turnover in the bioeconomy of the EU-15 countries is presented, followed by the construction of a trend line. And also formulated and predicted the value of trade in the bioeconomy of the EU-15 and EU-13 for the next decade.

Keywords

bioeconomy; innovative opportunities; clusters; investments; strategic development; biotechnologies; ecosystem.

Introduction

The authors of the article, in the course of studying an array of scientific studies, determined that in recent decades, the biotechnology industry has attracted more and more attention from investors around the world, and according to the forecasts of financial experts, biotechnologies that improve human life or the body itself can become one of the most dynamically developing and profitable businesses of the 21st century. The research problem posed by the authors is to analyze the prospects for the investment growth of biotechnology companies, to determine the impact of these companies on the formation and development of the bioeconomy. On the basis of the analysis, develop proposals for enhancing state initiatives for the development and

implementation of innovations in biotechnology companies, which will allow in the future to create an investment-attractive and competitive industry in any country.

So, we first of all studied scientific approaches to the definition of the definition of "biotechnology" as follows. We believe that this is a multicomponent and at the same time complex of interconnected industries, which often includes three main areas: biomedicine, industrial biotechnologies and agrobiotechnologies. In the first direction, research and implementation of new/modernized drugs, vaccines, molecular diagnostics and cell technologies can be singled out. The next direction includes high-tech and industrial processes using biological reactors, processing of microbial waste, as well as the production of biofuels, biodegradable polymers, etc. (Table 1).

Table 1. Bioinnovation is occurring in three key arenas. *Source: Compiled by the authors.*

Definitions	Biomolecules	Biosystems	Biomachine interfaces	Biocomputing
Mapping	In the study of omics, the subject of action is cellular processes and the functions of measuring intracellular molecules (such as DNA, RNA, proteins, etc.)	Complex biological functions and processes, as well as interactions between cells	The nervous system of organisms its structure and functions	Calculation of the output data of intracellular interactions under certain conditions
Engineering	Intracellular molecules (in selected cases via genome editing)	Technologies of various levels from cells, tissues, organs, to stem cells and their transplantation	The connection of the nervous system of the body and the machine in the form of a hybrid system	Selection, storage, processing and other actions of cells and their components for computing processes
Examples	Gene therapy for monogenic diseases and/or pathologies	Production of laboratory-grown meat	Motor control of human limbs (robot, hybrid) using neuroprocessing	Data storage in strands of DNA

For example, at the moment in the agricultural sector, one can observe the use of cultivation and soil reclamation, which improves pest resistance and plant fertility. In this case, we believe that this industry is attracting more and more attention over the last years of the 21st century, namely in the form of attracting investors at the international level. And if we rely on the opinion of well-known investment experts, then it is quite natural that at this stage of development, biotechnology should be considered the latest tool for improving human life due to the prospects for improving the quality of life, as well as the impact on the ecology of the whole world. The branch of our research, biotechnology, in comparison with other areas that are currently developing, but with difficulties, has a high popularity and necessity, as it affects almost all areas of human activity. In the conditions of modern risks, namely a general pandemic, many entrepreneurs, business entities, and, first of all, investors, are in no hurry to invest their funds with ambiguity in business structures [1,2]. Thus, if we consider the attention and influence of governments of various states, the media, society, medicine, scientific developments and other components of the search for drugs from COVID-19, it should be noted that there is a synergy of all of the above in the field of biotechnology, which has impressive prospects from the point of view investment perspective. In recent years, economic development during the worldwide COVID-19 pandemic has had a huge impact on the financial flows of most industries. It should be noted that few of them have recovered to the previous level, which distinguishes, on the contrary, biotechnologies, in which, after a short-term decline, there is a rapid improvement in indicators (Figure 1).

From the above, we can summarize that in 2021, the average value of shares of biotech companies in the countries of the European Union and the United States of America has more than doubled compared

to \$500. Accordingly, shares of Chinese companies increased by 106%, the United States and Europe by 39%, and the S&P 500 by 17%, that is, the increase in the first country increased by almost 6.5 times at an average price. In addition, it is biotechnologies that are advanced, even in comparison with other related and related companies, such as pharmaceuticals and virology [4–6]. In our opinion, these are obvious things, because modern conditions contribute to the close interaction of such areas in science and innovation as ecology, healthcare, sociology, as well as economics. These conditions of modernity form the radical changes that must be formed in Europe. Namely, it is necessary to form and change the approach to the production, use, consumption, processing, disposal and storage of all possible biological resources [7]. Accordingly, it is realistic and expected that the bioeconomy has emerged as a representation of the latest direction in the field of science, technology and innovation. Its main direction is to minimize the harmful impact on the environment in the process of doing business, subject to the achievement of operational, operational, strategic goals of sustainable development [8,9]. Between 2020 and 2021, biotechnology saw an annual increase in VC fundraising and deals (partnerships, joint developments, joint ventures) (Figure 2).

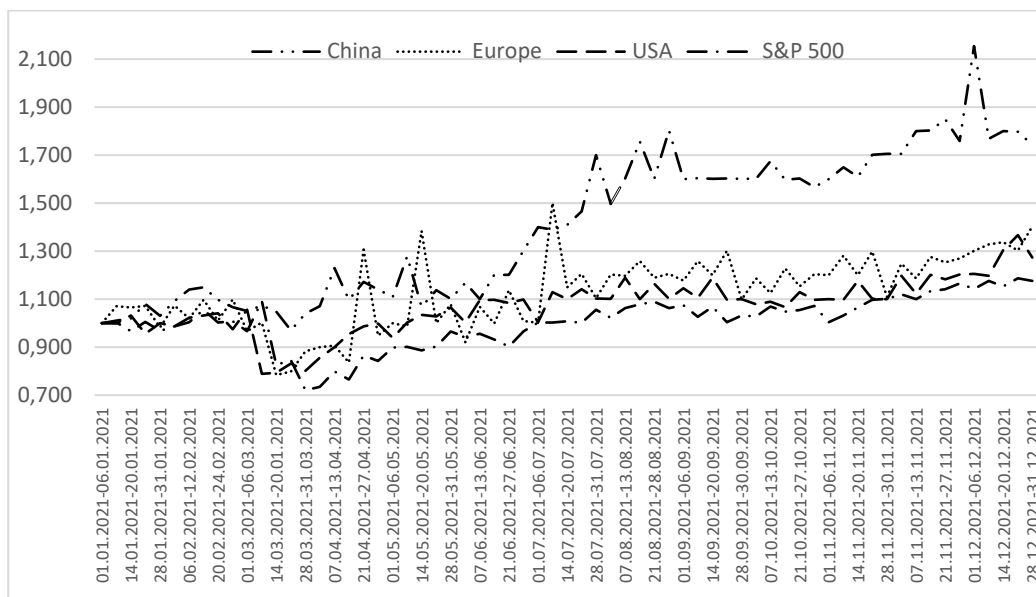


Figure 1. Recovery of biotechnologies in the period 01/01/2020 - 12/31/2021. Source: Own processing based on [3].

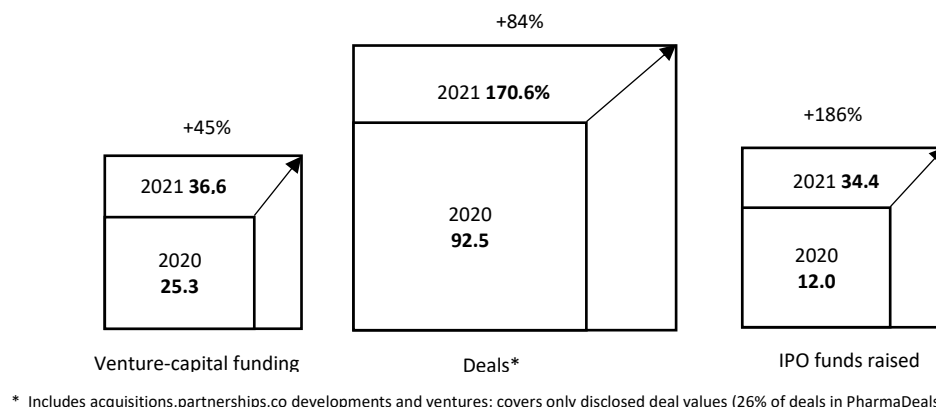


Figure 2. Recovery of biotechnologies in the period 01/01/2020 - 12/31/2021. Source: Own processing based on [10].

Venture activity in this area has increased by almost half over the past year, which has affected investments in this area, and at the time of mid-2021 the total amount was \$36.6 billion. From the point of view of assessing world leaders, the positions of the largest investments are distributed as follows - the USA, China, European countries. But it is worth noting that in the dynamics over the past year, the countries of the European Union (EU-15) in relative terms have more achievements in the development of investment in biotechnology. Thus, the volume of funding has more than doubled, and its growth rates are observed more rapidly than in the United

States. But it is fashionable to consider China as the leader of relative indicators in this case, since its indicators have increased by 4 times, even in comparison with the EU-15 countries. Accordingly, it is China that at the moment should be considered the leader in venture activity in the field of biotechnology.

Thus, having studied the opinion of venture investors, we can conclude that the field of biotechnology is now, more than ever, acceptable for deposits and has lower risks, compared to the period of the beginning of the 21st century. In contrast to this opinion, researchers of investment activity put forward their hypotheses that small contributions in the past affected the possible attractiveness in the present [11]. The other, third point of view, is more loyal and indicates that this activity in biotechnology is due only to the diversification of global investment portfolios. At the moment, the growth in investment activity is mainly due to quantitative growth in monetary terms in the United States. You can see the average amount of transactions doubled, and the total number increased by 25%. Among the EU-15 countries and China, rapid growth is also observed, but these rates are not supported by fundamental changes [12]. It is necessary to highlight the fact that the growth of investments in the bioeconomy is a strategically important indicator, which at the moment indicates growing financial benefits, and can also further increase the indicators of financial activity of related industries, which will form a new ecosystem. For example, some representatives of the strategic planning of large corporations expect to create and develop new enterprises not in urban areas, form import substitution of goods and services, and also strengthen the interaction between science and business [13]. In this direction, it should be noted that the bioeconomy has a direct impact even on such industries as biopolymers, fuel and its analogues, food additives and substitutes [14,15]. There is also a possibility of transformation, restructuring and formation of new processing processes [16,17] in the field of industrial biotechnology [13,18]. If we compare the development indicators of the bioeconomy five years ago, we can clearly see that in 2015 the indicator of 4.7% of the EU GDP accounted for this direction is very small. And in recent years, its development has stimulated representatives of science and entrepreneurs to deal with possible obstacles and risks. After we have studied a number of recent scientific studies in this industry, as well as the most popular theories and theorems [17,19–23] in the field of development of bioeconomics, it has been shown that the main direction regarding the development of this area is to reduce risks through the use of innovative systems at various levels business, industry, state, international relations.

Development prospects will be possible through the use of knowledge, the use of new materials, the inclusion of modern technologies and artificial intelligence in the process, as well as through the formation of rules, strategies and sustainable development [24]. Also, one should not forget that life cycles of development remain acceptable for any industry. In this case, it is necessary to predict development declines and form scenarios for getting out of them. In addition, the inherently collective nature of innovation requires a certain degree of shared imagination [25] and collective responsibility for developing capabilities [26]. In the case of a pessimistic scenario, only further observation and forecasting is necessary. The purpose of the study is to develop practical recommendations for the main provisions of the state level regarding initiatives to develop the potential of the biotechnology sector and increase the level of an international, strategic and competitive industry.

To achieve the goal, the following tasks were solved:

- the steps of strategic development and use of innovations (scientific transformation) in the field of biotechnology in the largest and most developed countries of the world were analyzed;
- the perspective of using innovations in biotechnology on the example of the EU-15 and EU-13 countries is determined, due to the identification of patterns (drivers) that the biotechnology of the EU (EU-15) countries is developed at a high national and international level;
- a dynamic model of trade in the bioeconomy of the EU-15 countries is presented, followed by the construction of a trend line with a forecast of the value of trade in the bioeconomy of the EU-15 and EU-13 for the next decade;
- strategic directions and potential prospects (intensification of state development initiatives) for innovations in the field of biotechnology are proposed, which will subsequently lead to increased investments in this field, which will provide each country with competitive advantages in the world.

Methods

In the process of the research, reporting and analytical information and the information base of the Ministry of Education and Culture were used [1,2,11–20,3,21–25,27,4–10]. To conduct the research, the dialectical

method was applied during the establishment of contradictions in methodological approaches regarding the determination of the features of strategic development and the use of innovations (scientific transformation) in the field of biotechnology in the largest and most developed countries of the world. Strategic directions and potential prospects for innovations in the field of biotechnology were proposed on the basis of the system-structural method based on the principle of a systematic study of socio-economic phenomena and processes, which will eventually lead to an increase in investments in this field. With the help of the historical-logical method during the study, the innovative drivers of development in biotechnology were singled out on the example of the EU-15 and EU-13 countries, due to the identification of patterns that the biotechnology of the EU (EU-15) countries is developed at a high national and international level. Based on the methods of quantitative and qualitative comparison, observation during the examination of patterns, resorting to the comparison of the state and structure of the compared indicators, the dynamics of turnover in the bioeconomy of the EU-15 countries was determined, followed by the construction of a trend line with the forecasting of the value of trade in the bioeconomy of the EU-15 and EU-13 for the next decade. As a result of the search for representatives of the bioeconomy, it is necessary to initially determine the possible existing clusters in this industry. Their presence indicates that joint work is already underway in the direction of development, learning processes, which may indicate a potential readiness for innovation. Such synergistic alliances can facilitate interaction with them, considering territorial, national, ethnic and other characteristics. In the future, the construction of trusting relationships can form sustainable management in the cluster. The analysis of the regional model of high-tech clusters of the EU based on the assessment of the development of the bioeconomy on the example of the EU-15 and EU-13 proves that the biotechnological industry of the "old" countries of the European Union (EU-15) is developed at a powerful level, both nationally and internationally. All opportunities for doing business and attracting investors have been created. The state plays an active role in developing initiatives and creating favorable risk control conditions for international investors. The results of monitoring companies associated with biotechnology showed that it is typical for them to use the latest developments in science and technology most effectively. A big role is played by the developed infrastructure and technological progress achieved by the "old" EU countries. Over the past 10 years, the biotechnological industry has been one of the development priorities in the national strategies of the "old" EU countries. In the course of the study, we formed a dynamic model of changes in commodity circulation in the bioeconomy of the EU-15 countries using the same trend line. The choice of the empirical function was carried out on the basis of linear, polynomial, logarithmic, power and exponential functions. Calculations with five trend lines were carried out to forecast the turnover based on the series of dynamics. The R^2 approximation reliability coefficient was used for the most optimal trend equation used in forecasting. If this coefficient approaches 1, then the trend equation can be a predictive model. The results of the forecast of changes in turnover in the EU-15 bioeconomy (Figure 3) showed optimistic results.

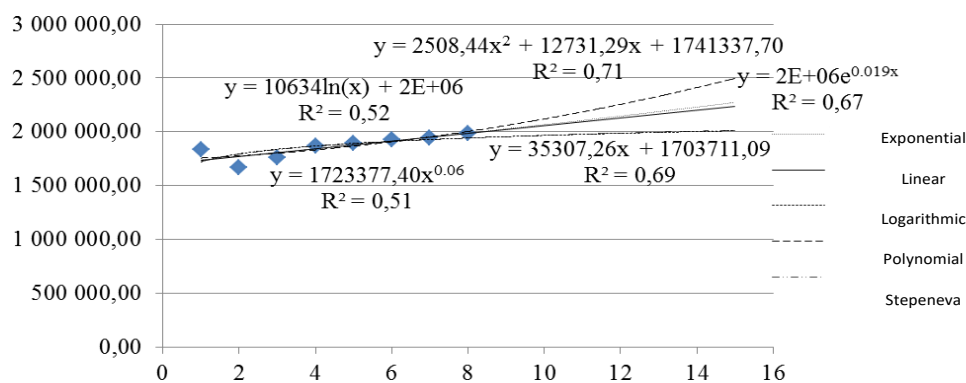


Figure 3. Forecast of changes in turnover in the EU-15 bioeconomy using the trend line. *Source: Developed by the authors.*

The highest approximation reliability was shown by the exponential function, R^2 is 0.71 (for polynomials of order 2). However, as the calculations showed, the reliability value of the approximation of all data/functions is disappointing. Carrying out calculations for polynomials of the 3rd order, we obtained the coefficient of determination coefficient $R^2 = 0.84$, for polynomials of the 4th order, $R^2 = 0.97$, and for polynomials of the 5th order, $R^2 = 0.997$ - that is, we obtained the largest value of reliable approximation. But, as a rule, the results calculated using polynomials of such orders, when compared with real data, should be rejected because they are inaccurate. So, the forecast values of turnover in the EU-15 bioeconomy for 7 years (2014-2021) are calculated using the obtained equations. The pessimistic forecast reflects the lower limit of the possible value of the indicator (due to the dominance of negative influencing factors), the optimistic one shows the upper limit

of the possible value (due to the predominance of positive factors), and the probable one reflects the most optimal development scenario. For optimistic forecasting, the highest R^2 (value of approximation reliability) was used - 0.71, for probable forecasting a linear function with R^2 - 0.69, and for pessimistic calculation R^2 - 0.51 was chosen. It can be asserted that the turnover in the bioeconomy of the "old" EU-15 countries in 2022 will amount to no less than 2 027 430.00 and no more than 2 496 706.05 euros (Figure 4). Forecasting the change in 2022 compared to 2008 showed that, according to the probable forecast, the turnover volume will increase by 28%.

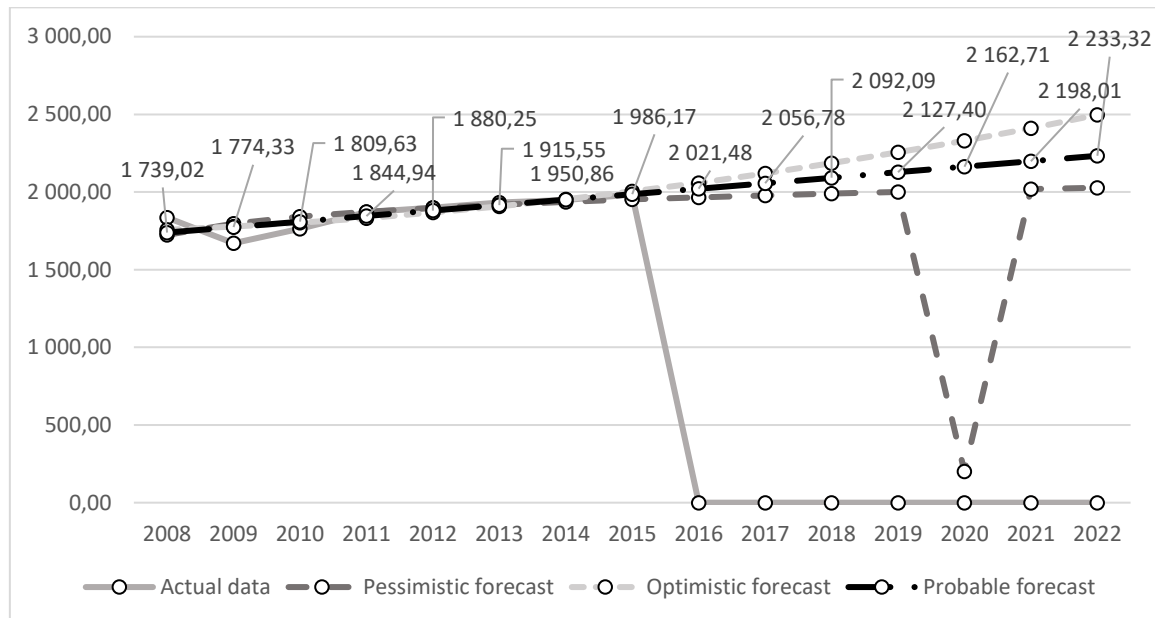


Figure 4. Optimistic, pessimistic, and probable/realistic scenarios of turnover growth in the EU-15 bioeconomy, 2008-2022 (thousand euros). Source: Calculated by the authors based on Data portal of agro-economics research: Bioeconomy.

Thus, according to the optimistic forecast of turnover in the bioeconomy of the "old" EU-15 countries, it will increase by 42% by 2022 compared to 2008. To forecast the turnover in the bioeconomy of the "old" EU-15 countries, a linear dependence was used for each country, because it's the probability ratio is 0.69 and shows steady growth. Disappointing results were shown by Greece, because its turnover in the bioeconomy may decrease by 7% in 2022, and in Spain, an increase in turnover is observed by 5%. The best changes in turnover are reflected in Luxembourg with an increase of 58%, Belgium – 51% and Denmark – 50%. The results of the forecast of changes in turnover in the EU-13 bioeconomy (Figure 4) are also optimistic. However, the reliability value of the data/function approximation is low, as it is for the EU-15. That is, the R^2 criteria is low-precision, which makes it difficult to predict. Shown in Figure 5 polynomial dependence shows that turnover in the EU-13 bioeconomy will increase.

Similarly, forecasting for the EU-13 was carried out as for the EU-15. From several functions, we choose the one that most likely approximates the dynamics of the indicator. For optimistic forecasting, the highest R^2 (value of 95 confidence approximation) was used - 0.59, for probable forecasting a linear function with R^2 - 0.57, and for pessimistic calculation R^2 - 0.50 was chosen. It can be argued that the turnover in the bioeconomy of the "new" EU-13 countries in 2022 will be no less than 283 541.05 and no more than 399 672.26 euros (Figure 6). Forecasting the change in 2022 compared to 2008 showed that, according to the probable forecast, the turnover volume will increase by 40%. A polynomial model was used for the best regression analysis, and according to its forecast, turnover in the bioeconomy of the "new" EU-13 countries in 2022 may increase by 70%.

Figure 7 presents the likely forecast of turnover in the bioeconomy of the "new" EU-13 countries. A negative trend is observed in 4 countries (Cyprus – 22%, Croatia – 19%, Slovenia – 5% and the Czech Republic – 6%). However, Cyprus is not a high-tech country, so these indicators are typical. Best forecasts in Estonia, Lithuania, Latvia and Poland. In the process of building forecast scenarios for the development of the bioeconomy in the EU-15 and EU-13, a second-order polynomial function was chosen, which has the most accurate results. The development of the optimistic scenario for the EU-15 is 42%, for the EU-13 – 70%, the onset

of the pessimistic prognosis is 18% and 24%, respectively, for the EU-15 and EU-13 countries, which is unlikely. The most realistic is the forecast for the growth of turnover in the bioeconomy at the level of 28% and 40% for the EU-15 and EU-13 countries, respectively. Therefore, according to all forecast development scenarios, there is a further increase in turnover in the bioeconomy of the EU, which proves the increasing role and importance of the development of the bioeconomy and biotechnologies in the future.

Over the past ten years, the European Patent Organization received 1 807.65 thousand applications for obtaining patents in the field of biotechnology from EU countries (Figure 8). The presented data (Figure 8) of submitted applications for patents in the field of biotechnology were presented by such countries as Belgium, Bulgaria, the Czech Republic, Denmark, Germany, Estonia, Ireland, Greece, Spain, France, Croatia, Italy, Cyprus, Latvia, Lithuania, Luxembourg, Hungary, Malta, the Netherlands, Austria, Poland, Portugal, Romania, Slovenia, Slovakia, Finland, Sweden, as well as Great Britain. The data for 2021 as a whole is the lowest for the period 2012 - 2021. The highest application activity was observed in 2015 – 3 053.99 thousand. The largest number of applications came from Germany, France and Great Britain, which were the constant leading countries throughout 2012 - 2021. On the other hand, Malta, Cyprus and Bulgaria show the lowest activity.

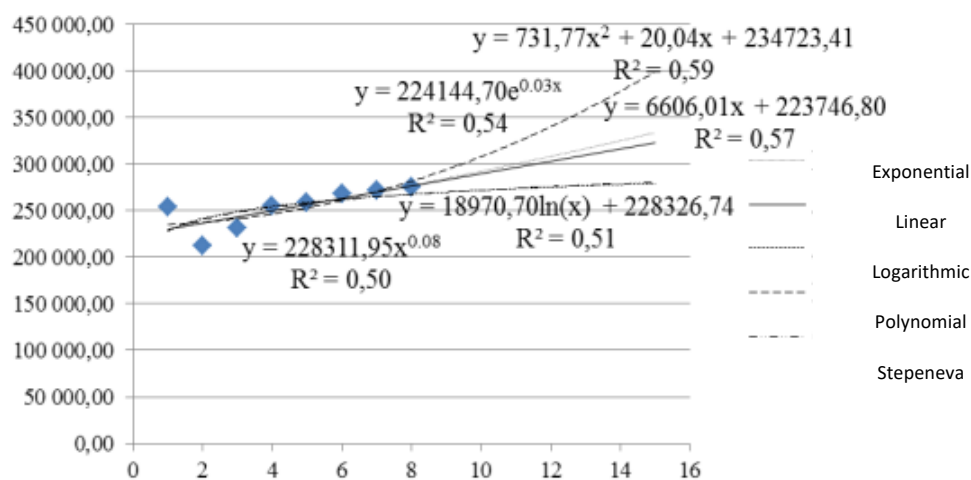


Figure 5. Forecast of changes in turnover in the EU-13 bioeconomy using the trend line. Source: Developed by the authors.

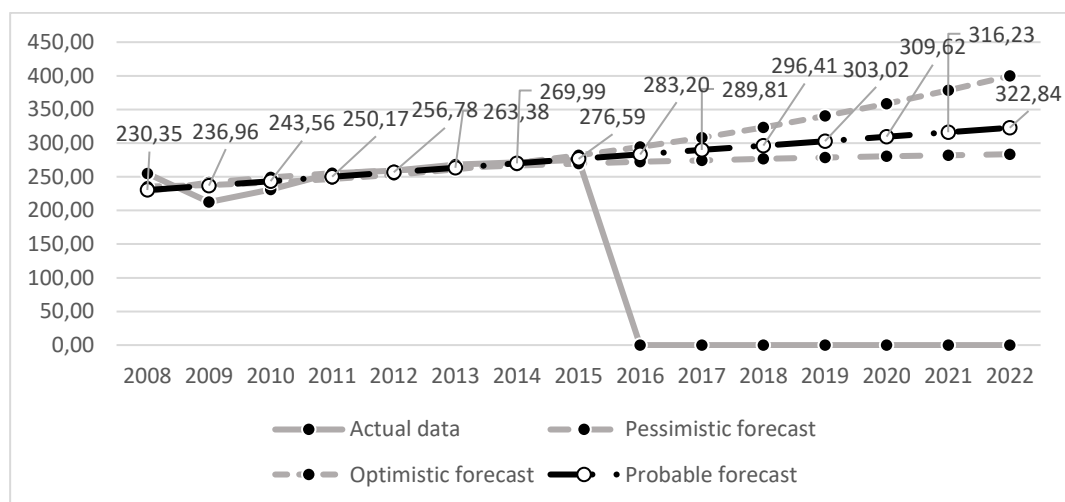


Figure 6. Optimistic, pessimistic, and probable/realistic scenarios of turnover growth in the EU-13 bioeconomy, 2008-2022 (thousand euros). Source: Calculated by the authors based on Data portal of agro-economics research: Bioeconomy.

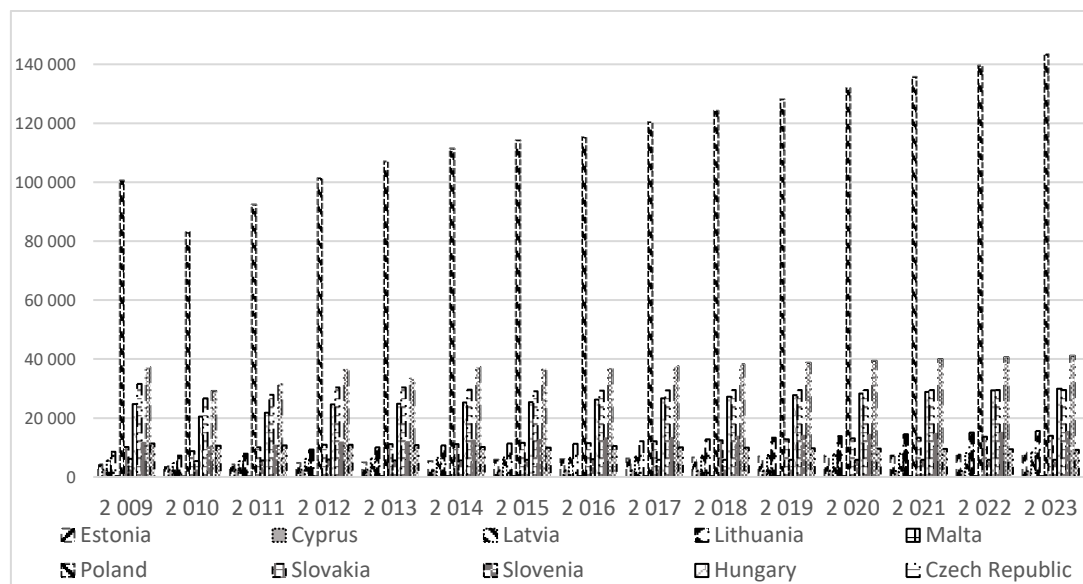


Figure 7. Dynamics of changes in the total trade turnover in the bioeconomy in the EU-13 countries, euro. *Source: Calculated by the authors based on [28].*

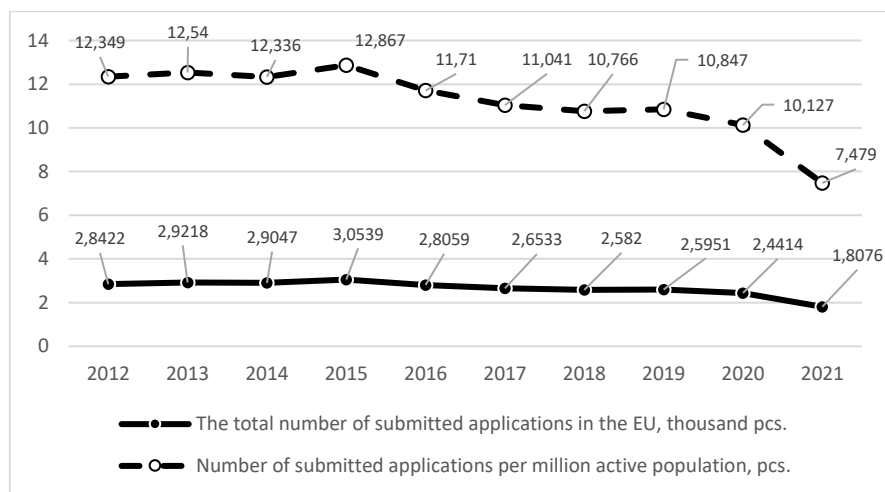


Figure 8. Submitted applications for patents in the field of biotechnology to the European Patent Organization, 2012-2021. *Source: Calculated by the authors based on Meta-network for public-to-public partnerships in the bioeconomy.*

Results

At the moment, the total world volume of biotechnologies is estimated at more than 1 billion dollars, and its constant annual growth is also estimated at an average of 14% until 2030 inclusive (Figure 9). The ever-increasing influence of person-centered medicine and the increase in orphan formulations are opening up new opportunities for biotech applications and driving the influx of new and innovative biotech companies, which in turn further increases their market revenues.

In the conditions of modern economic relations and the construction of business structures, it can be confidently stated that the conditions of restrictions as a result of the spread of the pandemic around the world had a negative impact on the majority of business entities, but at the same time, improvement in the field of biotechnology and bioeconomy can be identified as a positive factor. Thus, as of 2021, more than 11 billion doses of COVID-19 vaccines have been produced in the world, which made it possible, as a result of mass vaccination, to create conditions for the formation of herd immunity. Against this background, from an economic point of view, it is important to note that companies that produced vaccines are seeing sharp revenues from these industries. Industry leaders in the United States of America have revenues of almost \$31 billion in 2021 (Figure 9). In many countries of the world, a regulatory and legal framework has been developed, in particular, strategic programs for the long-term and short-term perspective regarding the development of public-private

partnerships (PPP) in the field of biotechnology. For example, the largest research and innovation program in EU countries to promote PPPs is Horizon 2020, the budget of which is almost 80 billion euros (from 2014 to 2020). Biotechnology in this program plays a leading role in the creation of industrial technologies (LEIT), which will develop in three directions:

- advanced biotechnologies as a future driver of innovation growth to ensure leadership positions in the medium and long term;
- biotechnologies based on industrial processes - a driver of increased competitiveness and sustainability to maintain European leadership in the field of industrial biotechnologies;
- innovative and competitive technology platforms for the development of new technology platforms related to biocatalysis and biodesign for industrial applications in a wide range of industries.

The number of biotechnological enterprises in EU countries is more than 1 700, of which 180 are public companies. To implement the Horizon 2020 program, a new institutionalized public-private partnership based on bio-industry (BBI) was created to overcome the "valley of death" on the way from research to market implementation. Projects on the creation of industrial biotechnologies in the "Horizon 2020" program (Table 2) are financed under three themes:

- synthetic biology - construction of organisms for new products and processes;
- expansion of industrial application of enzymatic processes;
- the following processes of unlocking biotechnological transformations.

From the above, it can be concluded that projects for the creation of industrial biotechnologies in the EU countries are mainly focused on: the application of modern synthetic biology to fill the main technical and scientific gaps in the biotechnological industry of Europe; expansion of the industrial use of robust oxidation biocatalysts for the conversion and production of alcohols; creation of interdisciplinary and interdisciplinary consortia as a powerful synergistic tool for promoting innovations in the field of formation of biocatalytic platforms in order to ensure the competitiveness of the European chemical and pharmaceutical industry; development of prophylactic vaccines with a low production cost, which will combine nano- and bioinnovations.

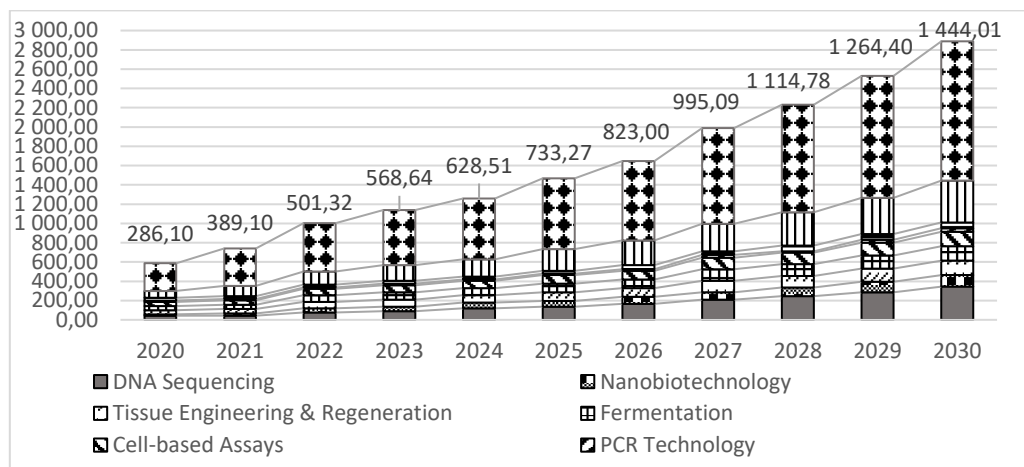


Figure 9. US Biotechnology Market Size Forecast 2020-2030 (million US dollars). Source: Calculated by the authors based on *Meta-network for public-to-public partnerships in the bioeconomy*.

Table 2. Projects on the creation of industrial biotechnologies in the Horizon 2020 program on the basis of PPP. *Source: Systematized by the author based on [29].*

Project name	Task	Cost, thousand €	Deadline	Participants
Biology is the construction of organisms for new products and processes				
EmPowerPutida	The development of three main factors in the field of biotechnology: 1. enables the transition from petrochemistry to bioeconomy; 2. diversification of new products, processes and markets; 3. provision of a strong, high-level platform for new industrial enterprises that find it too burdensome to implement new technologies	6 839	01.05.2015 – 30.04.2019	Industrial enterprises, scientific organizations of Germany, Spain, Switzerland, Portugal, Great Britain
MycoSynVac	Development of a universal Mycoplasma chassis that could be used to vaccinate animals against various types of mycoplasmas. Expected results of the project: 1. decrease in the level of infection caused by mycoplasmas; 2. improvement of animal safety; 3. cost-effective vaccines; 4. protection against new pathogenic microorganisms; 5. protection from the first time of use	8 057	01.04.2015 – 31.03.2020	Industrial enterprises, scientific organizations of the Netherlands, France, Great Britain, Germany, Austria, Denmark
P4SB	Biotransformation of plastic waste (e.g., polyethylene terephthalate and polyurethane) into alternative materials such as biodegradable plastic polyhydroxyalkanoates	7 057	01.04.2015 – 31.03.2019	Industrial enterprises, scientific organizations of Germany, Spain, Ireland, Great Britain, France
Diversification of new products, processes and markets				
ROBOX	Demonstration of the technical and economic viability of biological transformations of four types of stable oxidizing enzymes: monooxygenase (450), Bayer-Villiger monooxygenase (BVMOs), alcohol dehydrogenase (ADH) and alcohol oxidase (AOX), whose reactions have already been tested in laboratory conditions in the pharmaceutical, food industry, etc. . Implementation of ROBOX bio-oxidation processes is expected to result in significant reductions in cost (up to -50%), energy use (60%), chemicals (16%) and GHG emissions (-50%)	11 389	01.04.2015 – 31.03.201	Industrial enterprises, scientific and educational institutions of Switzerland, Belgium, the Netherlands, Germany, the Czech Republic, Austria, Italy, Spain, Great Britain
CARBAZYMES	Creation of an interdisciplinary and interdisciplinary consortium. The interdisciplinary approach will include: 1. a broad platform of 4 types of unique C-C bond forming enzymes; 2. the ability to quickly develop, work in industrial conditions with the help of new enzyme panels and massive screening methods; 3. application of microreactor technologies for biotechnological characteristics; 4. demonstration activities	9 251	01.04.2015 – 31.03.2019	Industrial enterprises, scientific and educational institutions in Spain, Germany, the Netherlands, Croatia, Great Britain
Processes of unlocking biotechnological transformations				
DiViNe	Development of preventive vaccines of various nature, which will combine nano- and bioinnovations: glycoconjugates, protein antigens and enveloped viruses	7 632	01.03.2015 – 29.02.2020	Industrial enterprises of France, Denmark, Germany, Portugal, Italy
NextBio PharmaDSP	Implementation of an integrated manufacturing platform for biosimilar monoclonal antibodies based on continuous chromatography combined with SingleUse methods for all single DSP sequencing operations together with state-of-the-art analytical tools	10 570	01.03.2015 – 28.02.2019	Industrial enterprises, scientific and educational institutions of France, Austria, Germany, Slovenia, and Italy

Discussion

Modern biotechnology and bioeconomics are closely intertwined with other areas such as agriculture. After all, it is obvious to introduce the latest technologies in this direction, namely in the processes of reproduction of flora and fauna at the micro and molecular levels, selection and crossing of various plant species for the purpose of their cultivation, transformation of wild plants, and so on. This kind of synergy allows plants to be more resistant to pests, use less herbicides, and improve their growth and productivity. At the moment, they already have positive results of introducing biotechnologies into the processes of growing bananas and rice in the countries of Asia and Africa. Against this background, clinical trials are constantly taking place, which also has good funding and stimulates the development of science and technology. According to the results of the total number of investments for 2020, they are estimated at \$19 billion, in 2021 this figure increased to \$23.1 billion, which is 16% more. The leader of such indicators is the company Intellia Therapeutics and Regeneron, which has produced the largest number of successful clinical trials. Such an example is a stimulating factor for increasing activity for other market representatives and the formation of a new range of drugs for currently incurable diseases (cancer, diabetes, etc.).

It is expected that such studies will stimulate further research in this area and stimulate the market. In the past few years, biotechnological methods have gained popularity, including stem cell technology, DNA fingerprinting, and genetic engineering (Figure 10).

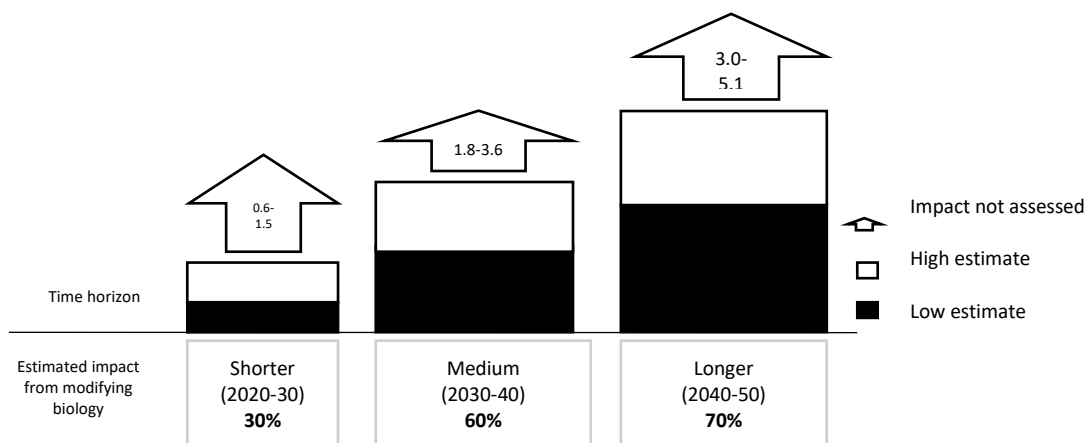


Figure 10. Estimated impact from modifying biology. Source: Compiled by the authors based on [30].

It should also be noted that more than half of biotechnological innovations are outside healthcare in agriculture, consumer and other areas (Figure 11). Thus, the development of biotechnologies has a direct impact on the spheres of science, life and healthcare, which forms new clusters of the economic space. Thus, the development of biotechnology has a direct impact on the spheres of science, life and healthcare, which forms new clusters of economic space. Accordingly, it is worth assuming that the bioeconomy combines many elements on the basis of production, using modern, innovative and progressive biotechnologies, while providing for the needs of the population. In this case, further discussion of possible discussion issues regarding the social impact of the bioeconomy is considered through food security, access to land plots and land use, employment, household income, lost working days due to injury, quality of life of the population in general, etc. At the current stage, the comparative analysis of countries is relevant to research with the help of the global innovation index. The Global Innovation Index was compiled by the World Intellectual Property Organization of Cornell University and the international business school "Insead". 143 countries of the world are represented in the rating. The structure of the index includes 7 indicators and their components. For the analysis of the countries of the European Union, information on their indicators for 2021 is presented (Table 3). The global innovation index reflects the main components of the country's innovation potential, so the index is a generalized assessment. There is a trend that the higher the country's position in the rating, the higher the development of high-tech industries, including biotechnology. Stock markets are also an important condition in the development of biotech companies for obtaining additional capital. Great optimism and new signs of confidence are observed in 2021, because 233 European biotechnology companies received 5.09 billion euros in financial resources, which is 54% more than in 2016 (3.30 billion euros). In 2021, investors show increased interest in European

biotechnology companies compared to 2020. By the end of 2021, 4.27 billion euros were allocated to biotechnology companies for follow-on offering, which is 56% higher in comparison with a similar period in 2020 - 2.75 billion euros. In 2021, according to analysts' forecasts, interest in the volume of initial public offerings (IPOs) in the European biotech sector on the stock market has improved compared to the previous year. The total amount of initial public offering of shares amounted to EUR 814.7 million, which shows an increase of 47% compared to 2020. Volumes of initial public offering of shares (IPOs), as well as their subsequent financing, increased, in particular, due to the upward trend on the NASDAQ stock exchange. An initial public offering of shares is increasingly becoming one of the financing options aimed at strengthening the future growth of business in the European biotech sector, because it involves the shares being offered to a wide range of investors for the first time and the company receiving a listing on the stock exchange. As a result of the search for representatives of the bioeconomy, existing clusters in this direction were identified, which emphasizes the formation and development of this industry. The authors set a goal to show the strategic directions and potential prospects of innovations in the field of biotechnology based on the system-structural method based on the principle of systematic study of socio-economic phenomena and processes [9–11]. Thanks to this, a dynamic model of changes in turnover in the bioeconomy of the EU-15 and EU-13 countries was formed along the trend line. In the future, calculations with five trend lines were carried out to forecast the turnover based on a series of dynamics. The R2 approximation reliability coefficient was used for the most optimal trend equation used in forecasting. If this coefficient approaches 1, then the trend equation can be a predictive model. It seems that the presented method of forecasting the turnover for building the strategic development of the bioeconomy contradicts the claims of research [8,10,13,14] about too much formalization and systematization of processes. The implementation of the authors' initiatives can be supported by efficient and effective communication channels, and the collection of results is automated in the bioeconomy company's IT systems. On the other hand, this confirms the statement of R. Bosman et al. [19] about the positive relationship between linear, polynomial, logarithmic, power, and exponential functions.

When analyzing the assumptions regarding the construction of the turnover strategy of bioeconomy companies in the EU countries, as well as the assumptions and the construction of five trend lines, a positive connection between them is visible, which turns into measurable advantages for the organization of clusters. A significant limitation of the research at this stage is the low level of knowledge regarding the future use of the main natural resources in the EU countries, considering the deterioration of the political situation. According to the authors, unfavorable conditions can delay positive forecast data for the sustainable development of trade in the field of bioeconomy.

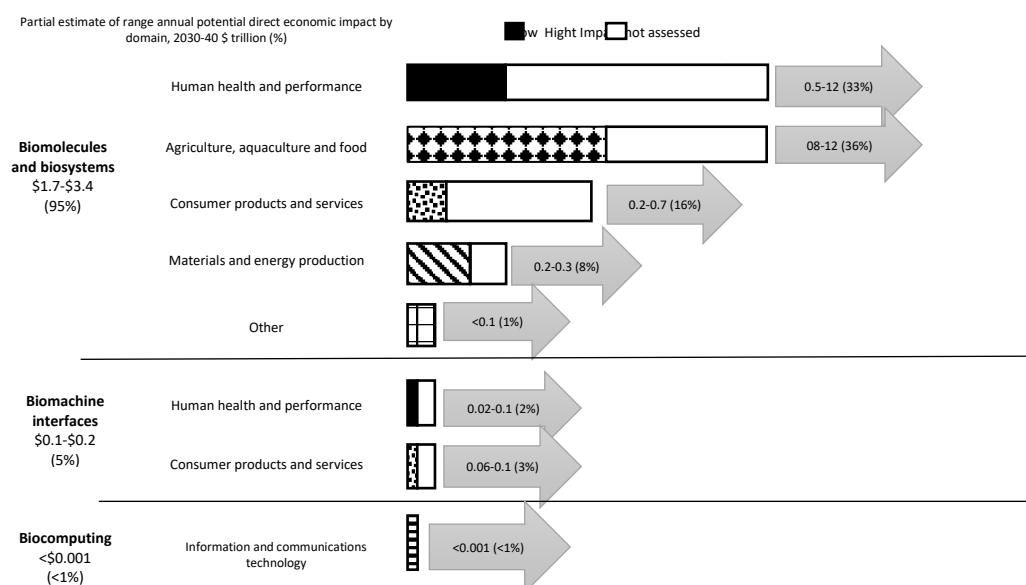


Figure 11. Partial estimate of range annual potential direct economic impact by domain, 2030-40 \$ trillion (%). Source: Compiled by the authors based on [30].

Table 3. Global innovation index of EU countries, 2021. *Source: Systematized by the author based on [31].*

Country	Place in the rating	Global Innovation Index	Institutional environment	Human capital and research	Infrastructure	Market experience	Business experience	Acquired knowledge and scientific and practical results	Results of creative activity
Sweden	2	68	88.3	63.7	69.1	64.9	62.6	62.5	53.3
Netherlands	3	63.4	88.2	54.7	63.3	63.3	59.0	62.9	59.0
Great Britain	5	60.9	88.4	63.3	67.1	70.2	52.2	46.5	60.5
Denmark	6	58.7	91.4	66.1	63.2	70.2	52.5	43.9	53.5
Finland	8	58.5	92.2	66.4	64.4	61.6	60.1	48.8	47.3
Germany	9	58.4	83.5	60.1	61.5	60.0	51.4	51.1	55.9
Ireland	10	58.1	87.6	55.1	62.1	55.0	54.5	55.9	50.9
Luxembourg	12	56.4	82.6	42.9	60.1	43.4	57.8	45.0	65.8
France	15	54.2	80.7	58.1	63.4	64.3	50.6	38.5	51.4
Austria	20	53.1	87.1	61.0	63.0	53.1	50.3	38.2	48.3
Czech Republic	24	51.0	77.6	47.6	57.3	50.2	45.9	45.8	46.7
Estonia	25	50.9	81.1	41.5	63.9	55.0	43.4	36.1	53.6
Malta	26	50.6	77.6	41.9	60.6	45.4	49.0	36.6	56.0
Belgium	27	49.9	80.5	59.7	57.2	51.8	48.5	33.2	47.1
Spain	28	48.8	75.9	48.9	64.3	59.0	38.4	36.3	44.4
Italy	29	47.0	71.9	46.3	61.8	52.6	39.6	36.1	42.9
Cyprus	30	46.8	81.0	39.9	48.1	57.9	42.7	41.3	38.2
Portugal	31	46.1	80.8	47.6	54.0	51.1	35.4	29.9	46.7
Slovenia	32	45.8	80.9	49.2	55.4	43.1	43.4	28.0	46.4
Latvia	33	44.6	77.8	35.2	53.1	52.1	38.2	26.5	49.4
Slovakia	34	43.4	74.5	34.4	55.3	45.8	38.3	33.5	40.8
Bulgaria	36	42.8	67.1	33.7	51.9	43.9	41.4	32.0	44.1
Poland	38	42	75.6	36.5	53.3	48.2	37.4	27.9	39.7
Hungary	39	41.7	70.7	39.5	52.3	41.5	37.8	32.3	37.9
Lithuania	40	41.2	74.1	37.5	57.2	53.0	37.8	21.3	39.6
Croatia	41	39.8	69.3	37.4	55.9	42.1	35.1	25.4	37.9
Romania	42	39.2	69.0	30.5	55.1	44.2	33.0	31.0	32.9
Greece	44	38.8	65.2	56.4	48.2	50.2	28.8	20.4	35.5

Impact

Regarding the impact of biotechnology on the development of the bioeconomy in different countries of the world, it is worth noting the rapid development and prospects. For example, systematic work on the development of biotechnology is already being carried out in the EU countries, with the main emphasis being placed on such a tool as strategic program documents for the medium and long term. Separately, each country strives to provide support for the development of this sector of the economy, creating quite powerful national strategic programs. For example, in Hungary there is a "National Research and Innovation Strategy Investments in the Future" (2013-2020), in Slovakia a "Strategy for Research and Innovation Development within Smart Specialization" (2014-2020), in Slovenia "Road and research infrastructure" (2012-2020), in South Africa "Ten-year innovation plan" (2008-2018), which allow to improve the well-being and quality of life of society. As you can see, most of them have already expired, but this does not mean that these programs will not be continued. In the future, the implementation of these programs ensures a reduction in the cost of food industry and agriculture products, allows to significantly improve and improve the field of environmental protection,

leads to the development of biomedicine and the emergence of new effective and affordable biopharmaceuticals, etc. At the same time, the analysis of the main ways of supporting the biotechnological sphere will allow to create a scientific basis for borrowing the best world experience in the conditions of Ukrainian realities.

Considering the joint efforts of scientific and governmental structures in increasing the share of the national biotechnology sector in the structure of the world, the leading player remains the USA. According to preliminary estimates, the total market value of the biotechnology sector is more than 360 billion dollars. In the USA, the total revenue provided by the biotechnology sector is about 60 billion dollars. USA and provides jobs for more than 100,000 workers. One of the ways to achieve such success, even during the financial crisis, is a number of programs to support the development of scientific, technological and innovative activities. According to experts of the international auditing company "EY" ("Ernst & Young"), the revenues of the biotechnology industry of public companies based in the USA amount to 71.9 billion dollars. USA per year. In relation to 2020, the revenues of the leaders of the biotech sphere in the USA increased by 15%, and expenses by 25%, while in Europe - by only 3%. The market capitalization of these companies in 2021 exceeded 400 billion dollars. of the USA (increased by more than 74% compared to the previous year), which indicates the efficiency of using own resources, strengthening and expansion of business, financial stability. According to the Financial Times Global 500 world ranking for 2021, the ranking of the Top 10 biological and pharmaceutical companies is distinguished by the indicators of the net profit obtained. In this rating, the 1st, 2nd, 7th, 8th, 10th places were occupied by US companies ("Pfizer" with a net profit of 22 billion USD; "Johnson & Johnson" 13.8 billion USD; "Amgen" 5.1 billion USD; "Eli Lilly" 4.7 billion USD; "Merck" 4.4 billion USD). According to the rating conducted by the American magazine "Forbes", where experts evaluated companies not only by indicators such as annual sales growth and total revenue over 5 years, but also by the so-called "innovation premium", in 2021, to the Top 100 the most innovative companies in the world included 8 companies represented in the field of pharmacy and biotechnology.

Conclusions

In the conditions of constant complication of biotechnological processes, their dynamics and innovative renewal, the determinants of further development of the main subsectors, which include intensive generation of knowledge, access to poststructuralist sources of financing, constant renewal of scientific and production infrastructure, creation of collaborative networks, a high degree of entrepreneurial culture, become extremely important. partnerships between government, business and universities, commercialization of existing and promising developments, and the creation of a new type of bio-based companies. Summarizing what has been said, for the perspective development and implementation of biotechnology innovations in the countries, it would be advisable to:

- prepare strategic program documents for the medium and long term to ensure effective legal regulation, in particular: management and protection of intellectual property; attraction of foreign investments for R&D, commercialization of their results, creation of competitive biotechnological clusters, etc.;
- develop a state program for the training, retraining and internship of specialists abroad in the field of biotechnology to ensure the acquisition of knowledge and experience of the future specialist in law-making activities, project management and scientific and technical activities;
- to initiate the development of measures to stimulate research and development works in the field of biotechnology with the aim of commercialization and development of innovations and ideas in various sectors of industry. Within the framework of this program, conduct various competitions with the payment of rewards for scientific and technical achievements in the field of biotechnology, etc.;
- promote, with the participation of the state and economic entities, the creation of organizational and institutional structures for the development of the biotechnological sphere, which will deal with the support of scientific and technical developments and the commercialization of their results, paying special attention to the current needs of the introduction of biotechnology in various sectors of the economy;
- to activate the participation of domestic specialists in international programs and projects of the biotechnological sphere, in particular, to involve domestic scientists as experts based on the results of international programs and projects, which will allow a more comprehensive consideration of the possibilities of creating innovative products (for example, biomedical products)

as responses to the current challenges of modernity simultaneous reduction of the consequences of adverse impact on the environment;

- create a state system of registration and accounting of scientific and technical research and development in the field of pharmaceuticals and biotechnology for the informatization of business entities, which will lead to the acceleration of their commercialization;
- expand public-private partnership by intensifying the development of innovative infrastructure through the creation of industrial parks, bio incubators, innovation towns, etc.;
- to concentrate efforts on the development of innovative medicinal products, with the involvement of talented students, postgraduates, scientists from both the state and corporate sectors, intended for the treatment of rare diseases, which will allow manufacturers to be competitive on the domestic and foreign markets in the long term.

The above proposals for the activation of state development initiatives and the introduction of biotechnological innovations will allow in the long run to create an investment-attractive and competitive industry that will provide competitive advantages in the world of each country.

Conflict of interest

There are no conflicts to declare.

Acknowledgements

The article will be funded at the author's expense.

References

- [1] K. Andriushchenko, A. Liezina, S. Vasylychak, M. Manylich, T. Shterma, U. Petrynyak, Management of the Development of the Innovative Potential of the Region, *TEM J.* 11 (2022) 339–347. <https://doi.org/10.18421/TEM111-43>.
- [2] K. Andriushchenko, A. Khaletska, N. Ushenko, H. Zholnerchyk, I. Ivanets, S. Petrychuk, S. Uliganets, Education Process Digitalization and Its Impact on Human Capital of an Enterprise, *J. Manag. Inf. Decis. Sci.* 24 (2021) 1–9.
- [3] I. Sotiropoulou, P. Deutz, Understanding the bioeconomy: a new sustainability economy in British and European public discourse, *Bio-Based Appl. Econ.* 10 (2021) 283–304. <https://doi.org/10.36253/bae-9534>.
- [4] V. Kovtun, K. Andriushchenko, N. Horbova, O. Lavruk, Y. Muzychka, Features of the management process of ambidextrous companies, *TEM J.* 9 (2020) 1–6. <https://doi.org/10.18421/TEM9131>.
- [5] Y. Bilan, V. Nitsenko, I. Ushkarenko, A. Chmut, O. Sharapa, Outsourcing in international economic relations, *Montenegrin J. Econ.* 13 (2017) 175–185. <https://doi.org/10.14254/1800-5845/2017.13-3.14>.
- [6] V. Nitsenko, I. Nyenno, I. Kryukova, T. Kalyna, M. Plotnikova, Business model for a sea commercial port as a way to reach sustainable development goals, *J. Secur. Sustain. Issues.* 7 (2017) 155–166. [https://doi.org/10.9770/jssi.2017.7.1\(13\)](https://doi.org/10.9770/jssi.2017.7.1(13)).
- [7] European Commission, Innovating for sustainable growth: A bioeconomy for Europe, 2012. <https://www.eea.europa.eu/policy-documents/innovating-for-sustainable-growth-a>.
- [8] N. Robert, J. Giuntoli, R. Araujo, M. Avraamides, E. Balzi, J.I. Barredo, B. Baruth, W. Becker, M.T. Borzacchiello, C. Bulgheroni, A. Camia, G. Fiore, M. Follador, P. Gurria, A. la Notte, M. Lusser, L. Marelli, R. M'Barek, C. Parisi, G. Philippidis, T. Ronzon, S. Sala, J. Sanchez Lopez, S. Mubareka, Development of a bioeconomy monitoring framework for the European Union: An integrative and collaborative approach, *N. Biotechnol.* 59 (2020) 10–19. <https://doi.org/10.1016/j.nbt.2020.06.001>.
- [9] U. Fritsche, G. Brunori, D. Chiaramonti, C.M. Galanakis, S. Hellweg, R. Matthews, C. Panoutsou, Future transitions for the bioeconomy towards sustainable development and a climate-neutral economy—knowledge synthesis. Final report, Luxembourg, 2020. <https://doi.org/10.2760/667966>.
- [10] I.M. Vlad, E. Toma, The Assessment of the Bioeconomy and Biomass Sectors in Central and Eastern European Countries, *Agronomy.* 12 (2022) 880. <https://doi.org/10.3390/agronomy12040880>.
- [11] T. Olejarz, V. Nitsenko, O. Chukurna, M. Mykhailova, Evaluation of factors influencing labour performance of machine-building enterprises in mining industry, *Nauk. Visnyk Natsionalnoho Hirnychoho Universytetu.* 1 (2018) 154–162. <https://doi.org/10.29202/nvngu/2018-1/2>.
- [12] European Commission, Regional Innovation Scoreboard 2019, Luxembourg, 2019. https://research-and-innovation.ec.europa.eu/statistics/performance-indicators/regional-innovation-scoreboard_en.
- [13] R. Wohlgemuth, T. Twardowski, A. Aguilar, Bioeconomy moving forward step by step – A global journey,

- N. *Biotechnol.* 61 (2021) 22–28. <https://doi.org/10.1016/j.nbt.2020.11.006>.
- [14] G.B. Frisvold, S.M. Moss, A. Hodgson, M.E. Maxon, Understanding the U.S. bioeconomy: A new definition and landscape, *Sustain.* 13 (2021) 1–24. <https://doi.org/10.3390/su13041627>.
- [15] S. Wydra, B. Hüsing, J. Köhler, A. Schwarz, E. Schirrmeister, A. Voglhuber-Slavinsky, Transition to the bioeconomy – Analysis and scenarios for selected niches, *J. Clean. Prod.* 294 (2021) 126092. <https://doi.org/10.1016/j.jclepro.2021.126092>.
- [16] S. Dahiya, A.N. Kumar, J. Shanthi Sraavan, S. Chatterjee, O. Sarkar, S.V. Mohan, Food waste biorefinery: Sustainable strategy for circular bioeconomy, *Bioresour. Technol.* 248 (2018) 2–12. <https://doi.org/10.1016/j.biortech.2017.07.176>.
- [17] H. Hellsmark, J. Mossberg, P. Söderholm, J. Frishammar, Innovation system strengths and weaknesses in progressing sustainable technology: The case of Swedish biorefinery development, *J. Clean. Prod.* 131 (2016) 702–715. <https://doi.org/10.1016/j.jclepro.2016.04.109>.
- [18] S. Wydra, Value chains for industrial biotechnology in the bioeconomy-innovation system analysis, *Sustain.* 11 (2019) 2435. <https://doi.org/10.3390/su11082435>.
- [19] R. Bosman, J. Rotmans, Transition governance towards a bioeconomy: A comparison of Finland and The Netherlands, *Sustain.* 8 (2016) 1017. <https://doi.org/10.3390/su8101017>.
- [20] C.C. Chung, Technological innovation systems in multi-level governance frameworks: The case of Taiwan's biodiesel innovation system (1997–2016), *J. Clean. Prod.* 184 (2018) 130–142. <https://doi.org/10.1016/j.jclepro.2018.02.185>.
- [21] A. Giurca, P. Späth, A forest-based bioeconomy for Germany? Strengths, weaknesses and policy options for lignocellulosic biorefineries, *J. Clean. Prod.* 153 (2017) 51–62. <https://doi.org/10.1016/j.jclepro.2017.03.156>.
- [22] T. Nevzorova, E. Karakaya, Explaining the drivers of technological innovation systems: The case of biogas technologies in mature markets, *J. Clean. Prod.* 259 (2020) 120819. <https://doi.org/10.1016/j.jclepro.2020.120819>.
- [23] A. Purkus, N. Hagemann, N. Bedtke, E. Gawel, Towards a sustainable innovation system for the German wood-based bioeconomy: Implications for policy design, *J. Clean. Prod.* 172 (2018) 3955–3968. <https://doi.org/10.1016/j.jclepro.2017.04.146>.
- [24] S. Leipold, A. Petit-Boix, The circular economy and the bio-based sector - Perspectives of European and German stakeholders, *J. Clean. Prod.* 201 (2018) 1125–1137. <https://doi.org/10.1016/j.jclepro.2018.08.019>.
- [25] D.D.T. Pham, P. Paillé, N. Halilem, Systematic review on environmental innovativeness: A knowledge-based resource view, *J. Clean. Prod.* 211 (2019) 1088–1099. <https://doi.org/10.1016/j.jclepro.2018.11.221>.
- [26] J. Stilgoe, R. Owen, P. Macnaghten, Developing a framework for responsible innovation, *Res. Policy.* 42 (2013) 1568–1580. <https://doi.org/10.1016/j.respol.2013.05.008>.
- [27] T. Kuosmanen, N. Kuosmanen, A. El-Meligi, T. Ranzon, P. Gurria, S. Lost, R. M'Barek, How big is the bioeconomy? Reflections from an economic perspective, Luxembourg, 2020. <https://doi.org/10.2760/144526>.
- [28] Eurostat, Patent applications to the EPO by priority year by NUTS 3 regions, (2015). <http://appsso.eurostat.ec.europa.eu/nui/submitViewTableAction.do>.
- [29] European Commission, CORDIS- Community Research and Development Information Service, (2022). http://cordis.europa.eu/project/rcn/193340_en.html.
- [30] Bio-Economy Technology Platforms (BECOTEPS), The European Bioeconomy in 2030: Delivering sustainable growth by addressing the grand societal challenges, *Bio-Economy Technol. Platforms.* (2011) 1–24. https://www.greengrowthknowledge.org/sites/default/files/downloads/resource/BECOTEPS_European Bioeconomy in 2030.pdf.
- [31] WIPO, Global Innovation Index 2021: Tracking Innovation through the COVID-19 Crisis, 2021. https://www.wipo.int/edocs/pubdocs/en/wipo_pub_gii_2021.pdf.

CHEMICAL HYDROLYSIS OF HEMICELLULOSE FROM SUGARCANE BAGASSE. A COMPARISON BETWEEN THE CLASSICAL SULFURIC ACID METHOD WITH THE ACIDIC IONIC LIQUID 1-ETHYL-3-METHYLIMIDAZOLIUM HYDROGEN SULFATE

Marcoaurélio Almenara Rodrigues

Unidade de Bioenergia, Laboratório Nacional de Energia e Geologia, I.P.
Estrada do Paço do Lumiar 22, 1649-038, Lisboa, Portugal

Permanent address: Departamento de Bioquímica, Instituto de Química
Universidade Federal do Rio de Janeiro

Av. Athos da Silveira Ramos, 149

Centro de Tecnologia, Cidade Universitária, 21941-909 Rio de Janeiro, Brazil, almenara@iq.ufrrj.br

 <https://orcid.org/0000-0002-5217-0082>

André M. da Costa Lopes

Unidade de Bioenergia, Laboratório Nacional de Energia e Geologia, I.P.
Estrada do Paço do Lumiar 22, 1649-038, Lisboa, Portugal

Permanent address: CICECO, Aveiro Institute of Materials, Department of Chemistry
University of Aveiro, 3810-193 Aveiro, Portugal, andremcl@ual.pt

 <https://orcid.org/000-0001-8855-6406>

Rafal M. Lukasik

Unidade de Bioenergia, Laboratório Nacional de Energia e Geologia, I.P., Estrada do Paço do Lumiar 22, 1649-038, Lisboa, Portugal, fax: +351217163636; phone: +351210924600 ext. 4224, rafal.lukasik@lneg.pt

 <https://orcid.org/0000-0002-7805-5744>

Article history: Received 28 August 2022, Received in revised form 3 October 2022, Accepted 4 October 2022, Available online 4 October 2022

Highlight

Sugarcane bagasse was pretreated with acidic ionic liquid and dilute sulfuric acid, high furfural yield was found at high ionic liquid concentration, high pentose yield was found at 46.4 wt.% ionic liquid concentration, a liquid fraction richer in pentose was found for the ionic liquid treated biomass, and the biomass pretreatment can be tuned to produce pentose or furfural using ionic liquid.

Abstract

Dilute sulfuric acid and acidic ionic liquids are pretreatment methods used to selectively hydrolyze hemicellulose from lignocellulosic biomasses. In this work, a comparison between these techniques is carried out by treating sugarcane bagasse both with 1-ethyl-3-methylimidazolium hydrogen sulfate at different ionic-liquid and water contents and with H₂SO₄ at the same conditions and equivalent ionic liquid molar contents. Results from the use of ionic liquid showed that it was possible to tune the biomass treatment either to achieve high hemicellulose hydrolysis yields of 72.5 mol% to very low furan and glucose co-production, or to obtain furfural at moderate yields of 18.7 mol% under conditions of low water concentration. In comparison to the use of ionic liquid, sulfuric acid pretreatment increased hemicellulose hydrolysis yields by 17%, but the 8.6 mol% furfural yield was also higher, and these yields were obtained at high water concentration conditions. Besides, no such tuning ability of the biomass treatment conditions can be made.

Keywords

sugarcane bagasse; acidic ionic liquid; biomass pretreatment; dilute sulfuric acid; pentose; furfural.

Introduction

Sugarcane bagasse, which is predominantly composed of cellulose, hemicellulose, and lignin [1], is the main by-product of the sugar/ethanol industry. This waste material is available in vast amounts and can be used for the production of high value-added products such as glucose, xylose furans, and other commodities [1–3]. The sugars glucose and xylose resulting from the enzymatic hydrolysis of cellulose and hemicellulose can be used in fermentation processes to produce fuel and chemicals [1,4–7]. Depending upon the biomass, pretreatment choice, and operational conditions, the cellulose-derived glucose can be transformed into 5-hydroxymethyl-

furfural (5-HMF) [2], and xylose can be transformed into furfural [3]. Because both furfural and 5-HMF are versatile chemical platform molecules in the biofuel and petrochemical industries [8], much effort has been devoted to converting biomass into these building-block molecules [2,9]. Lignocellulosic biomass can be pre-treated by several techniques to produce high value chemicals and fuels [3,10]. Pre-treatment with dilute sulfuric acid to selectively hydrolyze hemicellulose is the classic, most cost-effective reference method [3,10,11], reaching up to 85% of theoretical yield [5] and in some cases more than 95% [6]. However, this process has important drawbacks such as low selectivity and the formation of sugar dehydration products (e.g., furfural and 5-HMF), resulting in a highly impure and toxic pentose stream [12]. Besides, the sulfuric acid pre-treatment that has also been used to promote dehydration of xylose to furfural requires both the use of expensive construction materials to minimize corrosion, and the disposal of neutralization salts [6,10,13]. There is therefore great industrial interest in the development of more advanced processes for the production of a pentose syrup with very low furfural contamination and for the production of furfural in high yields without the use of sulfuric acid. Advances may come from a process option that avoids the detrimental industrial use of sulfuric acid and, more importantly, that enables the production of cleaner xylose or furfural currents more suitable to processing via biochemical or chemical pathways to higher value molecules.

Ionic liquids (ILs), particularly imidazolium based ILs, are an advantageous alternative to the use of sulfuric acid as they dissolve lignocellulosic biomass and can be used to convert biomass polysaccharides directly to furans [3,12,14]. ILs are made up of countless combinations of anions and cations and present highly tunable properties such as hydrophobicity, polarity, acidity, and miscibility with other solvents. Moreover, significant advances concerning the separation of biomass hydrolysis products from IL and the recovery of IL have been made, thereby decreasing the cost of using IL [15]. Acidic ILs have garnered special attention as they can act as both solvent and catalyst, selectively hydrolyze hemicellulose at high yield [16], and increase cellulose hydrolysability [17,18]. Novel superacid ILs have consequently been developed that improve hydrolysis of hemicellulose and its subsequent conversion to furfural [12]. In spite of the aforementioned wealth of information on the applications of IL for biomass processing, no thorough study has yet been done comparing hemicellulose hydrolyses from lignocellulosic biomass by acidic IL with the classic dilute sulfuric acid method. In the few studies found in the literature, the biomass used were either commercial hemicellulose [19] or cellulose [20]. Moreover, the sulfuric acid concentrations used in these studies were extremely low, less than 0.5 wt.%, which are inadequate to hydrolyze hemicellulose from lignocellulosic biomass since they result in low hydrolysis yields or require high temperatures (higher than 120°C) and/or treatment time longer than 1.5h to give hydrolysis yields higher than 50 mol% [21]. Accordingly, this work evaluated the treatment of sugarcane bagasse with the acidic IL 1-ethyl-3-methylimidazolium hydrogen sulfate ([EMIM][HSO₄]) in reaction mixtures presenting different ionic liquid and water contents. Results were compared to those obtained by treating the biomass, at the same temperature and time conditions, with dilute H₂SO₄ at the same molar content and similar concentration of the IL at the studied mass fraction of 6.5 wt.%, which corresponded to a sulfuric acid mass fraction of 5.6 wt.%. As expected, treatment with dilute sulfuric acid resulted in a pronounced hydrolysis of hemicellulose into xylose, nevertheless the liquid stream was also highly and undesirably contaminated with furfural and glucose. However, the use of ([EMIM][HSO₄]), besides resulting in hemicellulose hydrolysis into pentoses at high yield (69.2 mol%), presented a minimum of furfural, 5-HMF, and glucose contamination. Moreover, it was observed that the use of ([EMIM][HSO₄]) could be tuned, under conditions of low water content, for furfural production with a yield of as much as 18.7 mol%. Tuning is a valuable feature of the IL process that is not obtainable for the dilute sulfuric acid method.

Materials and methods

Biomass and chemicals

Sugarcane bagasse was milled to particles up to 0.5 mm in a knife mill (IKA WERKE GmbH & Co, Staufen, Germany) and kept dry at room temperature. The ionic liquid [EMIM][HSO₄] for the biomass treatment was purchased from Ionic Liquid Technologies GmbH in Heilbronn, Germany. The reagent presented 99% purity grade and water content of 1693.8 µg/g as determined by a volumetric Karl-Fischer titration method. Sulfuric acid of analytical grade was purchased from Panreac Química (Barcelona, Spain). The HPLC analysis standards, glucose, xylose, arabinose, furfural, and 5-HMF were purchased from Sigma Aldrich (St. Louis, USA). Deionized ultrapure Milli-Q grade water was used for the HPLC analysis and for the biomass treatment assays.

Biomass characterization

Biomass humidity was estimated according to the NREL/TP-510-42621 method [22]. Biomass characterization was performed by total acidic hydrolysis following the NREL/TP-510-42618 procedure [23]. The residual non-

hydrolyzed biomass was determined gravimetrically after incubation in a glass crucible at 100°C for 16h. The ash content was also determined according to the NREL/TP-510-42622 [24] procedure by igniting the non-hydrolyzed biomass at 550°C for 16 h. The acid-insoluble lignin content was assumed to be the difference between the non-hydrolyzed biomass and the ash content. All biomass characterizations were performed in triplicate.

Table 1. Mass composition (wt.%) of the reaction mixtures (dry mass of ionic liquid, dry mass of biomass and water) for the sugarcane bagasse treatment. Also showing control mixtures without catalyst at three representative biomass mass fractions. *Source: Authors results.*

[EMIM][HSO ₄]	Sugarcane biomass	Water
0.0	3.9	96.1
0.0	5.7	94.3
0.0	10.9	89.1
6.2	9.0	84.8
6.5	5.3	88.2
41.0	3.8	55.2
44.6	10.7	44.7
46.4	7.2	46.5
46.5	7.1	46.4
64.1	5.9	30.0
68.5	6.3	25.2
73.6	6.7	19.7
78.0	7.2	14.8
85.2	8.9	5.8

Biomass Treatment

■ Ionic liquid treatment

The mass composition (mass fraction) of the reaction mixtures (water, biomass, and IL) for sugarcane bagasse treatment is presented in Table 1. Four hundred milligrams of sugarcane biomass were treated with increasing IL and varying biomass concentration. The amount of IL and ultrapure Milli-Q grade deionized water that had to be added, to achieve the desired concentrations, was calculated considering the IL and biomass water contents, see the following section for calculation formulae and their deduction. The reaction mixtures were incubated for 83 minutes at 125°C in sealed flasks immersed in an oil bath under constant agitation [14,25]. These conditions were chosen based on a previous study that determined the optimum conditions to obtain xylose from wheat straw biomass with the similar IL 1-butyl-3-methylimidazolium hydrogen sulfate [BMIM][HSO₄] [14]. After cooling, unless the reaction mixtures already presented IL concentrations lower than 28.8 wt.%, a known amount of deionized water was added as an anti-solvent in order to reach a final IL concentration in the liquid phase of 28.8 wt.%. This threshold IL concentration prevented the IL interference in the subsequent sugar analysis [14]. For all treatments, the total mass added was recorded and it was assumed that no mass was lost by vaporization. The reaction mixture was filtered with a 0.45 µm nylon filter. The filtrate density was estimated by weighing a known volume of the solution in a pre-weighed volumetric flask and kept under refrigeration until its sugar composition determination by HPLC. The solid residue was washed with deionized water for the removal of soluble materials, dried for 20h at 70°C, and kept at room temperature. The yield of solid residue was determined gravimetrically, and its chemical composition analyzed using the same procedure applied to the untreated biomass as already described.

■ Biomass, ionic liquid and water contents calculations

The amounts of biomass, IL and water added to achieve the reaction mixtures compositions presented in Table 1 were calculated as follows:

The biomass mass fraction, $[Biomass]$, in the reaction mixture is described by equation (1).

$$(1) \quad [Biomass] = \frac{dmB}{mIL + mB + mw}$$

Where dmB is the dry mass of biomass added, mIL is the mass of IL to be added, mw is the mass of water to be added, and mB is the mass of biomass added, in this case, set in 400 mg.

The IL mass fraction in the reaction mixture, $[IL]$, is described by equation (2).

$$(2) \quad [IL] = \frac{dmIL}{mIL + mB + mw}$$

Where $dmIL$ is the dry mass of the IL added. Equations (1) and (2) can be rearranged in the following:

$$(3a) \quad \frac{dmB}{[Biomass]} = mIL + mB + mw$$

and

$$(3b) \quad \frac{dmIL}{[IL]} = mIL + mB + mw$$

Equating equations 3a and 3b and rearranging the following equation is deduced:

$$(4) \quad dmIL = \frac{[IL] \times dmB}{[Biomass]}$$

The IL and biomass dry masses are their masses subtracted from their respective mass of water.

$$(5a) \quad dmIL = mIL - wIL$$

and

$$(5b) \quad dmB = mB - wB$$

Where wIL and wB are their respective mass of water. However, wIL and wB are respectively the product of IL and biomass masses with their respective water content or humidity (hIL and hB).

$$(6a) \quad wIL = mIL \times hIL$$

and

$$(6b) \quad wB = mB \times hB$$

Therefore,

$$(7a) \quad dmIL = mIL \times (1 - hIL)$$

and

$$(7b) \quad dmB = mB \times (1 - hB)$$

Substituting equations (7a) and (7b) into equation (4) the following expression is deduced:

$$(8) \quad mIL = \frac{[IL] \times mB}{[Biomass]} \times \frac{1 - hB}{1 - hIL}$$

The mass of water to be added can be then, derived from equation (1)

$$(9) \quad mw = \frac{dmB}{[Biomass]} - mB - mL$$

Once the intended [IL] and [Biomass] are established, the IL and biomass humidities determined, and the biomass load set, the masses to be added of IL and water are calculated by equations (8) and (9).

▪ Dilute sulfuric acid treatment

In order to compare the biomass treatment with the acidic IL [EMIM][HSO₄] with the classic dilute sulfuric acid treatment, a different set of sugarcane bagasse biomass was treated with dilute sulfuric acid at the same molar content and concentration that was used for the ionic liquid treatment at mass fraction of 6.5 wt.% — that is, the concentrations either IL or sulfuric acid were set in 6.7 wt.%, which corresponded respectively to an IL and sulfuric acid mass fractions of 6.5 and 5.6 wt.%, see section below. The reaction mixture was incubated at 125°C for 83 minutes and deionized water was added to achieve a final liquid mass content of 10 g. The reaction mixture was then processed as already described for the treatment using IL.

▪ Sulfuric acid, water, and biomass content calculations.

For the design of the aforementioned comparative conditions, it was sought the same IL and sulfuric acid molar content, as well as the same concentration in the liquid phase of both chemicals, following the same rationale of previous works [19,20]. This approach secured comparative reaction conditions as the use of the same mass fraction for [EMIM][HSO₄] and H₂SO₄ would result in different concentrations of the reagents in the liquid phase as IL and sulfuric acid have different molar masses of 197.97 and 98.08 g/mol, respectively. The desired working conditions were designed as follows: (i) it was set the initial IL and biomass concentrations and considering the biomass load it was calculated the corresponding amount of IL; (ii) it was calculated the mass of the sulfuric acid solution corresponding to the same IL molar content; (iii) it was calculated the mass of the final solution for the same IL concentration; (iv) it was calculated the amount of deionized water to be added to achieve the mass of the final solution, considering the amount of water brought along with the biomass; (v) finally, the sulfuric acid and biomass concentrations were recalculated. The calculation and formulae deduction are described in the following:

The IL concentration in the liquid phase (*cIL*) is given by:

$$(10) \quad cIL = \frac{dmIL}{mIL + wB + mw}$$

The biomass concentration in the liquid phase (*cB*) is given by:

$$(11) \quad cB = \frac{dmB}{mIL + wB + mw}$$

The required IL dry mass (*dmIL*) to a given *cIL*, *cB*, and biomass dry mass load (*dmB*) can be deduced by analogy of the deduction of equation (4) as described previously:

$$(12) \quad dmIL = \frac{[cIL] \times dmB}{cB}$$

The IL and sulfuric acid molar contents (*nIL* and *nsa*) are given by the ratio of their masses (*dmIL* and *msa*) to their respective molar masses (*MMIL* and *MMsa*):

$$(13a) \quad nIL = \frac{dmIL}{MMIL}$$

and

$$(13b) \quad nsa = \frac{msa}{MMsa}$$

If nIL is equal to nsa , then (13a) = (13b) and msa can be derived after rearrangement;

$$(14) \quad msa = \frac{dmIL}{MMIL} \times MMsa$$

The sulfuric acid mass (msa) is the product of the mass of the sulfuric acid solution ($msasol$) to the concentration of sulfuric acid in the solution ($csas$):

$$(15) \quad msa = msasol \times csas$$

Substituting equations (12) and (15) into (14), $msasol$, the mass of sulfuric acid that gives the same IL molar content can be derived:

$$(16) \quad msasol = \frac{dmB}{cB} \times \frac{cIL}{MMIL} \times \frac{MMsa}{csas}$$

However, it is also desired that the IL and sulfuric acid concentrations in the reaction mixture (cIL and $csar$) are the same. The $csar$ is given by the expression:

$$(17) \quad csar = \frac{msa}{msasol + wB + mw}$$

Substituting equation (15) into (17) and making $csar = cIL$, the mass of water needed to satisfy this condition can be calculated by:

$$(18) \quad mw = msasol \times \left(\frac{csas}{cIL} - 1 \right) - wB$$

However, the biomass concentration no longer holds, and it must be recalculated by the expression:

$$(19) \quad cfB = \frac{dmB}{msasol + wB + mw}$$

Where cfB is the final biomass concentration in the reaction mixture. To calculate their respective mass fractions, the term wB must be replaced by mB , the mass of biomass, in equations (10), (11), (17) and (19).

Once the initial conditions are set, the amount of sulfuric acid solution and water needed to satisfy the conditions of equal molar content and concentrations can be calculated by these formulae however, it is not possible to keep the same biomass concentration. This approach differs from those previous works, where similar biomass load and concentrations of IL and sulfuric acid or similar biomass load and presumed $[H^+]$ concentrations were kept [19,20].

Sugar, furans and acetic acid analysis

The composition of the liquid stream of the IL or sulfuric acid treated biomass was determined by HPLC. Glucose, xylose, arabinose, acetic acid, furfural, and 5-HMF were identified against standards and quantified by the construction of standard analytical curves in the range of 0.5 to 20.0 g/L for glucose, xylose, and arabinose, 0.5 to 3.0 g/L for acetic acid, and 0.1 to 4.0 g/L for furfural and 5-HMF. HPLC analyses were performed using an Agilent Technologies Liquid Chromatographer 1100 Series System (Santa Clara, CA, USA) equipped with a diode

array for furans and refractive index detectors for organic acids and monosaccharides. It was used with an Aminex HPX-87H column (Bio-Rad, USA) in combination with a cation H⁺-guard column (Bio-Rad, USA). Elution was performed with H₂SO₄ 5 mmol·L⁻¹ at 50°C with a flow rate of 0.6 mL·min⁻¹ for liquors obtained by the biomass treatment with IL and dilute acid and a flow rate of 0.4 mL·min⁻¹ for the analysis of total acidic hydrolysates.

Calculation of the relative composition of the liquid phase

The relative composition regarding the glucose, pentose, furans and acetic acid mass contents was calculated using formulas (20) and (21). Firstly, the normalized mass content of each component (*C_i*) was calculated by dividing the component mass content (*m_i*) by the amount of dry biomass used (*dmB*). Its relative amount (*R_i*) was calculated by dividing it by the sum of the normalized content of each component, automatically by the MS Excel software.

$$(20) \quad C_i (\text{wt. \%}) = 100 \times \frac{m_i}{dmB_i}$$

$$(21) \quad R_i (\%) = 100 \times \frac{C_i}{\sum C_i}$$

Polysaccharide hydrolysis yield, furans and acetyl yields calculation

Polysaccharide hydrolysis yields were calculated using formulas (22) and (23) for glucan and arabinoxylan, respectively, where YG is the glucan hydrolysis yield (Glucose yield), Gb is the glucan content in the dry biomass, YAX is the arabinoxylan hydrolysis yield (Pentose yield), AXb is the arabinoxylan content in the dry biomass, and 90 and 88 are factors representing the conversion of sugar content into its respective polysaccharide equivalent.

$$(22) \quad YG(\text{mol}\%) = \frac{m_{\text{glucose}}}{dmB} \times \frac{90}{Gb}$$

$$(23) \quad YAX(\text{mol}\%) = \frac{(m_{\text{arabinose}} + m_{\text{xylose}})}{dmB} \times \frac{88}{AXb}$$

Furans and acetyl production yields were calculated similarly according to formulas (24), (25) and (26), where YHMF, YF, YAc are the respective yields of 5-HMF, furfural, and acetyl production. The numbers 128.7, 137.3 and 71.7 are conversion factors relating furans and acetic acid to their corresponding polysaccharide equivalent. Acb is the biomass acetyl content.

$$(24) \quad YHMF(\text{mol}\%) = \frac{m_{HMF}}{dmB} \times \frac{128.7}{Gb}$$

$$(25) \quad YF(\text{mol}\%) = \frac{m_{\text{furfural}}}{dmB} \times \frac{137.3}{AXb}$$

$$(26) \quad YAc(\text{mol}\%) = \frac{m_{HAc}}{dmB} \times \frac{71.7}{Acb}$$

Results

Biomass Composition

Sugarcane bagasse composition, with a humidity of 5.8±0.6 wt.%, was as follows: 36.9±0.5 wt.% glucan, 22.1±0.3 wt.% xylan, 2.6±0.2 wt.% arabinosyl group (corresponding to 24.7 wt.% arabinoxylan), 3.9±0.5 wt.% acetyl groups, 21.8±0.2 wt.% lignin, 4.5±1.1 wt.% ash, and 8.2 wt.% of others (all data on a dry weight basis).

Table 2. Composition of the liquid phase resulting from sugarcane bagasse treatment with [EMIM][HSO₄] or dilute H₂SO₄ at 125°C for 83 minutes at the indicated catalyst and biomass mass fractions and of control experiments without catalyst at three representative biomass mass fractions. Results are presented as gram of the component per 100 g of treated dry biomass and show at least, one significative algorism. *Source: Authors results.*

Catalyst	Catalyst mass fraction (wt.%)	Biomass mass fraction (wt.%)	Component content (wt.% dry biomass)					
			Glucose	Xylose	Arabinose	Furfural	5-HMF	Acetic Acid
[EMIM][HSO ₄]	0.0	10.9	0.2	0.07	0.2	0.00	0.00	0.14
	0.0	5.7	0.2	0.07	0.2	0.00	0.00	0.11
	0.0	3.9	0.2	0.06	0.2	0.00	0.00	0.10
	6.2	9.0	0.3	6.6	1.6	0.02	0.01	2.3
	6.5	5.3	0.3	6.8	1.6	0.03	0.02	2.4
	41.0	3.8	1.2	17.5	2.0	0.5	0.02	4.2
	44.6	10.7	1.0	15.5	1.9	0.4	0.02	4.1
	46.4	7.2	0.9	16.3	2.0	0.3	0.02	4.2
	64.1	5.9	1.3	15.8	2.0	0.8	0.03	4.0
	68.5	6.3	1.3	15.1	2.0	1.0	0.04	4.1
	73.6	6.7	1.2	14.1	1.9	0.7	0.03	4.1
	78.0	7.2	1.1	12.9	1.6	1.1	0.04	3.9
	85.2	8.9	1.0	7.5	1.4	3.4	0.08	2.1
H ₂ SO ₄	5.6	16.1	3.3	20.4	2.4	1.5	0.03	4.3

Liquid phase composition and hydrolysis yield

Composition of the liquid phase resulting from sugarcane bagasse treatment with [EMIM][HSO₄] or dilute H₂SO₄ at 125°C for 83 minutes at different catalyst and biomass mass fractions and that of control experiments without catalyst at three representative biomass mass fractions are shown in Table 2, and their relative composition in Figure 1. Table 3 shows the polysaccharide hydrolysis yields, and the furans and acetic acid production yields. Treatments without catalysts resulted in a low overall sugar content in the liquid phase with predominance of arabinose and glucose regardless the biomass mass fraction (Figure 1 and Table 2). Moreover, as their hydrolysis yields were very low (Table 3), it suggests that no auto-hydrolysis occurred at any biomass concentration, and probably that, these solubilized sugars are extractives components or hemicellulose labile structures. Quantitative acidic hydrolysis of these liquid fractions showed no further increment in the sugars content, suggesting the absence of extracted oligosaccharides.

Glucose and 5-HMF

Regarding glucose and 5-HMF, it was observed in the IL reaction mixtures a low glucose content and negligible degradation into 5-HMF whose maximal yield was of 0.3 mol% at IL mass fraction of 85.2 wt.%. The glucose mass content corresponded to 0.3 wt.%, (yield of 0.8 mol%) at IL mass fractions of 6.2 and 6.5 wt.%, increased to 1.3 wt.% (yield of 3.2 mol%) at IL mass fraction 68 wt.% and declined as the IL mass fraction increased. Glucose contributed to the range of 3.0 to 6.4% of the total solute mass, increasing its contribution as the IL mass fraction increased, reaching its highest value of 6.4% for the IL mass fraction of 85.2 wt.%. When treated with dilute sulfuric acid, glucose mass content was of 3.3 wt.% (yield of 8.0 mol%) and contributed to 10.3% of solute's total mass. The liquid phase resulting from dilute acid treatment presented 2.5-fold more glucose than those resulting from IL treatment. Negligible amounts of 5-HMF were formed for the biomass treatment with either [EMIM][HSO₄] or dilute sulfuric acid. The results indicate that the liquid phase obtained from dilute acid treatment is at least 1.6-fold richer in and contains at least 2.5-fold more glucose than those obtained from IL treatment.

Acetic Acid

The acetic acid mass contents and production yields in the liquid phase increased substantially in the presence of 6.2 wt.% of IL, from 0.10 wt.% (1.8 mol%) to 2.3 wt.% (41.8 mol%), rose to 77.2 mol% at 41.0 wt.% of IL, peaked at 46.4 wt.% of IL (78.5 mol%) and started to decrease slightly as the IL mass fraction increased. The mass contribution in the liquid phase was relatively constant (20%), and the acetic acid content increased contribution

in the liquid phase was relatively constant (20%), and the acetic acid content increased proportionally to the increase of all other components. At 85.2 wt.% IL its mass content, production yield and mass contribution decreased sharply, suggesting mass loss due to degradation or vaporization. When treated with 5.6 wt.% sulfuric acid, the acetic acid yield was as high as those obtained for treatment with IL at 46.4 wt.% but with a mass contribution of 13.5% against 17.9%, probably due to the increased pentose and glucose yields (Tables 2 and 3 and Figure 1).

Table 3. Glucan and hemicellulose hydrolysis yields after sugarcane biomass treatment with [EMIM][HSO₄] for 83 min at 120°C at several IL and biomass mass fractions. Biomass treatment with dilute H₂SO₄ at the same conditions are shown for comparison. Sugar, acetyl and furans yields were calculated as described in Materials and methods. *Source: Authors results.*

Catalyst	Catalyst mass fraction (wt.%)	Biomass mass fraction (wt.%)	Component hydrolysis yield (mol%)						
			Glucose	5-HMF	Xylose	Arabinose	Pentoses	Furfural	Acetyl group
[EMIM][HSO ₄]	0.0	10.9	0.4	0.0	0.3	8.2	1.1	0.0	2.7
	0.0	5.7	0.5	0.0	0.3	7.2	1.0	0.0	2.0
	0.0	3.9	0.4	0.0	0.2	6.9	1.0	0.0	1.8
	6.2	9.0	0.8	0.1	26.1	53.9	29.1	0.1	41.8
	6.5	5.3	0.8	0.1	27.2	52.7	29.9	0.2	45.0
	41.0	3.8	2.8	0.1	69.8	68.4	69.6	2.9	77.2
	44.6	10.7	2.3	0.1	61.9	64.0	62.1	2.1	75.1
	46.4	7.2	2.3	0.1	64.9	68.0	65.3	1.4	78.5
	64.1	5.9	3.1	0.1	62.8	67.8	63.3	4.2	74.8
	68.5	6.3	3.2	0.1	60.3	67.2	61.0	5.6	76.4
	73.6	6.7	2.8	0.1	56.3	63.1	57.1	3.9	75.4
	78.0	7.2	2.6	0.1	51.2	54.5	51.6	6.1	72.2
	85.2	8.9	2.4	0.3	29.9	48.0	31.8	18.7	38.4
H ₂ SO ₄	5.6	16.1	8.0	0.1	81.3	79.4	81.1	8.6	79.8

Pentoses and furfural

In the presence of 6.2 and 6.5 wt.% of IL (biomass concentrations of 9.0 wt.% and 5.3 wt.%), the pentose mass content showed a considerable increase when compared to treatment in the absence of catalyst, from 0.3 to 8.4 wt.%. Its yield reached 29.1 mol%, with negligible 0.1-0.2 mol% furfural yield. Maximal arabinoxylan conversion of 72.5 mol% (the sum of pentose and furfural yields) was observed upon increasing the IL concentration to 41.0 wt.% (biomass concentration of 3.8 wt.%), corresponding to a 2.4-fold increase relative to the previous treatment condition. The treatment also resulted in a pentose yield of 69.6 mol% and low furfural production of 2.9 mol% with corresponding mass contents of 19.5 and 0.5 wt.%. Treatments at IL concentration in the range of 41.0 to 46.4 wt.% resulted in similar pentose and arabinoxylan conversion yields, around 65.7 and 67.8 mol%, respectively. Furfural production at these IL concentrations showed a decrease of 33.3% with a final yield of 1.4 mol%.

The use of IL at concentrations in the range of 64.1 to 68.5 wt.% resulted in a steady decrease in pentose yield, reaching values found for treatments at IL concentration of 44.6 wt.%. This was accompanied by an increase in the furfural production, which resulted in similar arabinoxylan conversion. A further increase in IL concentration, from 68.5 to 78.0 wt.%, resulted in a sharp decrease in the pentose yield whereas the furfural yield increased reaching a final value of 6.1 mol% at IL concentration of 78.1 wt.%. Despite that, the sum of both components decreased continuously. The increment of IL from 78.0 to 85.2 wt.%, which corresponded to a water concentration of only 5.8 wt.%, had a dramatic effect on pentose and furfural production yields. Pentose yield decreased 38.4% to a final value of 31.8 mol%, and furfural yield increased sharply, reaching a final value of 18.7 mol%, however, the sum of both components yields decreased further 12.5% at the same rate. This increase of furfural yield occurred despite the increase of 41.3% in the biomass concentration; at IL 41-46 wt.% the increase in biomass concentration was followed by a decrease in the furfural production yields (Tables 2 and

3). The pentose relative mass contribution followed somewhat the same trend of pentose yield. Maximal values were observed at IL mass fraction of 41-46.4 wt.%, then it decreased steadily as the IL mass fraction increased and decreased sharply when the IL increased from 78.0 to 85.2 wt.%. However, the sum of pentose and furfural relative mass contributions showed a different pattern of their corresponding sum of yields, it remained relatively constant since the decrease in pentose mass contribution was accompanied by an increase of furfural relative mass contribution. These results suggest that at IL concentrations higher than 78.0 wt.% a considerable fraction of hydrolyzed pentose undergoes further conversion to furfural. Treatment of sugarcane bagasse with dilute sulfuric acid resulted in 89.7 mol% arabinoxylan conversion, 81.1 mol% pentose, 8.0 mol% glucose, and 8.6 mol% furfural production yields, as well as negligible 5-HMF production. The pentose relative mass contribution to the liquid phase was 71.2% whereas furfural was 4.8%. The arabinoxylan conversion and pentose yields when compared with those obtained after biomass treatment with a similar concentration of [EMIM][HSO₄], were 3.0 and 2.7-fold higher, respectively, and extremely higher for furfural production yield. Comparing with the results obtained by treating biomass with IL at concentrations ranging from 44.6 to 46.5 wt.%, where arabinoxylan hydrolysis yield was 65.3 mol%, the pentose content in the dilute acid hydrolysate was 24.3 to 30.6% higher. However, the amount of furfural produced was also 4 to six-fold higher resulting in a liquid stream 3.0 -4.4-fold richer in furfural and around 7.0% poorer in pentoses. Therefore, the pentose/furfural yield ratio was 4.0-fold higher, and the pentose/glucose ratio was 2.7-fold higher in the syrup obtained after IL biomass treatment, showing a greater specificity of IL hydrolysis towards hemicellulose. Thus, although the pentose content was 24.3 to 30.6% higher using the dilute acid treatment, the syrup obtained by treating biomass with [EMIM][HSO₄] at these concentrations contains a considerable amount of free pentose and much less contamination with glucose and the sugar degradation products. As the IL concentration increases and the pentose yields and relative mass contribution decreases whereas those of furfural increase, the pentose/furfural ratios decrease accordingly. The pentose content is 28-42% higher and the furfural content present at dilute acid hydrolysate is twice of that present in the hydrolysate of IL 64-73.6 wt.%. Nevertheless, the pentose mass contribution was similar in both treatments, but the furfural contribution was 1.5 times higher in the dilute acid treatment, and consequently the pentose/furfural ratio was still 1.6 higher in the IL syrup. A comparison of biomass treated with dilute H₂SO₄ and with IL at concentrations near 78.0 wt.% shows that, although the yield of free pentose at this IL concentration had decreased to 51.6 mol% (a yield 1.6 times lower than that obtained by dilute acid treatment), it still displayed a selectivity towards hemicellulose. The pentose/glucose yield ratio was twice that obtained by dilute acid treatment. However, given that the conversion of pentose into furfural increased at these IL concentrations, the pentose/furfural yield ratios were comparable. These results clearly indicate that the syrup obtained by treating biomass at these IL concentrations is enriched not only with pentose but also with large amounts of furfural, albeit 29% less furfural than was obtained with dilute acid treatment, its relative mass contribution is similar in both treatments. At the highest IL concentration, the pentose yield was 20.6% lower and furfural production yield was twice that obtained with dilute acid treatment, and the ratio of pentose/furfural was 5 times lower. However, the yield ratio of pentose/glucose was still 1.3 times higher than that obtained with dilute acid treatment. These results suggest that at these [EMIM][HSO₄] concentrations a syrup enriched with pentoses, and furfural can be obtained with low glucose and 5-HMF contamination, which allows for improvements to the furfural production process.

Characterization of residual biomass

▪ Solids yield

The solid yields, compositions, and polysaccharide contents from the IL and dilute sulfuric acid treatments are shown in Table . IL treatments in the range of 6.2 and 6.5 wt.% resulted in a similar yield of 81.4 wt.% indicating a 18.6% biomass dissolution despite their low yields (Tables 2 and 3). These yields were 24.6% higher in comparison to that for the sulfuric acid treatment at similar concentration which corresponded to 46.3% less biomass dissolution. The solids yield decreased steadily in response to the IL concentration increase up to 64.1 wt.% and fluctuated around values near 70.8 wt.% which were approximately 8.4% higher in comparison to that for dilute sulfuric acid treatment, showing that biomass treatment with 5.6 wt.% dilute sulfuric acid extracted more biomass than the highest IL at its highest concentration. Comparing the solids yields in Table 4 with the sum of the quantified components in the liquid streams in Table 2, after correction to their glycosyl or acetyl equivalent, it is found that the sum of the quantified components is smaller than the expected value suggested by the solid yields. At 6.2-6.5 wt.% IL concentration the quantified values were 50% less than expected. At 41.0-46.4 wt.% IL and dilute H₂SO₄ they were on average 19% less. At 64.1-78.0 wt.% IL they were 34% less, and at 85.2 wt.% IL they were 45% less. The reasons for these discrepancies can be partial hydrolysis with soluble oligosaccharide production (as might be the case for biomass treated at 6.2-6.5 wt.% IL), product degradation into either non quantified or volatile compounds (such as formic and levulinic acids, and CO₂) [26] that were lost

by vaporization, especially for those treatments with dilute sulfuric acid or with high IL concentrations.

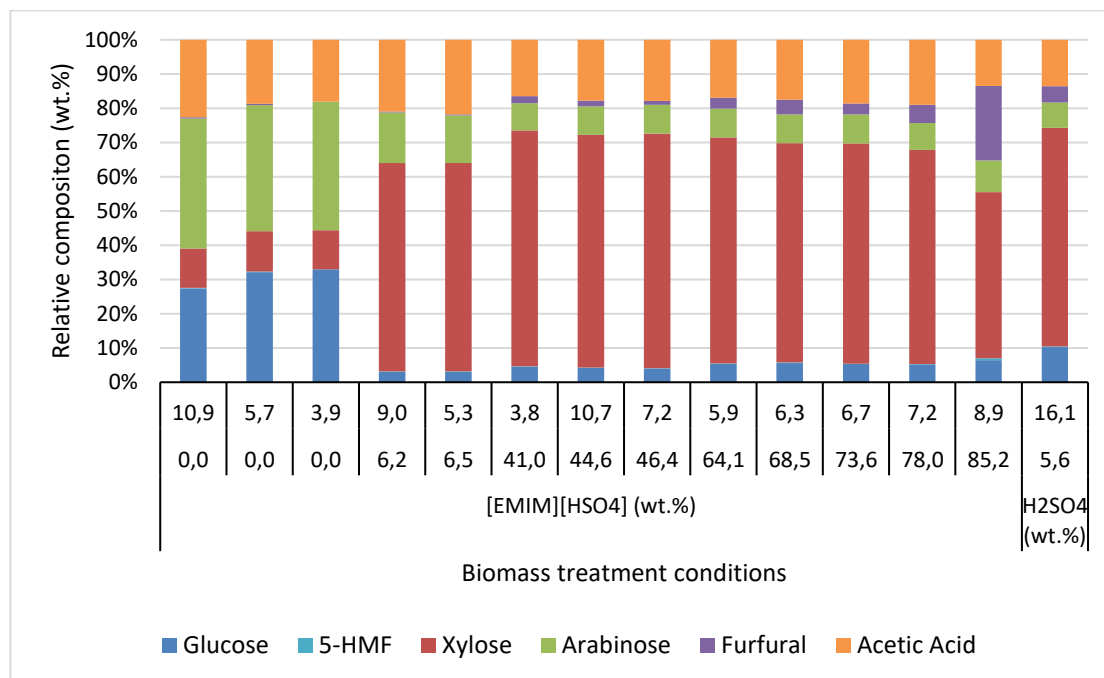


Figure 1. Relative composition of the liquid phase after sugarcane biomass treatment with [EMIM][HSO₄] or H₂SO₄ at the indicated conditions. The total component contents were set as 100% and each component relative content was calculated. In the horizontal axis, the upper values represent biomass mass fractions (wt.%) and the lower values, the catalyst mass fraction (wt.%). *Source: Authors results.*

▪ Glucan content

The polysaccharide content composition in the solids obtained after biomass treatment somewhat reflected the polysaccharide hydrolysis yield of the liquid phase. In all treatments there was an enrichment in glucan, lignin and ashes and impoverishment in xylan, arabinan and acetyl (Table 4). The glucan content, compared to the original biomass, enriched 18.7% by treating the biomass with 6.2-6.5 wt.% IL, reaching its maximal value of 38% enrichment at IL concentrations of 41.0 and 64.1 wt.% with respective biomass mass fractions of 3.8 and 5.9 wt.%. Treatments with IL in the range of 46.4-68.5 wt.% showed an average enrichment of 33.6% with corresponding 49.3 wt.% glucan. Treatments at IL concentrations higher than 68.5 wt.% resulted in a slow and steadily decrease in the glucan content with a final content of 47.8 wt.%, at IL concentration of 85.2 wt.%, corresponding to an enrichment of 29.0%. Solid residues obtained after biomass treatment with dilute sulfuric acid were 42.7% enriched in glucan with a content of 52.6 wt.%. These solids were from 3.4 to 20.4% richer in glucan than the solids obtained from IL, despite its higher glucan hydrolysis yield (Table 3).

▪ Lignin and ashes content

Although the contents of ashes and lignin increased in the solids obtained from biomass treatment with IL, there were no clear trends as the IL concentration increased. The lignin content in the solids averaged in 26.1 wt.% corresponding to an enrichment of 19.7%, nevertheless, they were 19.4% poorer in lignin when compared to the diluted acid treatment, in which the lignin content was 32.4 wt.%, an enrichment of 48.6%. This higher content may be the result of sugar decomposition, molecular condensation, and precipitation as nonhydrolyzable material. The ashes content in the solids obtained from biomass treatment with IL averaged in 7.8 wt.% an enrichment of 75.3% which was very similar to those obtained with 5.6 wt.% sulfuric acid treatment.

▪ Acetyl Content

The acetyl content diminished in the solids obtained from all biomass treatments, especially those treated with 5.6wt.% sulfuric acid where its content decreased 91.8%. Solids obtained from biomass treated with IL at 6.2 – 6.5 wt.% showed a decrease of 44.1% whereas those from biomass treated with IL at 41.0-85.2 showed an average decrease of 71.7%. The acetyl content in the solids at these IL concentrations was relatively constant and averaged in 1.1 wt.%, suggesting that at IL concentrations above 41.0 wt.% the hemicellulose hydrolysis achieved its maximum efficiency. Compared with the sulfuric acid treatment, the solids were in average, 6.8-fold

richer, for IL concentrations at 6.2-6.5 wt.%, and 3.4-fold richer for IL concentrations at 41.0-85.2 wt.% indicating a higher efficiency of dilute sulfuric acid to hydrolyze hemicellulose.

▪ Arabinoxylan content

Solids obtained from sulfuric acid treated biomass diminished 86.8% their arabinoxylan content when compared with the original biomass, whereas solids obtained from IL treated biomass decreased on average 17.9% at IL concentrations in the range of 6.2-6.5 wt.% and 42.5% for IL concentrations in the range of 41.0 to 73.6 wt.%, from then on, its content decreased continuously to a final decrease of 48.8% at IL concentration of 85.2 wt.%. These results show that the arabinoxylan hydrolysis efficiencies were relatively constant at IL concentrations between 41.0 to 73.6 wt.% and increased as the IL concentration increased further but decreased if the IL concentration was low. Compared to the sulfuric acid treatment, the arabinoxylan contents in the solids obtained from IL treatments were 4 to 5.5-fold higher indicating a far greater hydrolytic capacity of dilute sulfuric acid over IL.

Table 4. Solid yield and composition after sugarcane biomass treatment with [EMIM][HSO₄] for 83 min at 120°C at the indicated IL and biomass mass fractions. Biomass treatment with dilute H₂SO₄ at the same conditions are shown for comparison. *Source: Authors results*

Catalyst	Catalyst mass fraction (wt.%)	Biomass mass fraction (wt.%)	Component content in solids (wt.%)								Solid Yield (wt.%)
			Glucan	Xylan	Arabinan	Arabinoxylan	Acetyl	Lignin	Ashes	Others	
[EMIM][HSO ₄]	0.0	10.9	38.9	21.7	2.0	23.7	4.0	23.2	4.5	5.8	101.1
	0.0	5.7	40.0	22.4	2.4	24.8	4.1	21.9	2.6	6.6	101.0
	0.0	3.9	39.8	21.9	2.2	24.1	4.1	20.1	3.9	8.0	101.2
	6.2	9.0	43.9	16.2	1.7	18.0	2.2	26.5	9.1	0.3	82.1
	6.5	5.3	43.7	15.8	1.9	17.7	2.1	25.4	8.9	2.2	80.7
	41.0	3.8	50.9	13.7	1.3	14.9	1.2	25.8	5.6	1.5	74.3
	44.6	10.7	47.3	12.5	1.2	13.7	1.2	23.8	11.1	3.0	75.4
	46.4	7.2	49.1	12.9	1.0	13.9	1.2	24.7	8.3	2.9	73.2
	64.1	5.9	50.9	12.9	1.2	14.1	1.0	25.8	4.6	3.6	69.4
	68.5	6.3	49.4	12.5	2.1	14.6	1.2	28.4	5.7	0.7	68.4
	73.6	6.7	48.5	13.1	1.0	14.1	1.0	28.3	4.6	3.6	70.9
	78.0	7.2	47.6	12.2	1.0	13.3	1.1	28.2	7.7	2.2	72.8
	85.2	8.9	47.8	11.7	1.0	12.7	1.1	24.4	12.4	1.7	72.5
H ₂ SO ₄	5.6	16.1	52.6	2.5	0.7	3.2	0.3	32.4	7.9	3.5	65.3

Polysaccharide recovery

The recovery of the constituents was analyzed after calculating their yields in the solid residue and plotted against their yields and of their degradation products (furfural or 5-HMF) in the liquid phase.

Glucan recovery

The residual glucan yield fluctuated around 98 mol% up to an IL concentration of 46.5 wt.%, and then it decreased slightly up to an IL concentration of 68.5 wt.%, whereupon it fluctuated around 94 mol%, which also coincided with a decrease in its content in the solids (Table 4). When added to its and of 5-HMF yields in the liquid phase, the glucan recovery in the biomass treated with no catalyst was higher than 100 mol%, near 107.5 mol%. That might be the result of an overestimation of the glucan content in the solids. Glucan recovery for biomass treated with either 5.6 wt.% sulfuric acid or IL in the range of 6.2 – 64.1 wt.% was near 100 mol%, showing that at IL concentrations where the hydrolysis yields were the greatest (Table 3), there was no glucan loss. At higher IL concentrations the recovery oscillated near 96.1 mol% that might be the result of degradation into non quantified products. Nevertheless, results show a high glucan recovery in all biomass treatments and a greater contribution of hydrolyzed glucan at IL concentration in the range of 41.0 – 86.2 mol%. They also show a much greater hydrolyzed glucan in diluted sulfuric acid treated biomass, despite an obtained solid richer in glucan (Figure 2 and Table 4).

Arabinoxylan recovery

At IL concentration of 6.2 wt.%, 60 mol% of the biomass arabinoxylan remained in the solid. As the IL concentration rose from 46.4 up to 73.6 wt.%, the remaining arabinoxylan fluctuated around 40 mol% and decreased slightly as the IL concentration increased to 78.0 and 85.2 wt.%. Treatments in the range of 41.0 to 68.5 wt.% resulted with total arabinoxylan recovery with results constant near 107.0 mol%. As the IL rose, the recovery dropped with concomitant increase of furfural production yield. At the highest IL concentration, the recovery was 87.7 mol%, representing a 12.3 mol% loss. These indicate that the decrease in the observed pentose yield at the highest IL concentrations (Table 3) was not due to a decrease in the IL hydrolysis efficiency but due to further degradation of pentoses into furfural and into volatile and non-quantified compounds. If the hydrolysis efficiency had decreased under high IL concentrations, the arabinoxylan remained in the solids should have increased, rather than remaining constant in 40 mol%. A recovery of just 88.4 mol% for treatments at 6.2 – 6.5 wt.% IL concentration, and well above the 100 mol% for treatments at 41.0 wt.% IL concentration were observed for reasons not understood (Figure 3). Arabinoxylan recovery for biomass treated with dilute H₂SO₄ was 98.3 mol% showing almost a complete recovery of all biomass arabinoxylan. Its content in the residual solid was only 8.6 mol%, most of it was in the liquid phase either as hydrolyzed pentose or as furfural (Figure 3) explaining why the solid was so enriched in glucan (Table 4) despite the higher glucan hydrolysis yield (Table 3).

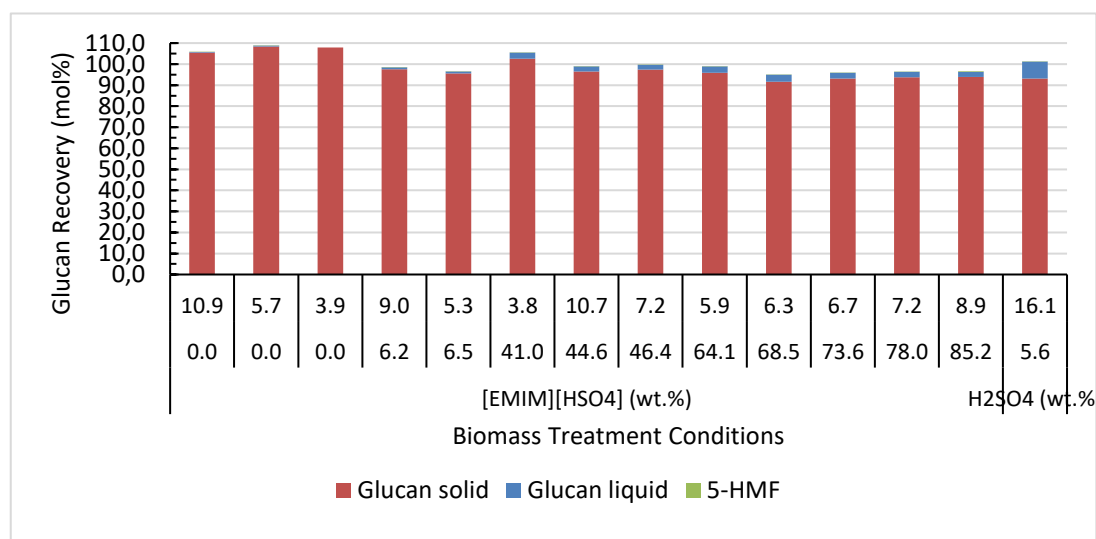


Figure 2. Glucan recovery after biomass treatment at different ionic liquid (upper line) and biomass (lower line) concentrations. Biomass treated with diluted sulfuric acid are shown for comparison. Biomass treatment conditions were as described in materials and methods. *Source: Authors results*

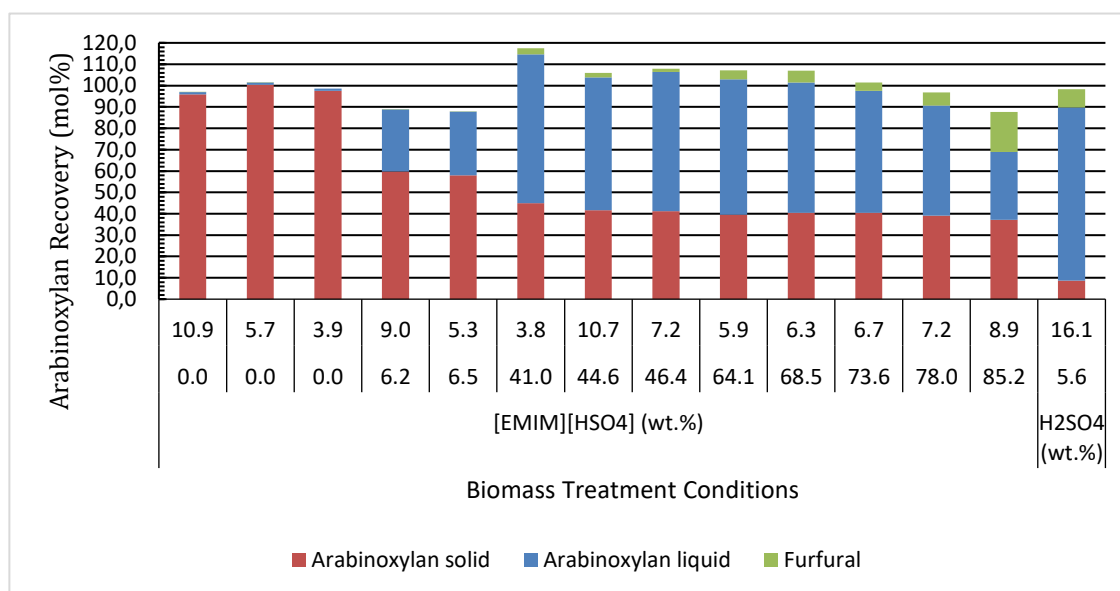


Figure 3. Arabinoxylan recovery after biomass treatment at different ionic liquid (upper line) and biomass (lower line) concentrations. Biomass treated with diluted sulfuric acid are shown for comparison. Biomass treatment conditions were as described in materials and methods. *Source: Authors results*.

Acetyl recovery

The acetyl group remaining in the solid residues showed the same trend observed for arabinoxylan, oscillating around 22.6 mol% in the IL concentration range of 41.0-46.4 wt.% and then around 19.1 mol% at IL concentrations of 64.1-85.2 wt.%, further suggesting that at high IL concentration there was no decrease in its hydrolysis efficiency (Figure 4). The acetyl recovery was almost complete at IL concentrations where the pentoses hydrolysis yield were the highest (Table 3). It showed a slight decrease to values near 93.6 mol% at 64.1-78.0 wt.% IL and decreased considerably to 58.3 mol% at the highest IL concentration, showing a high acetyl loss at this treatment condition. Biomass treated with dilute sulfuric acid resulted in solids with only 5.4 mol% acetyl group, four times lower than those obtained with IL, which indicates the higher hydrolytic efficiency of dilute sulfuric acid towards hemicellulose. Most of the acetyl group was in the liquid phase, yet the acetyl recovery was 85.2 mol% suggesting a 14.8 mol% of acetyl loss.

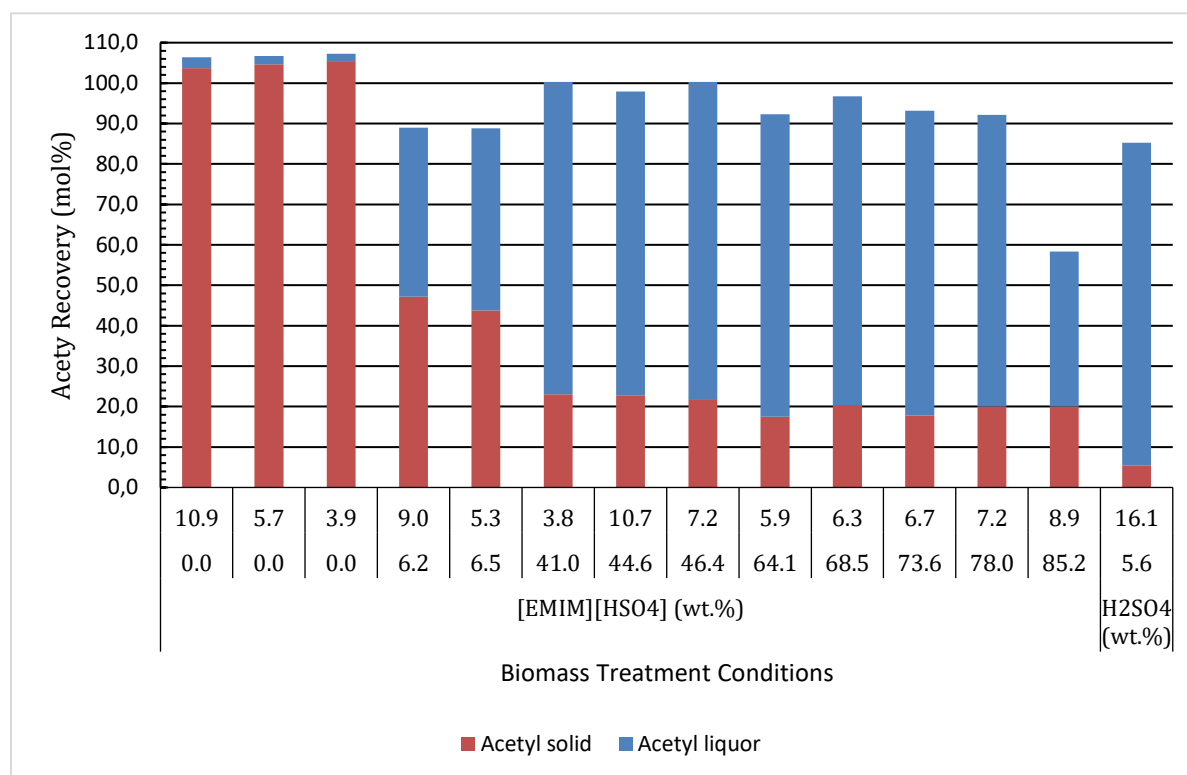


Figure 4. Acetyl recovery after biomass treatment at different ionic liquid (upper line) and biomass (lower line) concentrations. Biomass treated with diluted sulfuric acid are shown for comparison. Biomass treatment conditions were as described in materials and methods. *Source: Authors results.*

Discussion

This study compared the uses of [EMIM][HSO₄] and diluted sulfuric for the treatment of sugarcane biomass. Sugarcane biomass was treated at several IL and biomass fractions, or with diluted sulfuric acid with the same mass concentration and molar content used for the lowest IL concentration. Such condition was met by iterative calculations as demonstrated in section sulfuric acid, water, and biomass content calculations. Sugarcane biomass treated with IL up to 44.6 wt.% produced a syrup highly enriched in pentose with minimal contamination of glucose and furans. As the IL concentration increased, the furfural production yield increased concomitantly to the pentose yield decrease, resulting in a syrup with a high mass proportion of furfural, specially at the highest IL concentration. Furthermore, the pentose recovery decreased with the increase of the IL concentration, but at these higher IL concentrations, the arabinoxylan and acetyl contents in the solid were essentially the same of those found at 44.6 wt.% IL (Table 4), where the maximum pentose yield was obtained in the syrup, indicating that the observed decreased of the pentose yield at these high IL concentrations, consequently low water content, was not due to a lower IL hydrolysis efficiency, but due to further degradation of pentose and furfural into non quantified or volatile products. At very low water content, acidic ionic liquids tend to form degradation products along with biomass, particularly if treatment conditions are very severe [27,28]. Similar results were also found by da Costa Lopes et al. [16] when treating wheat straw with [EMIM][HSO₄] at different IL concentrations and temperatures. High pentose yields were obtained at moderate treatment severity with similar IL concentration and water content. At higher treatment severity, furfural yields rose to values near 30

butyl-3-methylimidazolium hydrogen sulfate [BMIM][HSO₄], where lignocellulosic biomass treatment at moderate IL concentrations results in hemicellulose hydrolysis near 40% with negligible furfural co-production [29]. Furfural production with yields in the range of 13-33% was favored when biomass was treated at low water content [14,17], especially when treated with superacidic ionic liquids [12]. Despite this, when biomass is treated with acidic ionic liquids, a syrup enriched with free pentoses and a cellulose-enriched solid are obtained. This solid is prone to enzymatic hydrolysis [16,30,31], and its hydrolysis yield is superior to that which results from treating biomass with dilute acid [32]. As compared with IL treatment, dilute acid treatment resulted in a solid residue not only enriched with but possessing a higher glucan content and far less arabinoxylan content (Table 4), making it an obvious substrate to produce glucose syrups via enzymatic hydrolysis, since dilute acid pre-treated biomass is more prone to enzymatic hydrolysis than the nontreated ones [33]. The hemicellulose hydrolysis yield (Table 3) and the pentose content in the resulting syrup were also higher (Table 2), and since the costs in using dilute sulfuric acid are much less than using ionic liquid, one may ask why ionic liquids should be used to treat lignocellulosic biomass after all. The reasons are many, despite the hemicellulose hydrolysis yield (Table 3) and the amount of free pentoses in the resulting syrup were smaller, they were significant at 41.0 to 64.1 wt.% IL concentration (Table 2). They were also richer in free pentoses and far less contaminated with glucose and furans, therefore treatments with IL result in a liquid stream with concentrated and purer free pentoses. It could also be argued that the higher amount of glucose and furans in the syrups obtained by treating sugarcane biomass with dilute sulfuric acid was due to the concentration used, 6.7 wt.% with a corresponding mass fraction of 5.6 wt.%. The acidic strength of H₂SO₄ is much stronger than that of HSO₄⁻, which pK_a at room temperature is 1.9, consequently the H⁺ molar content, in the sulfuric acid treatment would be equimolar to H₂SO₄ whereas in the IL treatment it would be less than HSO₄⁻ molar content. In fact, treatment of *Sorghum* biomass with 0.2 mol/L (approximately 2 wt.%) sulfuric acid at 121°C for 120 min [26], resulted in free pentose and furfural production yields close to those found by treating sugarcane biomass with IL in the range of 41-46.4 wt.%, however despite the temperature used was near of that used in this study, it took to 37 minutes longer to reach similar free pentose yield found in this study. High free pentose yields when treating lignocellulosic biomass with sulfuric acid with concentrations of 2 wt.% or less are achieved only at long treatment times or high temperatures but in this case, the furfural and glucose yields are similar to those found at this study [32]. When biomass of Bamboo was treated with 0.2 mol/L sulfuric acid for 2h the glucose production yield was not much different of that found when treated with 0.6 mol/L sulfuric acid, a concentration close to the one used in this work, besides the glucose production yield was also very near to that found at this work [32] (Table 3). Therefore, biomass treatment with dilute sulfuric acid in concentrations below or near 2wt.% must be performed at high temperatures and long times to achieve high hydrolysis yield. Acidic IL despite having lower acidic strength, its organic cation moiety interaction with biomass increases considerably its hydrolysis efficiency [18,19,34] explaining the efficiencies found at IL concentration in the range of 41.0-64.1 wt.%. The second reason in using IL against dilute acid is the concentration itself. While biomass can be treated with pure IL or with mixture of IL with very low water content, where some biomass degradation may occur, the same cannot be performed with mineral acids where considerable biomass degradation and loss of yield occur as the concentration increases. In other words, to achieve high hydrolysis yield with low degradation, biomass must be treated with dilute acid resulting in a liquid stream with a very large water content as opposed to IL where high hydrolysis yield can be accomplished with IL at 41-64 wt.% or even higher, resulting in a liquid stream with low water content, in the range 40-60 wt.% or less, which greatly facilitates the recovery of sugars and of the IL itself. The recovery of sugars and IL usually is done by the addition of anti-solvents, and as less water is present in the liquid stream, less anti-solvent and energy shall be required for the separation, thus making the whole process much more environmentally and economically sustainable, provided the IL is recycled. The third reason is the versatility that the acidic IL may offer regarding the desired product simply by tuning the biomass treatment conditions. At the highest IL concentration, a relatively high hemicellulose hydrolysis yield is achieved, and the obtained syrup is highly enriched with furfural. Moreover, furfural can be extracted with a green solvent and the hydrolyzed pentoses can be separated and recovered with considerable purity and the IL recycled [15] processes favored by the low water content. Treatments with dilute H₂SO₄, on the other hand, do not possess such versatility. Despite selectively hydrolyzing hemicellulose at a higher yield, the resulting syrup contains high amounts of glucose, furfural, and high-water content rendering the recovery process more difficult.

Impact

Furans, especially furfural and xylose are compounds of increasing interest, furans are important chemical platform [35] from which several compounds can be synthesized. Xylose is the precursor of furfural and also can be used to produce several other chemicals such as xylitol [36–38]. This increased interest has prompted several investigations in how to obtain these compounds in high yields and in an environmentally sustainable manner from lignocellulosic biomass [36,39–41]. To this end, biomass pretreatments methods applying dilute mineral

acid [36,37,39,42,43], solvolysis and green solvents, among them, molten salts [39], deep eutectic solvents [39,44–46] and ionic liquids [39,47–50] were investigated. Each of these approaches have clear advantages and disadvantages concerning the environmental impact, reusability, and economical feasibility. Nevertheless, the conventional processes still used for furfural production lignocellulosic biomasses are uneconomical since it is produced from a diluted xylose solution, obtained from acid-catalyzed hydrolysis of biomass rich in hemicellulose. Xylose on the other hand, can be recovered after evaporation of the excess of water and the addition of an antisolvent, resulting in an energy-intensive process [36,51]. This work contributes to the state of art of knowledge as it compares two hemicellulose hydrolysis methods: the classical dilute sulfuric acid, and the acidic ionic liquid [EMIM][HSO₄] using a different approach. It indicates that the biomass treatment with acidic IL has many advantages over the dilute sulfuric acid treatment, among them, the use of less water and less solvent to recover the products, xylose and furfural. This work shall contribute to the decision-making and paves the way to the development of new technologies to produce pentoses and furfural of high qualities in a sustainable manner. It is also an UpToDate investigation for the industrial technology still uses diluted acid to produce xylose and furfural, resulting in a diluted solution which is one of the difficulties to their recovery.

Conclusions

The stepwise evaluation of the reaction conditions for the use of the ionic liquid [EMIM][HSO₄] for sugarcane bagasse treatment enabled the identification of reaction conditions for the selective hydrolysis of hemicellulose into xylose with high yields, and at the same time, lessening the dehydration of xylose into furfural, and the release of glucose from the cellulose. In contrast, the use of dilute sulfuric acid results in xylose syrup highly contaminated with furfural and glucose. Unlike the use of sulfuric acid, the use of 1-ethyl-3-methylimidazolium hydrogen sulfate can be tuned either towards the predominant formation of xylose with very low degradation to furfural or towards an increase in furfural production. In both cases, a solid cellulose-lignin residue is obtained that can be further used for the production of glucose syrups via enzymatic hydrolysis. In a biorefinery context, these findings can enable the customized production of either a xylose-rich or a furfural-rich stream.

Author Contributions

Marcoaurélio Almenara Rodrigues contributed to the conception and execution of experiments, the analysis of data, and the writing of this manuscript. Andre M. da Costa Lopes contributed to the conception and execution of experiments, the analysis of data, and to the review and critique of this manuscript. Rafal M. Lukasik contributed to the conception of the scientific problem, the analysis and interpretation of the data, and the critical revision of this manuscript regarding both its coherence and scientific contribution. All authors have given approval to the final version of this manuscript.

Funding Sources

This work, done at the Biomass and Bioenergy Research Infrastructure (BBRI) – LISBOA – 01-0145-FEDER-022059, was supported by the Operation Program for Competitiveness and Internalization (PORTUGAL2020), by the Lisbon Portugal Regional Operation Program (Lisboa 2020), and by the North Portugal Regional Operation Program (Norte 2020) under the Portugal 2020 Partnership Agreement through the European Regional Development Fund (ERDF). Additionally, this research was supported by the Fundação para a Ciência e a Tecnologia (FCT, Portugal) through grants SFRH/BD/90282/2012 (AMdCL) and IF/00471/2015 (RML). This work was also supported by CAPES (Brazil) through the CAPES 371/14, AUXPE Nr 0005/2015, project 23038.002463/2014–98.

Conflict of Interest

There are no conflicts to declare

Acknowledgment

Dr. Marcoaurélio Almenara Rodrigues acknowledges the financial support received through a post-doctoral scholarship from CAPES (Brazil), BEX n° 10189/14-9. The authors also wish to thank Mrs. Maria do Céu Penedo for help in the execution of the HPLC analysis.

References

- [1] A. Pandey, C.R. Soccol, P. Nigam, V.T. Soccol, Biotechnological potential of agro-industrial residues. I: sugarcane bagasse, *Bioresour. Technol.* 74 (2000) 69–80. [https://doi.org/10.1016/S0960-8524\(99\)00142-X](https://doi.org/10.1016/S0960-8524(99)00142-X).
- [2] M.E. Zakrzewska, E. Bogel-Lukasik, R. Bogel-Lukasik, Ionic liquid-mediated formation of 5-

- hydroxymethylfurfural-A promising biomass-derived building block, *Chem. Rev.* 111 (2011) 397–417. <https://doi.org/10.1021/cr100171a>.
- [3] Y. Luo, Z. Li, X. Li, X. Liu, J. Fan, J.H. Clark, C. Hu, The production of furfural directly from hemicellulose in lignocellulosic biomass: A review, *Catal. Today.* 319 (2019) 14–24. <https://doi.org/10.1016/j.cattod.2018.06.042>.
 - [4] L. de F. Vilela, V.P.G. de Araujo, R. de S. Paredes, E.P. da S. Bon, F.A.G. Torres, B.C. Neves, E.C.A. Eleutherio, Enhanced xylose fermentation and ethanol production by engineered *Saccharomyces cerevisiae* strain, *AMB Express.* 5 (2015) 16. <https://doi.org/10.1186/s13568-015-0102-y>.
 - [5] P.J. Du Toit, S.P. Olivier, P.L. Van Biljon, Sugar cane bagasse as a possible source of fermentable carbohydrates. I. Characterization of bagasse with regard to monosaccharide, hemicellulose, and amino acid composition, *Biotechnol. Bioeng.* 26 (1984) 1071–1078.
 - [6] F.M. Girio, C. Fonseca, F. Carvalheiro, L.C. Duarte, S. Marques, R. Bogel-Lukasik, Hemicelluloses for fuel ethanol: A review, *Bioresour. Technol.* 101 (2010) 4775–4800. <https://doi.org/10.1016/j.biortech.2010.01.088>.
 - [7] V. Kumar, P. Binod, R. Sindhu, E. Gnansounou, V. Ahluwalia, Bioconversion of pentose sugars to value added chemicals and fuels: Recent trends, challenges and possibilities, *Bioresour. Technol.* 269 (2018) 443–451. <https://doi.org/10.1016/j.biortech.2018.08.042>.
 - [8] B. Kamm, P.R. Gruber, M. Kamm, Biorefineries—Industrial Processes and Products, *Ullmann's Encycl. Ind. Chem.* (2016) 1–38. https://doi.org/doi:10.1002/14356007.l04_l01.pub2.
 - [9] T. Ståhlberg, W. Fu, J.M. Woodley, A. Riisager, Synthesis of 5-(hydroxymethyl)furfural in ionic liquids: Paving the way to renewable chemicals, *ChemSusChem.* 4 (2011) 451–458. <https://doi.org/10.1002/cssc.201000374>.
 - [10] M.H.L. Silveira, A.R.C. Morais, A.M. Da Costa Lopes, D.N. Oleksyszzen, R. Bogel-Lukasik, J. Andreas, L. Pereira Ramos, Current Pretreatment Technologies for the Development of Cellulosic Ethanol and Biorefineries, *ChemSusChem.* 8 (2015) 3366–3390. <https://doi.org/10.1002/cssc.201500282>.
 - [11] V.T. de O. Santos, G. Siqueira, A.M.F. Milagres, A. Ferraz, Role of hemicellulose removal during dilute acid pretreatment on the cellulose accessibility and enzymatic hydrolysis of compositionally diverse sugarcane hybrids, *Ind. Crops Prod.* 111 (2018) 722–730. <https://doi.org/10.1016/j.indcrop.2017.11.053>.
 - [12] W. Hui, Y. Zhou, Y. Dong, Z.J. Cao, F.Q. He, M.Z. Cai, D.J. Tao, Efficient hydrolysis of hemicellulose to furfural by novel superacid SO₄H-functionalized ionic liquids, *Green Energy Environ.* 4 (2019) 49–55. <https://doi.org/10.1016/j.gee.2018.06.002>.
 - [13] N. Mosier, C. Wyman, B. Dale, R. Elander, Y.Y. Lee, M. Holtzapfel, M. Ladisch, Features of promising technologies for pretreatment of lignocellulosic biomass, *Bioresour. Technol.* 96 (2005) 673–686. <https://doi.org/10.1016/j.biortech.2004.06.025>.
 - [14] A. V. Carvalho, A.M. Da Costa Lopes, R. Bogel-Lukasik, Relevance of the acidic 1-butyl-3-methylimidazolium hydrogen sulphate ionic liquid in the selective catalysis of the biomass hemicellulose fraction, *RSC Adv.* 5 (2015) 47153–47164. <https://doi.org/10.1039/c5ra07159c>.
 - [15] A.M. da Costa Lopes, R.M. Łukasik, Separation and Recovery of a Hemicellulose-Derived Sugar Produced from the Hydrolysis of Biomass by an Acidic Ionic Liquid, *ChemSusChem.* 11 (2018) 1099–1107. <https://doi.org/10.1002/cssc.201702231>.
 - [16] A.M. da Costa Lopes, R.M.G.G. Lins, R.A. Rebelo, R.M. Łukasik, Biorefinery approach for lignocellulosic biomass valorisation with an acidic ionic liquid, *Green Chem.* 20 (2018) 4043–4057. <https://doi.org/10.1039/c8gc01763h>.
 - [17] J.R. Bernardo, F.M. Girio, R.M. Łukasik, The effect of the chemical character of ionic liquids on biomass pre-treatment and posterior enzymatic hydrolysis, *Molecules.* 24 (2019) 808. <https://doi.org/10.3390/molecules24040808>.
 - [18] A. Sant'Ana da Silva, S.H. Lee, T. Endo, E.P. Bon, Major improvement in the rate and yield of enzymatic saccharification of sugarcane bagasse via pretreatment with the ionic liquid 1-ethyl-3-methylimidazolium acetate ([Emim][Ac]), *Bioresour. Technol.* 102 (2011) 10505–10509. <https://doi.org/10.1016/j.biortech.2011.08.085>.
 - [19] B.M. Matsagar, P.L. Dhepe, Brønsted acidic ionic liquid-catalyzed conversion of hemicellulose into sugars, *Catal. Sci. Technol.* 5 (2015) 531–539. <https://doi.org/10.1039/c4cy01047g>.
 - [20] A.S. Amarasekara, B. Wiredu, Degradation of Cellulose in Dilute Aqueous Solutions of Acidic Ionic Liquid 1-(1-Propylsulfonic)-3-methylimidazolium Chloride, and p-Toluenesulfonic Acid at Moderate Temperatures and Pressures, *Ind. Eng. Chem. Res.* 50 (2011) 12276–12280. <https://doi.org/Doi10.1021/le200938h>.
 - [21] A. Rusanen, K. Lappalainen, J. Kärkkäinen, T. Tuuttila, M. Mikola, U. Lassi, Selective hemicellulose hydrolysis of Scots pine sawdust, *Biomass Convers. Biorefinery.* 9 (2019) 283–291.

- <https://doi.org/10.1007/s13399-018-0357-z>.
- [22] A. Sluiter, B. Hames, D. Hyman, C. Payne, R. Ruiz, C. Scarlata, J. Sluiter, D. Templeton, J. Wolfe, Determination of total solids in biomass and total dissolved solids in liquid process samples, National Renewable Energy Laboratory, Golden, Colorado, USA, 2008.
 - [23] A. Sluiter, B. Hames, R. Ruiz, C. Scarlata, J. Sluiter, D. Templeton, D. Crocker, Determination of structural carbohydrates and lignin in biomass - Laboratory Analytical Procedure (LAP), National Renewable Energy Laboratory, Golden, Colorado, USA, 2011.
 - [24] A. Sluiter, B. Hames, R. Ruiz, C. Scarlata, J. Sluiter, D. Templeton, Determination of Ash in Biomass, National Renewable Energy Laboratory - NREL, Golden, Colorado, USA, 2005.
 - [25] S.P. Magalhães da Silva, A.M. da Costa Lopes, L.B. Roseiro, R. Bogel-Lukasik, Novel pre-treatment and fractionation method for lignocellulosic biomass using ionic liquids, *RSC Adv.* 3 (2013) 16040–16050. <https://doi.org/10.1039/c3ra43091j>.
 - [26] N.N. Deshavath, M. Mohan, V.D. Veeranki, V. V Goud, S.R. Pinnamaneni, T. Benarjee, Dilute acid pretreatment of sorghum biomass to maximize the hemicellulose hydrolysis with minimized levels of fermentative inhibitors for bioethanol production, *3 Biotech.* 7 (2017) 139. <https://doi.org/10.1007/s13205-017-0752-3>.
 - [27] A. Brandt, M.J. Ray, T.Q. To, D.J. Leak, R.J. Murphy, T. Welton, Ionic liquid pretreatment of lignocellulosic biomass with ionic liquid–water mixtures, *Green Chem.* 13 (2011) 2489–2499. <https://doi.org/10.1039/c1gc15374a>.
 - [28] F. Tao, H. Song, L. Chou, Catalytic conversion of cellulose to chemicals in ionic liquid, *Carbohydr. Res.* 346 (2011) 58–63. <https://doi.org/10.1016/j.carres.2010.10.022>.
 - [29] Z. Chen, J. Long, Organosolv liquefaction of sugarcane bagasse catalyzed by acidic ionic liquids, *Bioresour. Technol.* 214 (2016) 16–23. <https://doi.org/10.1016/j.biortech.2016.04.089>.
 - [30] Z. Wang, J. Gräsvik, L.J. Jönsson, S. Winstrand, Comparison of [HSO₄][−], [Cl][−] and [MeCO₂][−] as anions in pretreatment of aspen and spruce with imidazolium-based ionic liquids, *BMC Biotechnol.* 17 (2017) 82. <https://doi.org/10.1186/s12896-017-0403-0>.
 - [31] P. Halder, S. Kundu, S. Patel, A. Setiawan, R. Atkin, R. Parthasarthy, J. Paz-Ferreiro, A. Surapaneni, K. Shah, Progress on the pre-treatment of lignocellulosic biomass employing ionic liquids, *Renew. Sustain. Energy Rev.* 105 (2019) 268–292. <https://doi.org/10.1016/j.rser.2019.01.052>.
 - [32] M. Mohan, N.N. Deshavath, T. Banerjee, V. V Goud, V.V. Dasu, Ionic Liquid and Sulfuric Acid-Based Pretreatment of Bamboo: Biomass Delignification and Enzymatic Hydrolysis for the Production of Reducing Sugars, *Ind. Eng. Chem. Res.* 57 (2018) 10105–10117. <https://doi.org/10.1021/acs.iecr.8b00914>.
 - [33] A.S. Patri, L. McAlister, C.M. Cai, R. Kumar, C.E. Wyman, CELF significantly reduces milling requirements and improves soaking effectiveness for maximum sugar recovery of Alamo switchgrass over dilute sulfuric acid pretreatment, *Biotechnol. Biofuels.* 12 (2019) 177. <https://doi.org/10.1186/s13068-019-1515-7>.
 - [34] A. Sluiter, B. Hames, R. Ruiz, C. Scarlata, J. Sluiter, D. Templeton, Determination of ash in biomass. NREL Laboratory Analytical Procedure (LAP), 2008. <http://www.nrel.gov/docs/gen/fy08/42622.pdf>.
 - [35] R. Bielski, G. Grynkiewicz, Furan platform chemicals beyond fuels and plastics, *Green Chem.* 23 (2021) 7458–7487. <https://doi.org/10.1039/d1gc02402g>.
 - [36] S.J. Chen, X. Chen, M.J. Zhu, Xylose recovery and bioethanol production from sugarcane bagasse pretreated by mild two-stage ultrasonic assisted dilute acid, *Bioresour. Technol.* 345 (2022) 126463. <https://doi.org/10.1016/j.biortech.2021.126463>.
 - [37] H. Xu, X. Li, W. Hu, L. Lu, J. Chen, Y. Zhu, H. Zhou, C. Si, Recent advances on solid acid catalytic systems for production of 5-Hydroxymethylfurfural from biomass derivatives, *Fuel Process. Technol.* 234 (2022) 107338. <https://doi.org/10.1016/j.fuproc.2022.107338>.
 - [38] Y. Dai, S. Yang, T. Wang, R. Tang, Y. Wang, L. Zhang, High conversion of xylose to furfural over corncob residue-based solid acid catalyst in water-methyl isobutyl ketone, *Ind. Crops Prod.* 180 (2022) 114781. <https://doi.org/10.1016/j.indcrop.2022.114781>.
 - [39] J.Y. Zhu, X. Pan, Efficient sugar production from plant biomass: Current status, challenges, and future directions, *Renew. Sustain. Energy Rev.* 164 (2022) 112583. <https://doi.org/10.1016/j.rser.2022.112583>.
 - [40] E.K. New, S.K. Tnah, K.S. Voon, K.J. Yong, A. Procentese, K.P. Yee Shak, W. Subramonian, C.K. Cheng, T.Y. Wu, The application of green solvent in a biorefinery using lignocellulosic biomass as a feedstock, *J. Environ. Manage.* 307 (2022) 114385. <https://doi.org/10.1016/j.jenvman.2021.114385>.
 - [41] S. Dutta, Valorization of biomass-derived furfurals: reactivity patterns, synthetic strategies, and applications, *Biomass Convers. Biorefinery.* (2021). <https://doi.org/10.1007/s13399-021-01924-w>.
 - [42] K. Świątek, S. Gaag, A. Klier, A. Kruse, J. Sauer, D. Steinbach, Acid hydrolysis of lignocellulosic biomass:

- Sugars and furfurals formation, *Catalysts*. 10 (2020) 437. <https://doi.org/10.3390/catal10040437>.
- [43] Y. Lu, Q. He, Q. Peng, W. Chen, Q. Cheng, G. Song, G. Fan, Directional synthesis of furfural compounds from holocellulose catalyzed by sulfamic acid, *Cellulose*. 28 (2021) 8343–8354. <https://doi.org/10.1007/s10570-021-04070-8>.
- [44] Z. Zhang, J. Xu, J. Xie, S. Zhu, B. Wang, J. Li, K. Chen, Physicochemical transformation and enzymatic hydrolysis promotion of reed straw after pretreatment with a new deep eutectic solvent, *Carbohydr. Polym.* 290 (2022) 119472. <https://doi.org/10.1016/j.carbpol.2022.119472>.
- [45] E.L.N. Escobar, M.J. Suota, L.P. Ramos, M.L. Corazza, Combination of green solvents for efficient sugarcane bagasse fractionation, *Biomass and Bioenergy*. 161 (2022) 106482. <https://doi.org/10.1016/j.biombioe.2022.106482>.
- [46] K.N. Guo, C. Zhang, L.H. Xu, S.C. Sun, J.L. Wen, T.Q. Yuan, Efficient fractionation of bamboo residue by autohydrolysis and deep eutectic solvents pretreatment, *Bioresour. Technol.* 354 (2022) 127225. <https://doi.org/10.1016/j.biortech.2022.127225>.
- [47] L. Huang, H. Peng, Z. Xiao, H. Wu, G. Fu, Y. Wan, H. Bi, Production of furfural and 5-hydroxymethyl furfural from *Camellia oleifera* fruit shell in [Bmim]HSO₄/H₂O/1,4-dioxane biphasic medium, *Ind. Crops Prod.* 184 (2022) 115006. <https://doi.org/10.1016/j.indcrop.2022.115006>.
- [48] L. Mesa, V.S. Valerio, M.B. Soares Forte, J.C. Santos, E. González, S.S. da Silva, Optimization of BmimCl pretreatment of sugarcane bagasse through combining multiple responses to increase sugar production. An approach of the kinetic model, *Biomass Convers. Biorefinery*. 12 (2022) 2027–2043. <https://doi.org/10.1007/s13399-020-00792-0>.
- [49] P. Liu, S. Shi, L. Gao, G. Xiao, Efficient conversion of xylan and rice husk to furfural over immobilized imidazolium acidic ionic liquids, *React. Kinet. Mech. Catal.* 135 (2022) 795–810. <https://doi.org/10.1007/s11144-022-02172-3>.
- [50] K.S. Khoo, X. Tan, C.W. Ooi, K.W. Chew, W.H. Leong, Y.H. Chai, S.H. Ho, P.L. Show, How does ionic liquid play a role in sustainability of biomass processing?, *J. Clean. Prod.* 284 (2021) 124772. <https://doi.org/10.1016/j.jclepro.2020.124772>.
- [51] H. Mao, S.H. Li, A.S. Zhang, L.H. Xu, H.X. Lu, J. Lv, Z.P. Zhao, Furfural separation from aqueous solution by pervaporation membrane mixed with metal organic framework MIL-53(Al) synthesized via high efficiency solvent-controlled microwave, *Sep. Purif. Technol.* 272 (2021) 118813. <https://doi.org/10.1016/j.seppur.2021.118813>.

EVALUATION OF DESIGN AND INSERTION ANALYSIS OF A CONICAL SHAPED POLYMERIC BASED MICRONEEDLE FOR TRANSDERMAL DRUG DELIVERY APPLICATIONS

Aswani Kumar Gera*

Department of Electrical Electronics and Communication Engineering, School of Technology
GITAM, Deemed to be University, Visakhapatnam, India, agera@gitam.edu
 <https://orcid.org/0000-0002-8375-7580>

Rajesh Kumar Burra

Department of Electrical Electronics and Communication Engineering, School of Technology
GITAM, Deemed to be University, Visakhapatnam, India, rburra@gitam.edu
 <https://orcid.org/0000-0001-5081-7711>

Article history: Received 1 September 2022, Received in revised form 6 October 2022, Accepted 10 October 2022, Available online 10 October 2022

Highlight

This article focuses on structural design of an eco-friendly, recyclable featured conical-shaped PMMA polymeric based microneedle for medical applications.

Abstract

Transportation of drug through parental routes are conventionally followed through hypodermic injection methods, where hypodermic injections are administered into the human skin for drug release. However, there are some issues observed when these hypodermic needles are being used, there are instances where the needle is being inserted leaves some needle fractures in the skin. To cater to the issue scientific researchers are voraciously working on designing and developing polymeric type of microneedle structures for various medical diagnostic applications for glucose monitoring, drug delivery, and other applications. This article presents the structural design of a conical-shaped polymeric microneedle and the insertion force while being pierced into the skin. Simulations at different insertion angles on microneedle are analyzed by arriving with total needle displacements in the process of insertion. The von mises stress is also analyzed with applied force at different insertion angles resulted in incremental change in stress exerted by the microneedle. The resultant stress is below the yield stress which makes the microneedle pierce into the skin without breakage.

Keywords

eco-friendly polymers; drug delivery; micro needle; transdermal drug delivery.

Introduction

Transdermal drug delivery method (TDD) generally refers to the delivery of therapeutics which are channelized across the skin's innermost layers. This method of drug being delivered into the skin's layers overcomes issues like routing the drug through oral passage which can lead to gastrointestinal tract irritability and poor compliance from the patient point of view [1]. However, this method of transdermal means of delivering the drug offers better release over a period of time when being compared with that of administering the drug through oral cavity [2,3]. Polymeric microneedles are receiving attention in medical and biological sciences especially drug delivery due to their prime advantages which are their biocompatibility properties when being compared with that of the other materials. Polymeric microneedles have improved method for transdermal transportation of drugs as they are routed into the skin's stratum-corneum barrier with minimal invasiveness and with ease [1]. Pharmaceutical giants and biotechnology based companies are focusing on drug research and developmental of microneedles with loaded protein based drugs [4–6]. This will tend towards progress and extensive technological outburst in the production of microneedles which clinically important for the upcoming future [4]. As discussed with regards to the microneedles the mechanical properties and their biocompatibility of the material chosen plays a key role in manufacturing and in their performance analysis. In general, for mass production manufacturers are keen on low production cost with exceptional mechanical stability towards their fabrication. To cater this, need an ideal and viable option is to choose a material from polymeric family with good mechanical stability which can be tailor-made for different mechanical strengths with appropriate functions [7]. To be able to successfully penetrate into the skin's surface, depends on various factors which are the length of the microneedle, density, tip and base diameters. Microneedles which tend to have higher value of

Young's Modulus will aid in better mechanical stability and with good penetration capacity [8]. A higher Young's Modulus tends with better stability and when the tensile strength is considered the shape and size of the microneedle need to be considered [9]. The design of a microneedle is a prime factor for determining the effectiveness of a microneedle [10,11]. Microneedles are commonly designed as an array of structures either they resemble in a conical form or in a pyramidal shape which are used to pierce through the skin surface to transport the drugs [12]. The materials which are used in micro needle fabrication are considered to be the one of the utmost factors in the designing aspects, since this factor totally governs the mechanical strength and medicinal drug transportation viabilities for the micro needle. Consequently, other pivotal issues which need to be considered are the density of the material, the overall height from (base to tip), the diameter and also the width of the tip, [8]. Microneedles with either conical shapes or pyramidal-shaped structures are fabricated or formed with the application of various materials which typically range from 250mm and can even go up to 2000 mm in height which has the technique to travel across the human skin's internal layers to deliver the targeted drug molecules [12]. Scientific researchers and scientists have worked upon various microneedle lengths, widths, and thickness and on tip size portions towards optimized penetration [13].

Methods

Material selection:

Lately in the recent times, polymeric based micro needles are gaining a tremendous interest in the field of medical and biological sciences. Most of the polymers in polymeric family exhibit good rate of rigidity with an added biocompatibility compliance, which enables the polymeric-based micro needles which evades the fractures and side effects when they are administered into the skin. Some polymers in the polymeric family are also soluble in water as its medium. Thus, drugs can be encapsulated in dissolving kind of micro needles. As these polymeric micro needles also have property of relatively low melting point of temperature, fabrication techniques like microinjection molding can be used in the preparation of polymer micro needles. A common widely used molding technique which injection molding technique wherein the process the materials are melt widely used are polymeric based materials, they are allowed to flow with high force by maintaining high pressure through a plunger based setup which enters into a mold cavity, after passing, opens up to a phase of solidification and thereafter gets ejected thereby produces an exact replicate structure on the surface. Thus, mold based fabrication technique could further reduce the manufacturing cost and still remains to be the most viable option for mass production [14]. Solid truncated conical shaped micro needles which are made with poly methyl methacrylate (PMMA) material, measuring the tip radius of 20 μm and with a diameter of 40 μm and 650 μm in height with a bottom dimensional radius of 100 μm and 200 μm diameters is chosen for the model. Polymeric micro needles are ideally considered as they tend to show exhibit excellent properties of biocompatibility, added to that their property of rigidity and their built quality, makes them capable enough for transportation of wide range of drugs without any hindrance to in their dimensional mechanical properties [15]. Hence there is a dire need to contribute to the overall development of polymeric-based microneedles. More importantly considering the type of polymer used, an efficient and intricate design of the micro needle tip, length and width of the needle, and the manufacturing modality are the prime parameters in the overall development of the micro needle [16]. One of the prime challenges being linked with polymeric type of micro needles are their penetrating capacity through the skin's layers. In many cases, the mechanical strength tends to be weaker in polymers that are soluble in water compared to that of the materials which do not dissolve like silicon or in metals, and encapsulation of the drug to be introduced will be a factor of compromising on the rigidity and strength of the Microneedles [16,17]. When polymeric microneedles are taken into consideration, their uniqueness pertains to their mechanical stability and in their strength, add to that their modulus of elasticity and fracture rigidity, they are the pivotal factors. Mechanically stronger based polymeric microneedles are sufficiently capable enough to withstand the forces without deformations i.e., their bending and breakage limits [18]. Apart from this, the tissue under target for MN's is it the application through the transdermal means or the non-transdermal method must be taken into consideration with the right kind of polymeric microneedles. However, the method of application for non- transdermal means for the target areas like the tissue of an eye, vascular linked tissues, and of the digestive tract system polymeric microneedles are the viable option which can bend and they are simple to use through surgical means, with an ideal balance of their strength and flexibility options, only when targeting soft type of tissues which require comparatively less pressure in terms of their insertion strength [19].

Design Parameters

The fundamental characteristic of micro needles is that they should meet some pivotal requirements for achieving the desired need of penetrating into the skin layers with ease subjective to pain free when being administered. To achieve the objective, the micro needles which are designed are to made sharp enough

meeting a rigidity to handle the requirement. Simultaneously when they are administered there should not be any mechanical damage or fracture pertaining to the material. The micro needles which are designed and manufactured should not compromise on the length of the micro needle and in diameter, to avoid contacts with other organs. The authors clearly illustrated in [20], after taking into consideration the skin deformation allied issues and concluded that length of the micro needle can be further restricted to 300 μ m-400 μ m range. Further it can be assumed by considering the flexibility issue of the skin, the assumed length will not be sufficient to penetrate into the skin layers effectively. Thus, the micro needle length in this work is considered to be 650 μ m. Figure 1 shows the schematic diagram and dimensions of the designed microneedle.

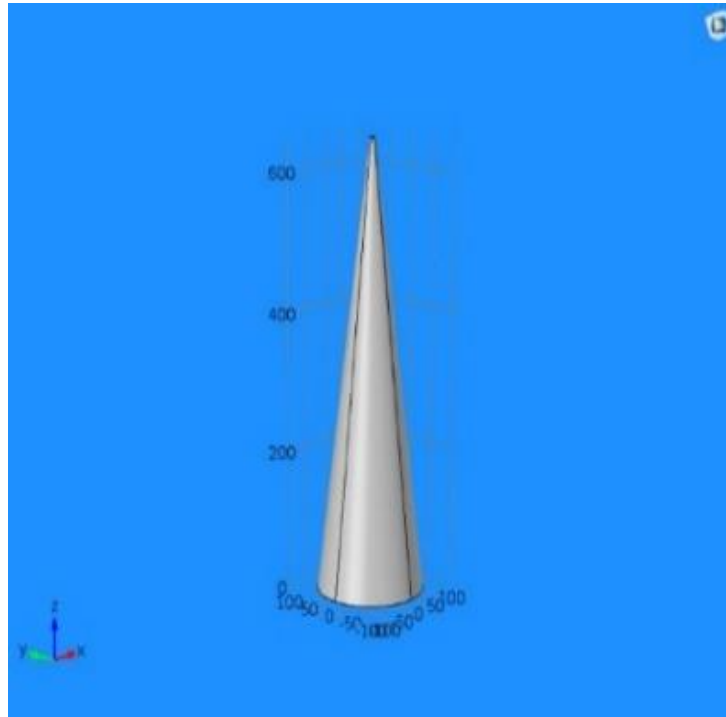


Figure 1. Geometrical shape of a micro needle (MN) in Longitudinal view. *Source: Author.*

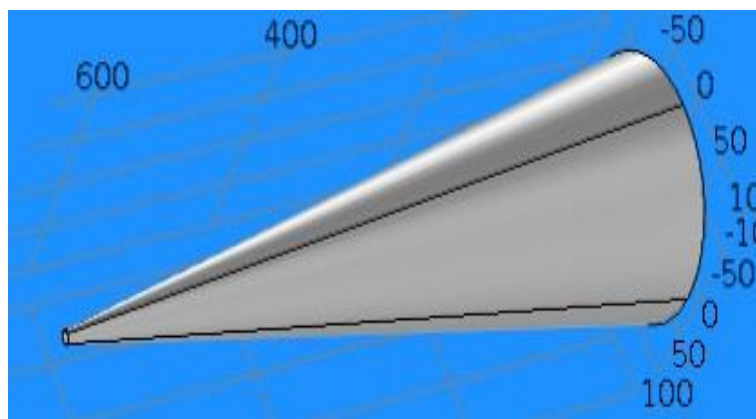


Figure 2. Geometrical shape of a microneedle (MN) in Lateral view. *Source: Author.*

The designed micro needle in this study is considered to be a solid truncated cone like structure, the base being with broader and narrows like a tip as it goes to the tip which is illustrated in Figure 1. The shape is designed in such a manner, to minimize the effects of bending stress on the micro needle when exerted and also the deformities failure of buckling, during the process of insertion of micro needle into the skin when being compared with other high aspect ratios or column-like structures [21]. Evidently by sharpening the tip of the micro needle and reducing the tip diameter (L) by simultaneously increasing the angle of bevel i.e. (θ), will lessen the impact of the insertion force on the micro needle. In spite of working to lessening the effect of insertion force, leads in resulting in tip fractures when the micro needle is in the process of penetration and also a trade-off between the sharpness and mechanical strength of the tip which should be considered. The material properties are given

below in Table 1.

Table 1. Properties of PMMA Material. *Source: Author.*

Elastic modulus	3 GPa
Poisson's Ratio	0.400
Shear Modulus	3.202 GPa
Density	1900 kg/m ³
Tensile Strength Factor	1.434 GPa
Yield Strength Factor	1.394 GPa

The mechanical properties of micro needles pertaining to their (elasticity modulus values and the value of fracture forces) need to be analyzed in order to make sure that micro needles will not undergo any sort of deformity in their structure or breakage issues also called as fracture issues during the process of skin insertion tests. Mechanical testing is quite common practice when the necessity arises to measure the maximum for exerted axially, which is the common cause for micro needle failure. However even if the Young's modulus of the material and the base of the diameter dimensions are strengthened will give rise to an increase in the yield force exerted of the micro needles. On the contrary if a condition arises wherein force of failure of the micro needle is increased by simultaneously decreasing the overall length of the micro needle, which leads to a condition of critical buckling (lateral way of deflection) load of a column decreases by increasing column's length [5,22].

These explanations are proved analytically by referring to Euler's formula, the equation for critical buckling load [23].

$$(1) \quad P_{cr} = \pi^2 EI / (KL)^2$$

where:

P_{cr} is the critical load;

E is considered as the Young's modulus

I is the cross sectional area of the micro needle;

L being the total length of the needle

K to be considered as the effective length factor.

K is related to the boundary conditions of the column. All the above conditions are applied considering the micro needle as a fixed-free column or fixed-pinned column, the corresponding effective length factor is K is considered to be value of 2 or nearly $K = 0.699$, respectively [24,25]

Design Criteria of Interest

Insertion angle and counting on the Von misses stress on the polymeric microneedle was the interest of this paper. In this simulation model a parametric sweep analysis different angle of deflection was performed for various angles of (Θ) and the stress is analyzed. Thus, the range of insertion angle was considered to be from 0 radians to 0.26 radians (i.e., from 0 degree to 15 degree of deflections. A coarse meshing type is selected for analysis. The surface stress exerted on the needle tip is very low at 0 radians and stands out to be 1.91MPa and surface stress is radiated throughout the needle and stands out to be 6.28 MPa. The microneedle reflects their typical angle of insertion criteria at the two extremity values. The material applied to the microneedle stands out to be Poly-methyl-methacrylate (PMMA).

The applied force on the microneedle was subjected to be kept at a constant value of 0.058N. The computations of the model were generated by using the governing equations of motion and strain displacement equations. The base of the microneedle was set as a fixed constraint, and the tip of the microneedle was chosen as the boundary load location. A parametric sweep was used to sweep the insertion angle from 0 rad to 0.26 rad in steps of 0.010 rad. The resultant Von Mises Stress from this simulation is analyzed and discussed.

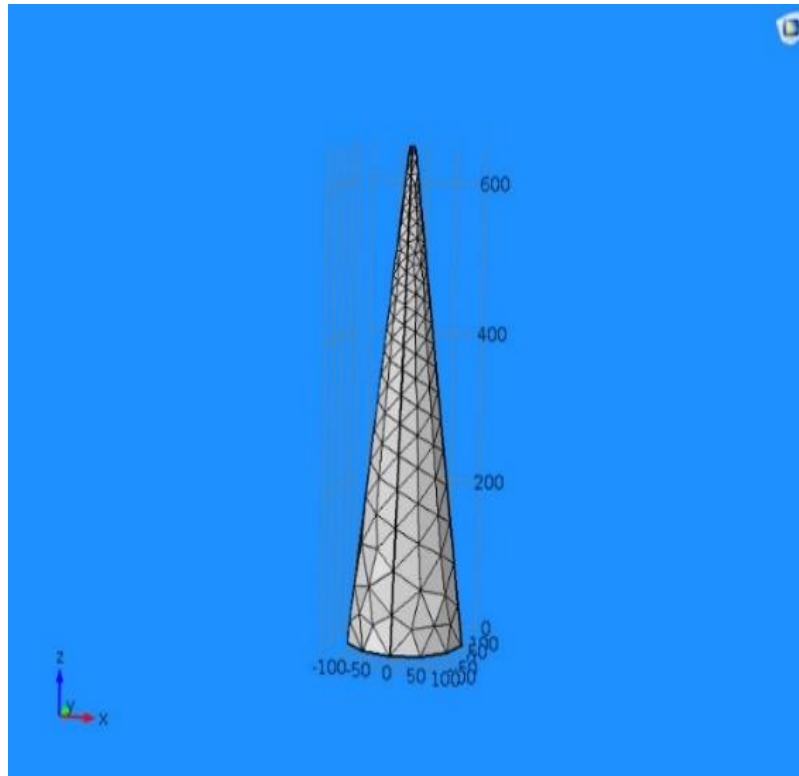


Figure 3. Mesh Analysis of the PMMA Polymeric Microneedle. *Source: Author.*

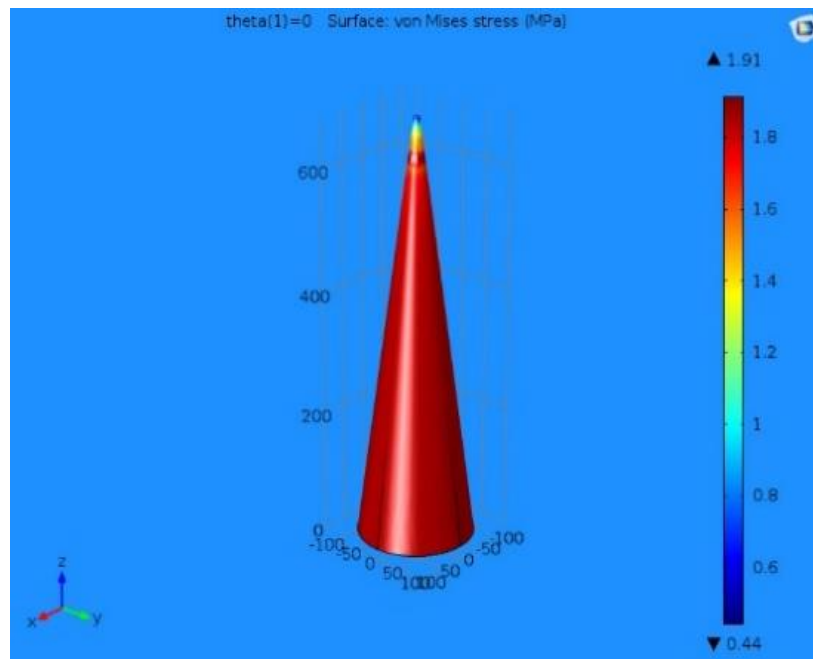


Figure 4. Surface stress on a PMMA Polymeric Microneedle at 0 radians. *Source: Author.*

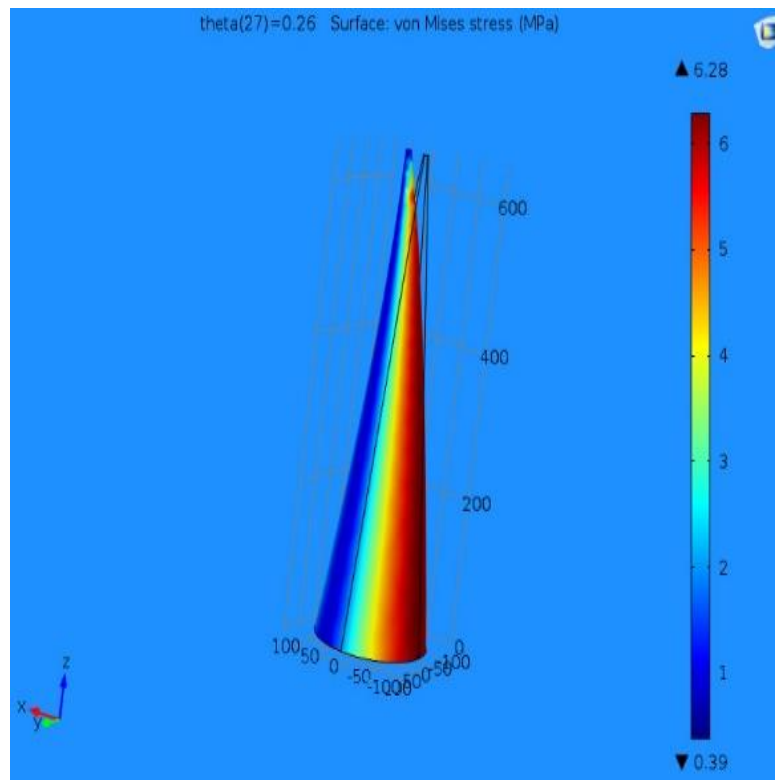


Figure 5. Surface Stress on a PMMA Polymeric Microneedle at 0.26rad. *Source: Author.*

Mathematical modeling & Governing equations

Equation of Motion can be written as:

$$(2) \quad \nabla \cdot \sigma + F \cdot v = \rho \frac{\partial^2 U}{\partial t^2}$$

General Strain Displacement Equation can be written as

$$(3) \quad \varepsilon = \frac{1}{2} [\nabla u + (\nabla u) \cdot T]$$

Equation of motion can be written as

$$(4) \quad -\Delta \sigma = Fv$$

Simulations

Conical shaped polymeric microneedle at different eigen frequencies and the relative stress surface displacement distributions are carried out with simultaneously observing the deformations in the microneedle structure. The polymeric microneedle is designed to withstand the breakage failure while being inserted into the skin's surface. However, when the microneedle is inserted into the skin's surface the microneedle exerts some reaction forces onto it. When the reactive forces are more than the incidental forces the microneedle exerts a state deformation leading to breakage called the fracture. These anomalies need to be taken into consideration while designing the microneedle and while loading the microneedle into the skin. In the above simulation it is observed that the needle retains its shape without any deformation and the entire stress is equally distributed from the tip of the base needle to the base of the needle. The stress being concentrated maximum at the tip of the needle and minimum at of the needle. The stress factor changes in accordance with the change in the Eigen frequency. Total surface displacement to the corresponding frequency are being simulated in the above figure.

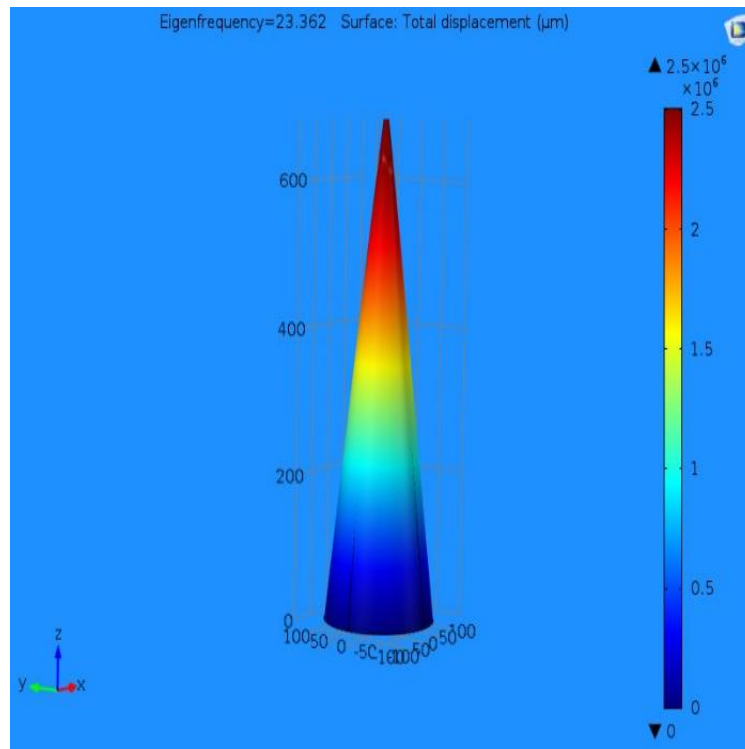


Figure 6. Total Displacement without deformation of the needle structure (Longitudinal View). *Source: Author.*

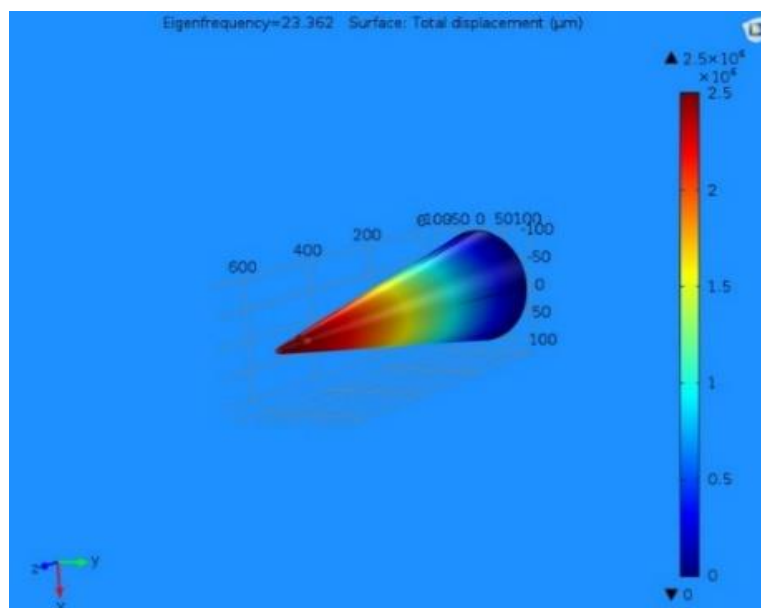
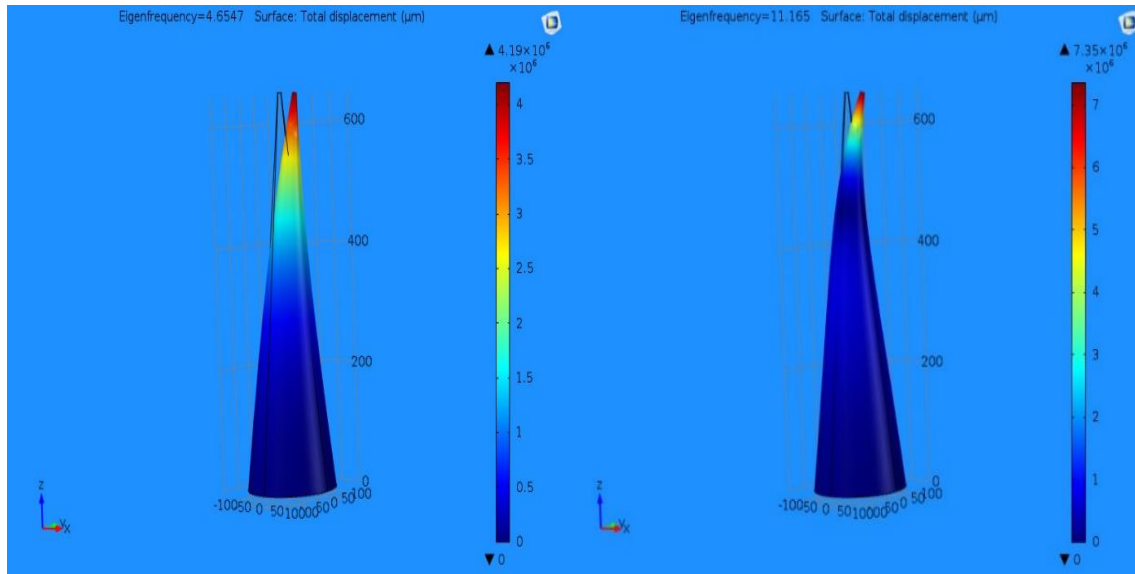


Figure 7. Total Displacement without deformation of needle structure (Lateral View). *Source: Author.*

Total surface displacement of the polymeric microneedle is shown in a lateral view where the stress distribution is evident from the tip of the microneedle to the base of the microneedle. The stress distribution is equally spread along the whole length of the microneedle. It exerts a maximum at the tip of the microneedle and a minimum at the base diameter of the microneedle. The importance of maintaining a sharp tip for the microneedle is that the insertion will be smooth and effective on the skin surface. Sharp tips and corrugated tips, slant tips of different designs are used for microneedle.

Here in the above simulation, it is observed that by varying the frequency there also observed that there is a change in the structure of the needle, a bulge is observed at 200µm to 400µm and also slightly on the above heights. The maximum stress tends to shift to the middle portion of the needle.



Figures 8 and 9. Total Displacement with initial stages of deformation. *Source: Author.*

Figures 8, 9 depicts the displacements exerted by the microneedle at different eigen frequencies, structural deformations on the microneedle. In the initial stages of the deformation, the stress is shifted towards the tip and distributed throughout the microneedle. It is analyzed that after an eigenfrequency of 4.567, with a minimum stress is distributed from the lower half of the microneedle to its base. It is evident from the literature that the minimum stress required for a microneedle to pierce into the skin is found to be as 3.18MPa and as it surpassed the value the needle can pierce into the skin at this particular frequency with a total displacement of 4.19MPa. Further, there is an increase in the stress component concerning the structural deformation of the microneedle. It is evident from the simulations that as there is an increase in the eigenfrequency.

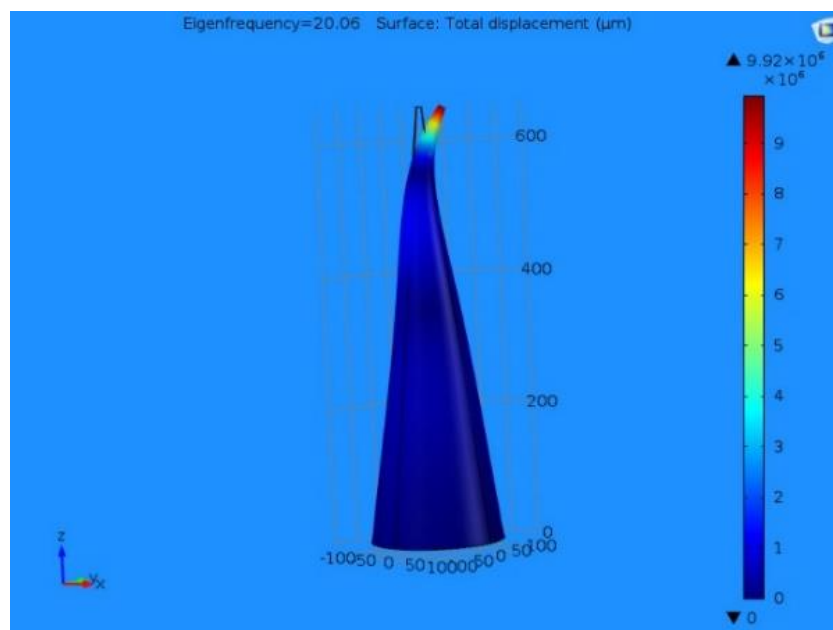


Figure 10. Displacement at mediocre stages of deformation. *Source: Author.*

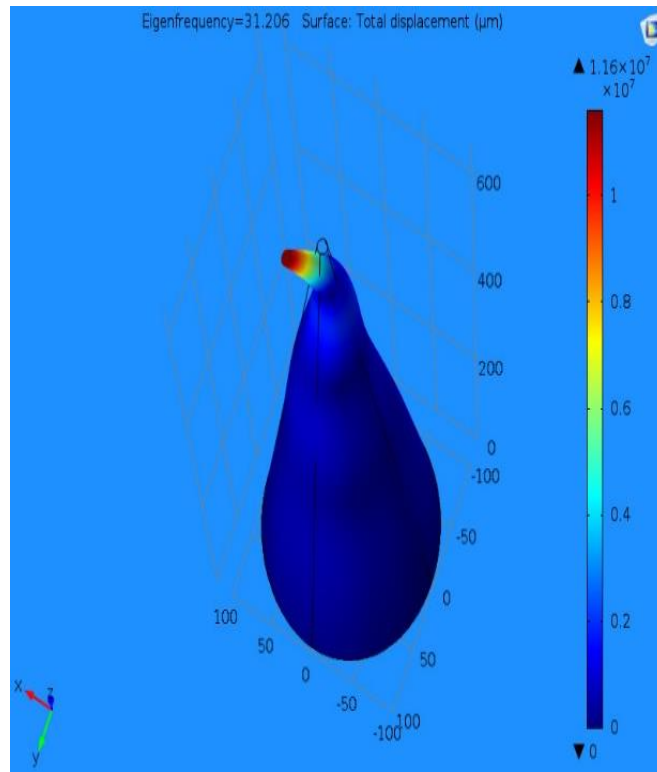


Figure 11. Total Displacement with deformation of needle structure. *Source: Author.*

At this point of eigenfrequency 31.206, the polymeric microneedle gets deformed exhibiting a maximum deformation stress-based Surface displacement of $0.116 \mu\text{m}$.

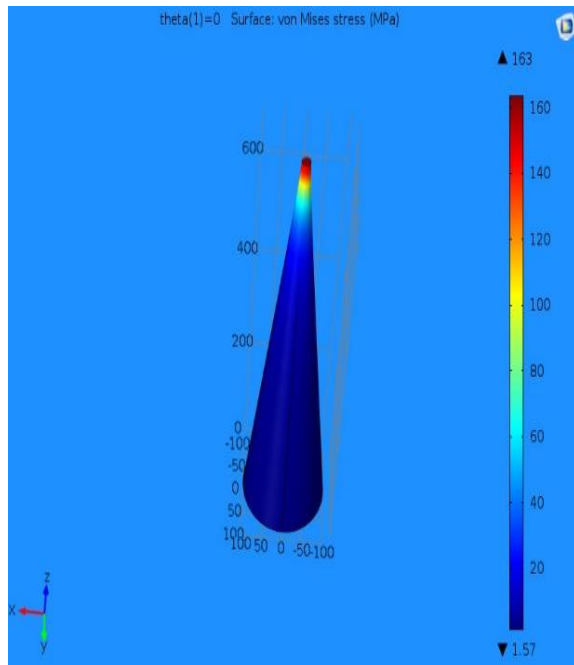


Figure 12. Stress observation at 0 degree. *Source: Author.*

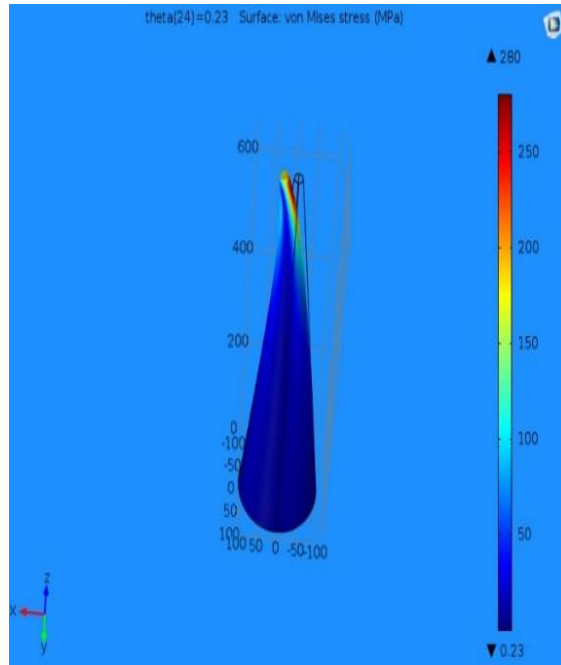


Figure 13. Stress observed at 0.21 degree. *Source: Author.*

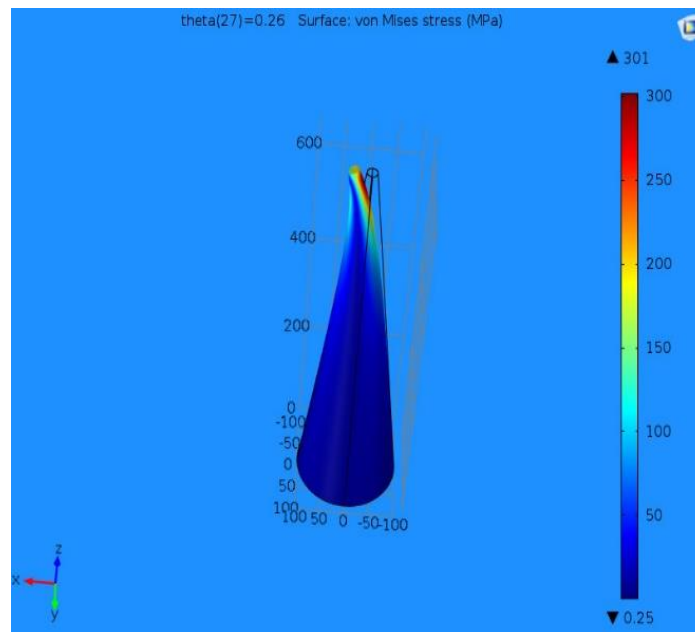


Figure 14. Stress observed at 0.25 degree. *Source: Author.*

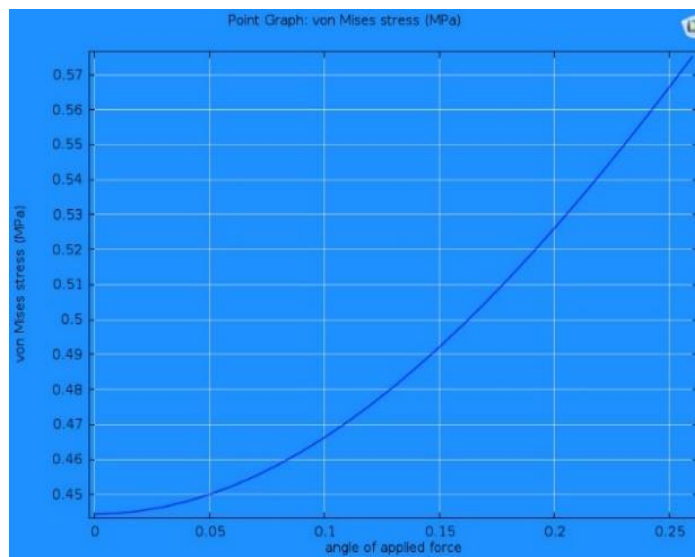


Figure 15. Angle of Applied Force Vs von Mises Stress. *Source: Author.*

The angle of applied force concerning the von Mises stress is depicted. It is evident that as the angle of applied force is changing there is an incremental change in the von Mises stress factor. The angle of applied force is directly proportional to the von Mises stress on the microneedle structure.

Impact

In the past few decades, there has been a substantial increase towards the materials which are reusable especially in the areas of agriculture cultivation, medicine and other allied areas. Polymers and their families are standing as the big head for the current plastics, and they are expanded into versatile areas. Research communities are steadfastly working out in these areas of polymeric materials to make them more and more user-friendly and there on to design and fabricate a new composite type of materials [26]. In the days to come these kinds of biodegradable polymeric materials will significantly reduce the need for polymeric materials which are synthetic in nature by reducing the fabrication costs, which in turn have progressive effects in the environment and an economically feasible option.

Conclusion

This model was designed to study the relationship between a single conical shaped polymeric PMMA micro

needle's insertion angle with that of the resultant Von Mises stresses. The results of this simulation study depict that the resultant von Mises stresses tend to be increased when there is an incremental change in the insertion angle; the minimum Von Mises stress of 163 MPa occurred at an angle of 0 rad and the maximum Von Mises stress of 301.00 MPa occurred at angle = 0.26 rad. To penetrate the skin, the micro needle's Von Mises stress needed to exceed the skin's resistive pressure of 3.18MPa, and to prevent yielding, the microneedle's Von Mises needed to remain below 400 MPa. As was determined from the Von Mises stress range of 163 to 301 MPa, all angles of insertion were below this yield stress of 400 MPa. The results clearly show that the microneedle is sufficient can be able to penetrate the skin layers and be capable enough to resist the needle breakage for all possible angles of insertion.

Conflict of interest

The authors declares that there is no conflict of interest.

Funding information

There is no funding involved in this work.

Acknowledgments

The authors of the manuscript would like to thank the Department of EECE, School of Technology, GITAM Deemed to be University for the Research Lab facility. This research has not been supported by any external funding.


References

- [1] K. Ahmed Saeed AL-Japairai, S. Mahmood, S. Hamed Almurisi, J. Reddy Venugopal, A. Rebhi Hilles, M. Azmana, S. Raman, Current trends in polymer microneedle for transdermal drug delivery, *Int. J. Pharm.* 587 (2020) 119673. <https://doi.org/10.1016/j.ijpharm.2020.119673>.
- [2] K. Ita, Transdermal delivery of drugs with microneedles—potential and challenges, *Pharmaceutics*. 7 (2015) 90–105. <https://doi.org/10.3390/pharmaceutics7030090>.
- [3] C. Pegoraro, S. MacNeil, G. Battaglia, Transdermal drug delivery: From micro to nano, *Nanoscale*. 4 (2012) 1881–1894. <https://doi.org/10.1039/c2nr11606e>.
- [4] J.S. Kochhar, J.J.Y. Tan, Y.C. Kwang, L. Kang, *Microneedles for Transdermal Drug Delivery*, Springer International Publishing, Cham, 2019. <https://doi.org/10.1007/978-3-030-15444-8>.
- [5] G. Ma, C. Wu, Microneedle, bio-microneedle and bio-inspired microneedle: A review, *J. Control. Release*. 251 (2017) 11–23. <https://doi.org/10.1016/j.jconrel.2017.02.011>.
- [6] Y.C. Ryu, D.I. Kim, S.H. Kim, H.M.D. Wang, B.H. Hwang, Synergistic Transdermal Delivery of Biomacromolecules Using Sonophoresis after Microneedle Treatment, *Biotechnol. Bioprocess Eng.* 23 (2018) 286–292. <https://doi.org/10.1007/s12257-018-0070-6>.
- [7] M.S. Lhernould, M. Deleers, A. Delchambre, Hollow polymer microneedles array resistance and insertion tests, *Int. J. Pharm.* 480 (2015) 8–15. <https://doi.org/10.1016/j.ijpharm.2015.01.019>.
- [8] E.Z. Loizidou, N.T. Inoue, J. Ashton-Barnett, D.A. Barrow, C.J. Allender, Evaluation of geometrical effects of microneedles on skin penetration by CT scan and finite element analysis, *Eur. J. Pharm. Biopharm.* 107 (2016) 1–6. <https://doi.org/10.1016/j.ejpb.2016.06.023>.
- [9] E. Larrañeta, R.E.M. Lutton, A.D. Woolfson, R.F. Donnelly, Microneedle arrays as transdermal and intradermal drug delivery systems: Materials science, manufacture and commercial development, *Mater. Sci. Eng. R Reports*. 104 (2016) 1–32. <https://doi.org/10.1016/j.mser.2016.03.001>.
- [10] S.P. Davis, M.R. Prausnitz, M.G. Allen, Fabrication and characterization of laser micromachined hollow microneedles, in: *TRANSDUCERS 2003 - 12th Int. Conf. Solid-State Sensors, Actuators Microsystems*, Dig. Tech. Pap., 2003: pp. 1435–1438. <https://doi.org/10.1109/SENSOR.2003.1217045>.
- [11] M. Wang, L. Hu, C. Xu, Recent advances in the design of polymeric microneedles for transdermal drug delivery and biosensing, *Lab Chip*. 17 (2017) 1373–1387. <https://doi.org/10.1039/C7LC00016B>.
- [12] T. Tomono, A new way to control the internal structure of microneedles: a case of chitosan lactate, *Mater. Today Chem.* 13 (2019) 79–87. <https://doi.org/10.1016/j.mtchem.2019.04.009>.
- [13] G. Yan, K.S. Warner, J. Zhang, S. Sharma, B.K. Gale, Evaluation needle length and density of microneedle arrays in the pretreatment of skin for transdermal drug delivery, *Int. J. Pharm.* 391 (2010) 7–12. <https://doi.org/10.1016/j.ijpharm.2010.02.007>.
- [14] Matec Web Conference Volume 192, Exploring innovative solutions for smart society, in: 4th Int. Conf.


- Eng. Appl. Sci. Technol. (ICEAST 2018), 2018.
- [15] G. Du, X. Sun, Current Advances in Sustained Release Microneedles, *Pharm. Front.* 02 (2020) e11–e22. <https://doi.org/10.1055/s-0040-1701435>.
 - [16] Q. Wang, G. Yao, P. Dong, Z. Gong, G. Li, K. Zhang, C. Wu, Investigation on fabrication process of dissolving microneedle arrays to improve effective needle drug distribution, *Eur. J. Pharm. Sci.* 66 (2015) 148–156. <https://doi.org/10.1016/j.ejps.2014.09.011>.
 - [17] R.F. Donnelly, D.I.J. Morrow, T.R.R. Singh, K. Migalska, P.A. McCarron, C. O'Mahony, A.D. Woolfson, Processing difficulties and instability of carbohydrate microneedle arrays, *Drug Dev. Ind. Pharm.* 35 (2009) 1242–1254. <https://doi.org/10.1080/03639040902882280>.
 - [18] L.K. Vora, A.J. Courtenay, I.A. Tekko, E. Larrañeta, R.F. Donnelly, Pullulan-based dissolving microneedle arrays for enhanced transdermal delivery of small and large biomolecules, *Int. J. Biol. Macromol.* 146 (2020) 290–298. <https://doi.org/10.1016/j.ijbiomac.2019.12.184>.
 - [19] H. Juster, B. van der Aar, H. de Brouwer, A review on microfabrication of thermoplastic polymer-based microneedle arrays, *Polym. Eng. Sci.* 59 (2019) 877–890. <https://doi.org/10.1002/pen.25078>.
 - [20] K.J. Lee, M.J. Goudie, P. Tebon, W. Sun, Z. Luo, J. Lee, S. Zhang, K. Fetah, H.J. Kim, Y. Xue, M.A. Darabi, S. Ahadian, E. Sarikhani, W.H. Ryu, Z. Gu, P.S. Weiss, M.R. Dokmeci, N. Ashammakhi, A. Khademhosseini, Non-transdermal microneedles for advanced drug delivery, *Adv. Drug Deliv. Rev.* 165–166 (2020) 41–59. <https://doi.org/10.1016/j.addr.2019.11.010>.
 - [21] S.J. Moon, S.S. Lee, *Micromech, Microeng.* 15 (2009) 903–911.
 - [22] A.P. Sgouros, G. Kalosakas, K. Papagelis, C. Galiotis, Compressive response and buckling of graphene nanoribbons, *Sci. Rep.* 8 (2018) 9593. <https://doi.org/10.1038/s41598-018-27808-0>.
 - [23] M.R. Maschmann, Q. Zhang, R. Wheeler, F. Du, L. Dai, J. Baur, In situ SEM observation of column-like and foam-like CNT array nanoindentation, *ACS Appl. Mater. Interfaces.* 3 (2011) 648–653. <https://doi.org/10.1021/am101262g>.
 - [24] E.R. Parker, M.P. Rao, K.L. Turner, C.D. Meinhart, N.C. MacDonald, Bulk Micromachined Titanium Microneedles, *J. Microelectromechanical Syst.* 16 (2007) 289–295. <https://doi.org/10.1109/JMEMS.2007.892909>.
 - [25] E.R. Parker, M.P. Rao, K.L. Turner, C.D. Meinhart, N.C. MacDonald, Bulk micromachined titanium microneedles, *J. Microelectromechanical Syst.* 16 (2007) 289–295. <https://doi.org/10.1109/JMEMS.2007.892909>.
 - [26] I.M. Shamsuddin, S. N, A. M, A. MK, Biodegradable polymers for sustainable environmental and economic development, *MOJ Bioorganic Org. Chem.* 2 (2018). <https://doi.org/10.15406/mojboc.2018.02.00080>.

SIMULATION AND DESIGN OF AN ENERGY ACCUMULATOR AROUND THE HYDROGEN ENERGY VECTOR


Laince Pierre Moulebe*

Department of Thermal Engineering, Faculty of Technology
Laboratory of Complex Cyber-Physical Systems (LCCPS) of ENSAM Hassan II University
150 Bd du Nil, Casablanca 20670, Morocco, mpierrelaince12@gmail.com
 <https://orcid.org/0000-0001-7149-5694>


Abdelwahed Touati

Department of Thermal Engineering, Faculty of Technology
Laboratory of Complex Cyber-Physical Systems (LCCPS) of ENSAM Hassan II University
150 Bd du Nil, Casablanca 20670, Morocco, touati_2010@hotmail.com
 <https://orcid.org/0000-0001-9589-0090>

Eric Akpoviro Obar

Department of Thermal Engineering, Faculty of Technology
Laboratory of Complex Cyber-Physical Systems (LCCPS) of ENSAM Hassan II University
150 Bd du Nil, Casablanca 20670, Morocco, akposobar@yahoo.com
 <https://orcid.org/0000-0002-4776-4708>

Nabila Rabbah

Department of Thermal Engineering, Faculty of Technology
Laboratory of Complex Cyber-Physical Systems (LCCPS) of ENSAM Hassan II University
150 Bd du Nil, Casablanca 20670, Morocco, nabila_rabbah@yahoo.fr
 <https://orcid.org/0000-0002-2221-4830>

*Article history: Received 7 August 2022, Received in revised form 8 September 2022, Accepted 6 October 2022,
Available online 6 October 2022*

Highlight

Reduction of greenhouse gases thanks to an energy generator using green hydrogen.

Abstract

This work demonstrates the study of the numerical modelling and a design of a compact energy generator based on green hydrogen. This generator aims allowing the energy storage, electricity, cold and heat productions as well as a supply the energy for the production of the sanitary hot water. The generator is considered to be powered by 30 solar cells panels and will mainly consist of a Proton Exchange Membrane (PEM) electrolyzer compiled with a Metal Hydride (MH) tank, a PEM fuel cell, and a system of heat exchangers sized to recover the heat from the electrolyzer, PEM fuel cell and MH tank. Furthermore, the generator will contain an adsorber to manage air conditioning (cooling and heating) and a production of the sanitary hot water. A converter block is included in the generator, in particular, a Buck-booster to raise the voltage of the solar panels and the DC-AC converter for the electricity consumption in the household. The desorption of the hydrogen contained in the tank MH will take place using the heating resistance. In overall, the designed generator is foreseen to have a dimension of $1800 \times 1000 \times 500$ mm and its role is to allow integration of the hydrogen energy for the tertiary and residential sectors. As such it is a suitable choice of components for the cost reduction and high yield hydrogen production, storage, and consumption.

Keywords

energy storage; thermal energy; green hydrogen; trigeneration; energy transition.

Introduction

Facing the challenges to act against global warming, reducing the world's energy consumption is one of the big challenges. Sustainable development is the main action that will enable our planet to address the challenges of global warming. Considering the World population increase, and the climate changes observed in the World [1], indeed a paradigm shifts in the energy sector is essential for the future of humanity. The circular economy,

renewable energy, and energy efficiency are key aspects of current economies and allows changing the way the World consumes the energy. To address all these challenges, the production and storage of energy play a key role. Therefore, the number of power plants producing electricity from renewable energy is growing considerably around the World. However, with an increase in the renewable energy production, there is proportional growth in energy storage systems (ESS). ESS occupies an equally important place in the energy transition because electricity from renewable energies such as solar energy and wind energy is unstable over time due to the intermittency of these energy sources. Hence, it is important to store this energy for consumption corresponding to the actual needs of the humankind. There are several types of energy storage systems [2,3]. The effects of the global warming observed and those planned require the use of a so-called clean ESS. To meet this need, the strategy for ESS, especially for the energy produced from renewable sources, in particular solar and wind power, relies in the hydrogen production and storage [4]. The use of hydrogen continues to increase and today, several countries have allocated a considerable percentage of their GDP in the R&D on the hydrogen area [5]. On the other hand, the hydrogen can find its application in all scales, ranging from the tertiary sector to industry including transport [6,7]. Nowadays, the main obstacle in the use of green hydrogen as an energy storage is its production cost. The solution to improve the economic analysis of the hydrogen production is to consider the recovery of thermal energy, resulting from the production of hydrogen. Several studies demonstrated integrated cogeneration and trigeneration as an approach to increase in the energy efficiency and to reduce the cost of ESS of green hydrogen [8–11]. Other technical and economic studies [9,11] highlighted a possible cost reduction of the hydrogen production by recovery of the generate heat. It should be noted that one of the energy-intensive sectors in terms of demand for thermal energy, especially for air conditioning and for the sanitary hot water, is the tertiary sector. Hence, this work aims to demonstrate the integration of green hydrogen production in the households. For this purpose, this work proposes the study on a modelling and a design of an energy generator based on hydrogen storage for use at the medium and small scales. This work is an advance in comparison to already existing batteries, such as the first hydrogen fuel cell for domestic use [12], which mark the importance of the use of hydrogen in the tertiary sector.

Methods

The results presented in this study rely on the conceptual modelling of the hydrogen generator. This considers the bibliographic data and implementation of them in the numerical modelling of the entire designed system. The modelling was performed using MATLAB® Simulink R2013a. The heart of MATLAB is the MATLAB language, a matrix-based language allowing the most natural expression of computational mathematics. The modelling was performed until the coherent iteration all of elements was satisfactory and obtained results were consistent. PVsyst 6.8.1 software was used to perform the calculations regarding the energy production by the photovoltaic systems. PVsyst is a PC software package for the study, sizing and data analysis of complete PV systems. It deals with grid-connected, stand-alone, pumping and DC-grid (public transportation) PV systems, and includes extensive meteorological and PV systems components databases, as well as general solar energy tools.

Results and discussion

Energy conception profile

To properly model and design the generator, the energy consumption profile of a standard household was considered. The simulation of energy consumption was established on the basis of PVsyst software. This simulation allowed evaluating the energy to be produced by the generator and the number of photovoltaic panels needed to power it. The study of household energy consumption was done over three intervals, the day (6 a.m. - 6 p.m.), the evening (6 p.m. - 12 a.m.), and the night (12 a.m. - 6 a.m.).

Table 1. The consumption behaviour between 6 a.m. and 6 p.m. *Source: Author.*

Number	Appliance	Power (W)	Daily use (h/day)	Daily energy (Wh)
8	Lamps	20	1	160
2	Fridge	110	12	2640
1	Washing machine	600	0.5	300
1	TV	150	6	900

Table 2. The consumption behaviour between 6 p.m. and midnight. *Source: Author.*

Number	Appliance	Power (W)	Daily use (h/day)	Daily energy (Wh)
8	Lamps	20	7	1120
2	Fridge	110	6	1320
1	Washing machine	600	0.5	300
4	Lamps exterior	36	6	864
1	TV	150	6	900
1	Stand-by consumer	24	1	24

Table 3. The consumption behaviour between midnight and 6 a.m. *Source: Author.*

Number	Appliance	Power (W)	Daily use (h/day)	Daily energy (Wh)
8	Lamps	20	1.5	240
2	Fridge	110	6	1320
4	Lamps exterior	36	6	864
1	TV	150	1	150
1	Stand-by consumer	24	1	24

Tables 1-3 give us an overview of the profile standard consumption evaluated on PVsyst. The estimated power consumed was 980W without heating and air conditioning. The simulation of the number of solar panels presented in Figure 1 shows the need for 24 solar panels to satisfy the expected consumption.



Figure 1. PVsyst simulation of solar panels needed to support the household energy consumption: 1 type of the regulation mode and the regulator; 2 - the power of the inverter sized for the total consumption; 3 - the number of solar panels to be put in series, i.e., 4 and in parallel, i.e., 6; 4 - the total power supplied by the 24 solar panels. *Source: Author.*

The proposed generator is expected to cover the previously defined consumption. Furthermore, the proposed generator uses components such as electrolyzer, MH storage tank, fuel cell, and converter from different manufacturers presented below. The manufacturers were selected taking into consideration the expected dimensions and in terms of technical characteristics corresponding to the defined design.

Selection of the PEM fuel cell (PEMFC) [13,14].

The selected generator can deliver 1000 W, which is necessary to cover the demand of 980 W observed in this case study.

The maximum useful power provided by the battery fuel is:

$$(1) \quad P_{ufc} = \eta_{fc} \times P_{abs_fc}$$

where P_{ufc} - the utile power; η_{fc} - the fuel cell efficient, P_{abs_fc} - the power absorbed, Q_{max} (L/min) – the maximum volume flow; P_c - the power consumed; Q_{ch} - the hydrogen volume flow generated; t_c – the production or consumption time; E_c - the energy consumed; h_2l - the quantity of hydrogen produced

in liters. As presented above, the consumption profile is divided into 3 parts. For a maximum power of 1000 W, the maximum flow rate is 23.4 L/min, therefore, to produce 335.33 W required to supply the household between 6 a.m. and 6 p.m., the flow rate should be reduced for a proper management of the hydrogen stock in the generator. The power production is needed to be adjusted according to the power demand as given in Tables 4, 5 and 6 in the corresponding consumption periods using the following formula.

$$(2) \quad Q_i = P_i \times \frac{Q_{max}}{1000}$$

Table 4. The fuel cell behaviour between 6 a.m. and 6 p.m. *Source: Author.*

Components	Rating values
P_{abs_fc} (W)	2000
Q_{max} (L/min)	23.4
Production time (h)	12
P_c (W)	335.33
Q_{hc} (L/min)	7.84
t_c (h)	12
E_c (Wh)	4024
h_{2l} (L)	5649.69

Table 5. The fuel cell behaviour between 6 p.m. and midnight. *Source: Author.*

Components	Rating values
Q_{hc} (L/min)	16.49
E_c (Wh)	4229
P_c (W)	704.83
h_{2l} (L)	5937.52
t_c (h)	6
h_{2l}	12.56

Table 6. The fuel cell behaviour between midnight and 6 a.m. *Source: Author.*

Components	Rating values
Q_{hc} (L/min)	10.13
E_c (Wh)	2598
P_c (W)	433
t_c (h)	6
h_{2l} (L)	3647.59

Data given in Tables 4-6 allows estimating the quantity of hydrogen to be stored. Table 4 shows that for the estimated consumption between 6 a.m. and 6 p.m., i.e., 4024 kWh, the fuel cell consumes 5650 L of hydrogen. For other periods, i.e., from 6 p.m. until midnight and from midnight until 6 a.m., the consumptions are of 5937 L and 3647 L, respectively. In total, as much as 15235 L of hydrogen is needed.

Selection of the PEM electrolyser [15].

The hydrogen production in the electrolyser is done mainly due to the photovoltaic energy, which is only available during day. Therefore, a key to cover the energy demand during the night is a choice of the proper electrolyser (Table 7) able to ensure the adequate hydrogen flow rate also to obtain the desired quantity of hydrogen to be stored. The average sunshine time is estimated at 8 hours as given by PVgist.

Table 7. The electrolyser production performance for 8 hours. *Source: Author.*

Components	Rating values
Q_{elh}	1.57
η_{el}	75
Nominal power (kW)	5
tc (h)	8
h2f (Nm ³)	12.56
m_{h2}	1.11
h2s (L)	15737.196

The estimated quantity of hydrogen stored in 8 hours can be calculated using the following equations:

$$(3) \quad V_{h2} = Q_{elh} \times t$$

where V_{h2} (Nm³) is the volume of hydrogen produced during 8h, Q_{elh} (Nm³/h) is the maximum flow rate of hydrogen in the electrolyser, and tc represents the total production time in hours.

$$(4) \quad m_{h2} = 0.044 \times M_h \times V_{h2}$$

where m_{h2} is the total mass of hydrogen produced in kg.

Therefore, the total volume of hydrogen produced in liters can be calculated using the following formula:

$$(5) \quad V_h = 14128 \times m_{h2}$$

where 14128 represents the volume of 1 kg of hydrogen expressed in liters.

The volume of hydrogen produced by the selected electrolyzed corresponds to 15737.2 liters, which is superior to expected consumption of the PEM fuel cell, which is 15235 liters as given in Table 7. It is fundamental to note that the selected fuel cell provides an output voltage between 24 – 40 Vdc and will provide a maximum current of 80 A.

Thus, this voltage range is suitable for a 24 Vdc-220 Vac/2000 VA [16] inverter intended for the supply of undulating current. In addition, a buck-booster [17] is integrated into the generator to raise the voltage of the photovoltaic field to 125 Vdc nominal voltage of the electrolyser.

Selection of MH tank

Evaluation of storage characteristics in a MH tank according to the electrolyser productivity is given in Table 8.

Table 8. Electrolyser productivity. *Source: Author.*

Components	Rating values
h2f (L)	15737.196
h2f (Nm ³)	13.29
h2f (m ³)	5

Several types of MH tanks for hydrogen storage are available in the industry. Hence, exist a vast number of the research studies on MH tanks [18–23]. For the purpose of this work, a model given in Figure 2 was selected according to its storage capacity, its weight, the size, and the thermal energy dissipated. To address the demand for the hydrogen storage capacity, i.e., 1.11 kg, as many as 24 MH tanks are need.



Figure 2. MH tube [22].

Table 9. Fundamental characteristics of the MH tank given in Figure 2. *Source: Author.*

Components	Rating values
Diameter (m)	0.0508
Storage capacity (g)	50
Height (m)	0.64
weight (kg)	4.4
Number	24
Clutter (m)	$0.6096 \times 0.116 \times 0.64$
Weight (kg)	101.2

Selection of an adsorber

In the design of the generator intended to provide electricity, heating, air conditioning, and sanitary hot water, besides the heat loss management system, one of the most important elements is the absorber. The adsorber must be sized to provide the air conditioning and heating power required for a standard household adapted in this study. According to Fernandez et al. [24] it can be estimate that an average annual consumption of 125.54 kWh/m², 22.24 kWh/m², and 13.025 kWh/m² for heating, air conditioning, and the sanitary hot water, respectively is needed. In the case of the tropical regions of Africa, the consumption related to air conditioning is at 200 kWh/m² [25]. Therefore, in this study, an adsorber capable of producing 12500 kWh/year, 2200 kWh/year, and 1300 kWh/year for heating, air conditioning, and the sanitary hot water, respectively should be considered. This data is given in Table 10.

Table 10. Heating Ventilation and Air Conditioning (HVAC) consumption. *Source: Author.*

Heating	Air conditioning	Sanitary hot water
12500 kWh/year	2200 kWh/year	1300 kWh/year
32.24 kWh/day	6.027 kWh/day	3.56 kWh/day

The adsorber selected in this system is based on the models presented in the literature [26–31]. Table 11 presents the characteristics of the main component of the adsorber.

Where m is the mass of the adsorbent or the refrigerant, respectively in the adsorption/desorption chambers and the condenser and the evaporator (kg), C_p is the heat capacity (J/(kg·K)), U heat transfer coefficient (W/(m²·K)), A is exchange area (m²), q is the amount of water vapour uptake (kg/kg), t is the fluid circulation time (s).

Through the numerical simulation and the dimensions of the internal components of the adsorber defined in Table 11, the total dimension of the absorber can be estimated using the following equation:

$$(6) \quad A_{ad} = 2 \times \left(\sum_{i=1}^4 A_i \right)$$

where A_i is the surfaces of the adsorption/desorption chambers, condenser, and evaporator.

Table 11. Characteristic of the adsorber. *Source: Author.*

Units	Adsorber	Desorber	Evaporator	Condenser
m (kg)	50	50	20	25
Q (l/min)	0.35	0.35		
Cp (J/(kg·K))	20	20	15	20
UA (w/k)	85.45	90.47	257.05	475.73
Cp.m (J/K)	347.37	231.58	744.91	935.16
t cycle(s)	120	120	120	120
U (W/(m ² ·K))	1700	1800	2557	4115
A (m ²)	0.050	0.050	0.1005	0.1156
Cp (Cu)	386	386	386	386
Cp (H ₂ O)	4185	4185	4185	4185

Selection of the heat exchanger management system

As mentioned above, one of the characteristics of the proposed generator is its heat recovery system. The electrolyser, the fuel cell, and the MH hydrogen storage tanks emit a considerable amount of heat, which is generally lost. In the proposed energy generator, two flat tubes heat exchangers are designed to recover the heat losses. In addition, the MH tank is contained in a heat exchanger similar to a Shell- and tube exchanger (Figure 3).

Table 12. Exchanger characteristics. *Source: Author.*

Air to water exchanger	Exchanger in electrolyser	Exchanger in fuel cell	Exchanger MH
Q min (kg/s)	0.0017	0.0017	
Q max (kg/s)	0.0588	0.0588	
Dc (mm)	15	15	508.8
L (m)	1.42	2.48	0.64
Material	Coil	Coil	Coil
Dimensions (mm)	230x110x50	260x150x50	370x240x660
Tube number	6	8	23
Fins number	20	24	
Thickness (mm)	3	3	5

Using data given in Table 12, the various flow rates and the approximate stored quantities of water can be calculated using the following equations:

$$(7) \quad S_{inx} \cdot v_{inx} = S_{ox} \cdot v_{ox}$$

$$(8) \quad t_D = \frac{V}{v \cdot S}$$

where S_{inx} (m²) is the section of the vein of the entering fluid, v_{inx} (m/s) is the flow velocity of the entering fluid respectively, S_{ox} is the section of the outgoing fluid pipe, v_{ox} is the outgoing fluid velocity, t_D (s) is a duration of the water course in the MH exchanger and Dc is the intern diameter. Therefore, after defining all the devices necessary for the generator, they are installed in the most suitable ergonomics according to the dimensions obtained in the design study as shown in Figure 4. A medium-sized generator obtained is of 1800 × 1000 × 500 mm size.

Such proposed energy generator allowed obtaining different profiles of variation of the energy flows. To validate its adequacy the modelling of the system in the real environment was modelled. As such Figure 5 presents

the solar irradiation over 24 hours. During the experiment, the simulation of the entire system lasted 50 min in real time for implementation of 5 s on MATLAB Simulink.

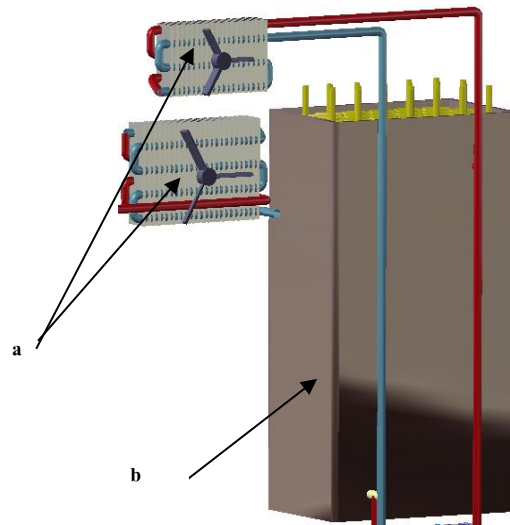


Figure 3. Heat exchanger system: (a) two flat tubes heat exchangers; (b) Shell- and tube exchanger. *Source: Author.*

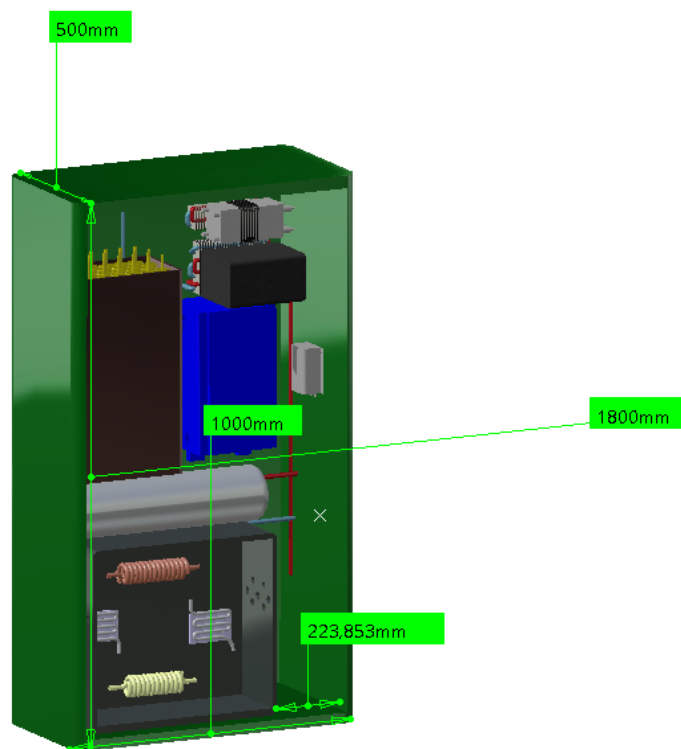


Figure 4. Internal view of the energy generator by hydrogen storage. *Source: Author.*

Thus, it was note that the solar irradiation increases between 1 s-2.5 s, i.e., between 6 a.m. and 1 p.m., then decreases between 1 p.m. and 7 p.m. The results presented below are basis of this solar radiation profile.

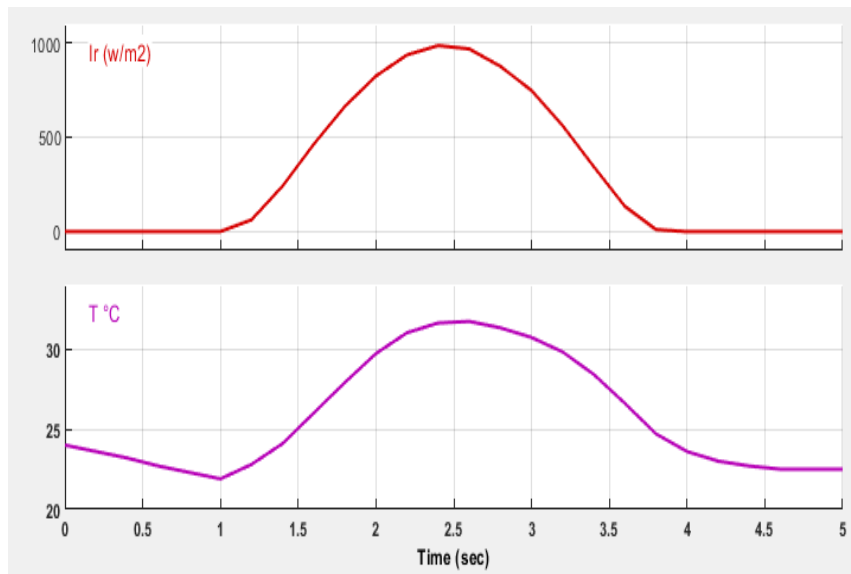


Figure 5. Solar irradiation in Morocco between 1 a.m. and 12 a.m. *Source: Author.*

Figure 6 presents the characteristics of the variations of the thermal flows according to the time of operation of the electrolyser.

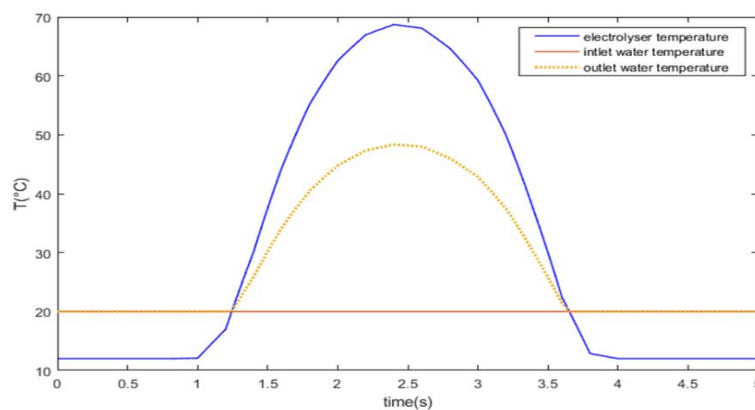


Figure 6. Electrolyser-exchanger heat flux curve. *Source: Author.*

The photovoltaic field produces useful energy in the time interval of 1.25-3.25 s, i.e., between 9 a.m. and 5 p.m., which corresponds to approximately 8 h. It can be noticed that during this time, the temperature in the electrolyser increased and reached 68°C. Thus, the cold water that enters the exchanger at a temperature of 22 °C can be heated up to 49 °C. During the heating period, which lasts about 6 hours, from 9 a.m. to 3:30 p.m. the quantity of hot water stored is approximately 38 liters. Figure 7 shows the heat flow characteristics in MH tanks responsible for hydrogen storage. As it can be observed, the variation of heat in the heat exchanger occurs and a temperature in the MH increases rapidly until it reaches maximum during the exothermic period, i.e., 130°C. During this time, the cold water, which enters at 25°C can increase its temperature from 80°C to 100°C. This increase in heat is observed between 9 a.m. to 3:30 p.m.

Following results given in Figure 7, the evolution of the temperature in the fuel cell during its operation can also be noticed as given in Figure 8. The heat generated by the PEM cell reaches 80°C and it allows heating up the cold water, which enters the exchanger at a temperature of 25°C, to temperature of 68°C. In this experiment, the adsorber is fed by hot water coming from the storage tank coming from the heat exchanger of the electrolyser, the MH tank, and the fuel cell combustion. The energy of hot water stored in the storage tank can be calculated using the following equation:

$$(9) \quad \varphi = m_{T1}C_{p1}(T_1 - T_f) = m_{T2}C_{p2}(T_f - T_{T2})$$

where C_p is the specific heat capacity and m_{T2} is the mass.

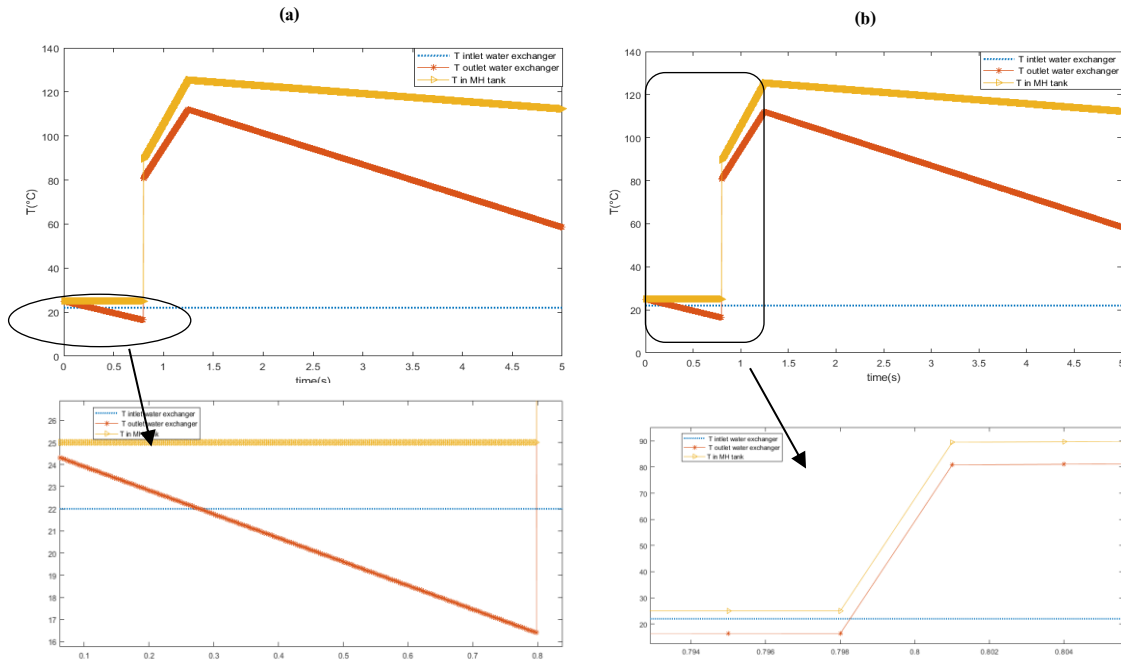


Figure 7. Characteristic of the heat exchange of the system MH-exchanger with enlarged views: a – up to 0.8 s, and b – from 0.793 to 0.805 s. *Source: Author.*

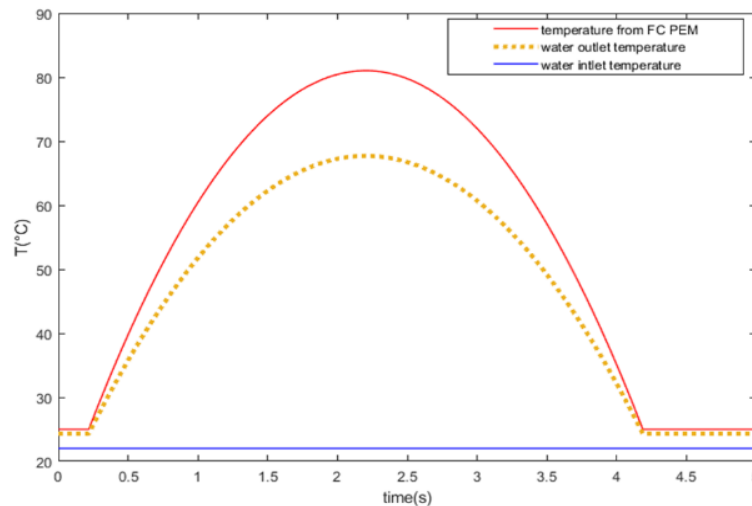


Figure 8. Heat variation in the fuel cell and its heat exchanger. *Source: Author.*

Figure 9 demonstrates the changes in the hot water temperature. The water stored in the tank reaches 85°C and the evolution of the temperature of the water stored in the tank occurs between 9 a.m. and 3 p.m. for the hot water coming from the MH and the one coming from the electrolyser. The total quantity of water stored is approximately 949 liters. The data3 curve represents the variation of data1 and data2 temperature curves mixed. The water stored in the container allows the supply of the absorber, which provides the air conditioning and heating of the building and the supply of hot water to the MH tank for the desorption of the stored hydrogen and to cover the needs for the sanitary hot water. During the period from sunshine on, the storage and the adsorber is supplied with hot water from the mixture as given in Figure 9. Figure 10 demonstrates the thermal and cooling production power where the productivity of the adsorber is fed by the hot water mixture MH-electrolyser and MH-electrolyzer- fuel cell.

Note that the desorption of hydrogen in the MH is carried out by the hot water stored in the balloon, and to accelerate the desorption this water is superheated by resistors, which raise the temperature from 80 to 120°C . The resistors integrated in the exchanger are powered by a $2\text{V}/100\text{Ah}$ battery allowing overheating for

more than 12 hours. Table 13 demonstrates basic characteristics resulting from the sizing justifying the choice of a 2V/100Ah battery. The following equations allows obtaining the characteristics of resistant present in Table 13.

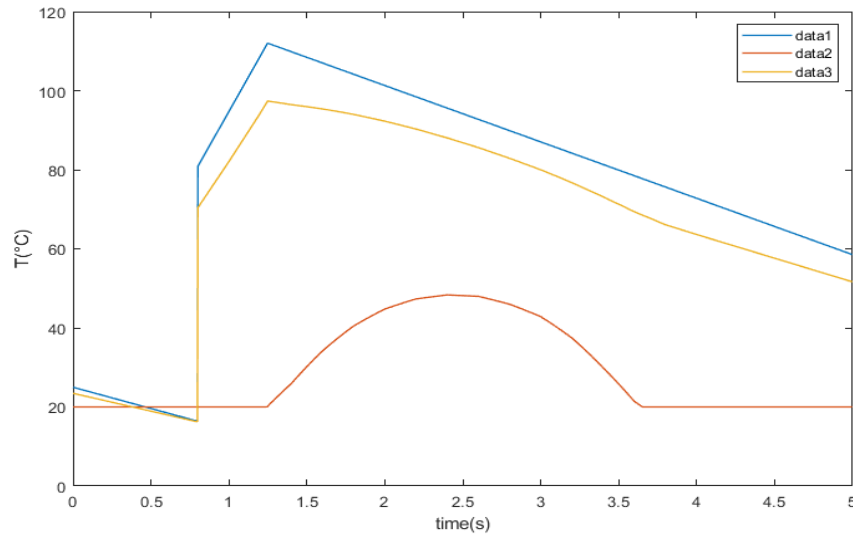


Figure 9. Hot water temperature in the storage tank (data1 and data2 represent the hot water Coming from the MH exchanger and the electrolyser exchanger, respectively. Data3 represents the variation of data1 and data2 mixed). *Source: Author.*

$$(10) \quad R = \rho \frac{L}{S} = m_{T2} C_{p2}$$

$$(11) \quad (T_f - T_{T2})$$

$$(12) \quad R_{45} = R[1 + (\Delta\theta\alpha_{cu})]$$

$$(13) \quad R_{120} = R_{80}[1 + (\Delta\theta\alpha_{cu})]$$

$$(14) \quad U = RI$$

Where R , R_{45} , R_{120} are the resistances of the heating rods at 0 °C, 45 °C et 120 °C, ρ is the resistance of copper ($\Omega \cdot m$), α_{cu} (K) is the temperature coefficient, $\Delta\theta$ (K) is temperature, L (m) is the rod length, $S(m^2)$ is the rod section, $U(V)$ is the voltage and I (A) is the current sent to the heating resistor, C is the battery capacity (Ah).

Table 13. Characteristics of the 24 heating resistors integrated into the MH heat exchanger. *Source: Author.*

Components	Rating values
S (m^2)	0.000020568
L (m)	0.64
ρ ($\Omega \cdot m$)	$1.725 \cdot 10^{-8}$
α_{cu} (K)	0.00393
R (Ω)	0.000536
R_{120} ($\Omega \cdot m$)	0.471
U (V)	2
I (A)	4.245
C (Ah)	76.4180

As presented in the section related to the adsorber selection, thermal and cooling consumption is on average 125.54 kWh/m², 22.24 kWh/m², and 13.025 kWh/m² for heating, air conditioning, and the sanitary hot water, respectively. The proposed absorber produces as much as 13.42 kW as cooling power and 33.29 kW as thermal power during the 50 min, which represents a day according to the performed simulation. Thus, to compare this data to this given in Table 10 it can be concluded that the proposed solution satisfies the estimated needs.

Thus, the evolution of the heating and cooling powers from the adsorber is shown in Figure 10.

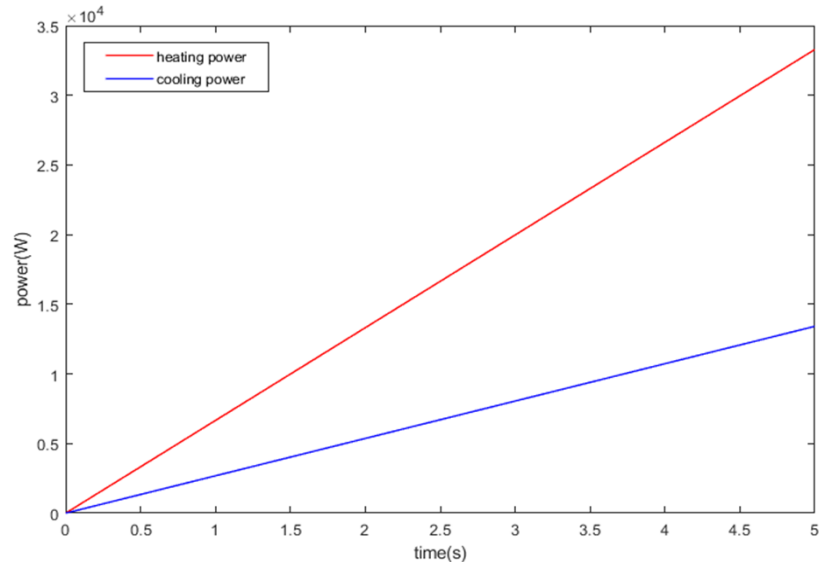


Figure 10. Characteristics of the heating and cooling capacities of the absorber. *Source: Author.*

Impact

This work contributes to the area of green hydrogen production and use. In more general term, this work helps to create solutions for more renewable energy use and contributes to the general changes against the global warming. This work depicts the role and importance of an energy storage based on technologies relied on hydrogen. Through this article, it can be seen that an energy storage based on green hydrogen will have a considerable impact especially when integrated with co- and trigeneration approaches combined with the process of production and storage of hydrogen for further electricity production. The real impact of this research is the innovative design of an all-in-one energy generator, based on the use of green hydrogen. This model shows that a generator is capable to store energy by means of green hydrogen, providing electricity, the sanitary hot water, cold and heating. Consequently, it contributes to the reduction of green hydrogen cost and in parallel impact the fight against global warning provoked by the energy production. Knowing that the electricity production sector generates approximately 40% of global pollution [32] and that the tertiary sector is among the largest energy consumers (electricity, the sanitary hot water, heating and cooling), the design and marketing of such an energy generator will contribute to the reduction of the CO₂ emissions resulting from the use of electricity in this sector. The particularity of this article is that it presents a novel technical energy efficiency solution allowing obtaining a favourable economic performance. It is possible to achieve by the green hydrogen production via electrolysis of water and the hydrogen storage in MH to be later used for electricity production by a PEM fuel cell. The process is completed by a thermal energy recovery system. This in turn, makes possible to demand for the sanitary hot water and heating. In addition, due to the use of absorber the needs for cold is ensured too. Ultimately this article demonstrates energy innovation approach by showing that even at household size an energy storage can be efficient and can play an important role for the tertiary sector.

Conclusion

This work showed the design of an energy generator as an energy storage system, the production of hydrogen by electrolysis of water via a PEM electrolyser through photovoltaic energy. The proposed energy efficiency generator allows for a maximum heat recovery from production, storage, and electricity generation obtained from green hydrogen. All the main components were dimensioned so that the size of the generator is suitable for a common use in the residential - tertiary and industrial sectors. It is mainly composed of a 5kW PEM

electrolyser, a 2 kW PEM fuel cell, 24 MH tubes with a capacity of 50 g each, an absorber, heating resistors, a 2V/100Ah battery, an oxygen storage tank, a DC-AC converter, a boost DC-AC converter, and several heat exchangers. The overall dimension of the generator block is $1800 \times 1000 \times 500$ mm. Through modelling, component sizing, and simulation, it was possible to confirm that the proposed solution can store up to 949 liters of hot water in the temperature range from 49 to 85°C and ensure the storage of 1.11 kg of hydrogen for the energy consumption of 6.9 kWh from 6 p.m. to 6 a.m. In addition, the absorber integrated into the generator makes it possible to produce 33.29 kW of heating power with 13.42 kW of cooling power per day. This study allowed to demonstrate that the PEM electrolyser - PEM fuel cell - MH tank combination provides significant thermal power that can be used to cover heating, the sanitary hot water, and air conditioning needs. Thermal and cooling consumption is of 125.54 kWh/m², 22.24 kWh/m², and 13.025 kWh/m² for heating, air conditioning, and the sanitary hot water, respectively. It can be also noted that absorber produces 13.42 kW as cooling power and 33.29 kW as thermal power during the period equivalent to full day of simulation. The results obtained in this study confirm that an energy generator coupled to the hydrogen storage can have an optimal yield due to high energy efficiency and thus make it possible to obtain a cost of integration of hydrogen for very competitive small and medium scale use.

Conflict of interest

There are no conflicts to declare.

Acknowledgments

This research has not been supported by any external funding.

References

- [1] Working Group I Contribution to the Sixth Assessment Report of the Intergovernmental Panel on Climate Change, Climate Change 2021: The Physical Science Basis Summary for Policymakers, 2021. <https://reliefweb.int/report/world/climate-change-2021-physical-science-basis>.
- [2] M.S. Guney, Y. Tepe, Classification and assessment of energy storage systems, *Renew. Sustain. Energy Rev.* 75 (2017) 1187–1197. <https://doi.org/10.1016/j.rser.2016.11.102>.
- [3] A.B. Gallo, J.R. Simões-Moreira, H.K.M. Costa, M.M. Santos, E. Moutinho dos Santos, Energy storage in the energy transition context: A technology review, *Renew. Sustain. Energy Rev.* 65 (2016) 800–822. <https://doi.org/10.1016/j.rser.2016.07.028>.
- [4] M. Kayfeci, A. Keçebaş, Hydrogen storage, in: *Sol. Hydrog. Prod.*, Elsevier, 2019: pp. 85–110. <https://doi.org/10.1016/B978-0-12-814853-2.00004-7>.
- [5] GEA34805 (03/22), Hydrogen for power generation; Experience, requirements, and implications for use in gas turbines, (2022).
- [6] Fuel Cells and Hydrogen 2 Joint Undertaking, A sustainable pathway for the European Energy Transition Hydrogen Roadmap Europe, 2019.
- [7] D. Parra, M. Gillott, G.S. Walker, Design, testing and evaluation of a community hydrogen storage system for end user applications, *Int. J. Hydrogen Energy.* 41 (2016) 5215–5229. <https://doi.org/10.1016/j.ijhydene.2016.01.098>.
- [8] K. Maeda, M. Suzuki, H. Aki, R&D and deployment of residential fuel cell cogeneration systems in Japan, in: 2008 IEEE Power Energy Soc. Gen. Meet. - Convers. Deliv. Electr. Energy 21st Century, IEEE, 2008: pp. 1–5. <https://doi.org/10.1109/PES.2008.4596046>.
- [9] P.M. Laince, T. Abdelwahed, O.E. Akpoviroro, R. Nabila, Mathematical modeling of re-electrification by green hydrogen storage through the PEM fuel cell integrating a 10-year economic study applied to a hotel, *E3S Web Conf.* 229 (2021) 01038. <https://doi.org/10.1051/e3sconf/202122901038>.
- [10] M.. L. Pierre, T. Abdelwahed, R. Nabila, Implementation of an Advanced PEM Hydrogen Storage System Based Cogeneration Using Photovoltaic System in a Building, in: 2020 Int. Conf. Control. Autom. Diagnosis, IEEE, 2020: pp. 1–6. <https://doi.org/10.1109/ICCAD49821.2020.9260552>.
- [11] G. Zubi, Technology mix alternatives with high shares of wind power and photovoltaics—case study for Spain, *Energy Policy.* 39 (2011) 8070–8077. <https://doi.org/10.1016/j.enpol.2011.09.068>.
- [12] B. Deboyser, La toute première batterie domestique à hydrogène : quel est son intérêt ?, (2021). <https://www.revolution-energetique.com/la-toute-premiere-batterie-domestique-a-hydrogene-quel-est-son-interet/>.
- [13] Techfine 24v 48v Hybrid Solar Inverter 1/2/3/4/Skva Off Grid Mppt Solar Power Inverter - Buy Hybrid Solar Inverter Product on Alibaba.com, <https://french.alibaba.com/product-detail/techfine-24v-48v->

- hybrid-solar-inverter-1-2-3-4-5kva-off-grid-mppt-solar-power-inverter-1600209524603.html?spm=a2700.galleryofferlist.normal_offer.d_image.49d22addEBzw3O&s=p,(2021)
- [14] G-HFCS-2kW25V (2kW Hydrogen Fuel Cell Power Generator), <https://www.fuelcellstore.com/g-hfcs-2kw25v-1kw-hydrogen-fuel-cell-power-generator>, (2021).
- [15] PEM-Elektrolyse-Stack S30: H-TEC Systems Produkte, <https://www.h-tec.com/en/products/>, (2021).
- [16] Techfine Pur Onde Sinusoidale 8kw Ondeuleur Hybrid 10kva Onduleur 48kv Onduleur Solaire Systeme-Buy 8kw Hybrid Inverter 10 kva Power Inverter Solar Power Inverter System Product on Alibaba.com, https://french.alibaba.com/product-detail/techfine-pure-sine-wave-8kw-hybrid-inverter-10kva-power-inverter-48v-solar-power-inverter-system-1600196276975.html?spm=a2700.galleryofferlist.normal_offer.d_image.26121e7fqUESJT&s=p, (2021).
- [17] M.N. Wg-s, Globle Shipping Globle Shipping.
- [18] M. Marinelli, M. Santarelli, Hydrogen storage alloys for stationary applications, *J. Energy Storage*. 32 (2020) 101864. <https://doi.org/10.1016/j.est.2020.101864>.
- [19] M.V. Lototsky, I. Tolj, L. Pickering, C. Sita, F. Barbir, V. Yartys, The use of metal hydrides in fuel cell applications, *Prog. Nat. Sci. Mater. Int.* 27 (2017) 3–20. <https://doi.org/10.1016/j.pnsc.2017.01.008>.
- [20] G. Karagiorgis, C.N. Christodoulou, H. von Storch, G. Tzamalīs, K. Deligiannis, D. Hadjipetrou, M. Odysseos, M. Roeb, C. Sattler, Design, development, construction and operation of a novel metal hydride compressor, *Int. J. Hydrogen Energy*. 42 (2017) 12364–12374. <https://doi.org/10.1016/j.ijhydene.2017.03.195>.
- [21] B.P. Tarasov, P.V. Fursikov, A.A. Volodin, M.S. Bocharnikov, Y.Y. Shimkus, A.M. Kashin, V.A. Yartys, S. Chidziva, S. Pasupathi, M.V. Lototsky, Metal hydride hydrogen storage and compression systems for energy storage technologies, *Int. J. Hydrogen Energy*. 46 (2021) 13647–13657. <https://doi.org/10.1016/j.ijhydene.2020.07.085>.
- [22] D. Brayton, A. Narvaez, Low Cost, Metal Hydride Based Hydrogen Storage System for Forklift Applications (Phase II), 2013.
- [23] M. V. Lototsky, M. Davids, T.I. Wafeeq, Y. V. Klochko, B.S. Sekhar, S. Chidziva, F. Smith, D. Swanepoel, B.G. Pollet, Metal hydride systems for hydrogen storage and supply for stationary and automotive low temperature PEM fuel cell power modules, *Int. J. Hydrogen Energy*. 40 (2015) 11491–11497. <https://doi.org/10.1016/j.ijhydene.2015.01.095>.
- [24] M. Fernandez, B. Cener, Heating and cooling energy demand and loads for building types in different countries of the EU, March (2014).
- [25] F. Foudazi, M. Mugendi, N.A. Rithaa, Sustainable solutions for cooling systems in residential buildings case study in the Western Cape Province, South Africa, 2010. <https://www.thesustainabilitysociety.org.nz/conference/2010/papers/Foudazi-M'Rithaa.pdf>.
- [26] Q. Pan, J. Peng, R. Wang, Experimental study of an adsorption chiller for extra low temperature waste heat utilization, *Appl. Therm. Eng.* 163 (2019) 114341. <https://doi.org/10.1016/j.applthermaleng.2019.114341>.
- [27] B.B. Saha, A. Akisawa, T. Kashiwagi, Silica gel water advanced adsorption refrigeration cycle, *Energy*. 22 (1997) 437–447. [https://doi.org/10.1016/S0360-5442\(96\)00102-8](https://doi.org/10.1016/S0360-5442(96)00102-8).
- [28] B.B. Saha, S. Koyama, T. Kashiwagi, A. Akisawa, K.C. Ng, H.T. Chua, Waste heat driven dual-mode, multi-stage, multi-bed regenerative adsorption system, *Int. J. Refrig.* 26 (2003) 749–757. [https://doi.org/10.1016/S0140-7007\(03\)00074-4](https://doi.org/10.1016/S0140-7007(03)00074-4).
- [29] M. Bilgili, Ö.E. Ataer, Numerical analysis of hydrogen absorption in a P/M metal bed, *Powder Technol.* 160 (2005) 141–148. <https://doi.org/10.1016/j.powtec.2005.08.018>.
- [30] B. Saha, A. Akisawa, T. Kashiwagi, Solar/waste heat driven two-stage adsorption chiller: the prototype, *Renew. Energy*. 23 (2001) 93–101. [https://doi.org/10.1016/S0960-1481\(00\)00107-5](https://doi.org/10.1016/S0960-1481(00)00107-5).
- [31] B. Han, A. Chakraborty, Adsorption characteristics of methyl-functional ligand MOF-801 and water systems: Adsorption chiller modelling and performances, *Appl. Therm. Eng.* 175 (2020) 115393. <https://doi.org/10.1016/j.applthermaleng.2020.115393>.
- [32] GEA33861 (02/2019), Power to gas: Hydrogen for power generation, (2019).

PHOTOVOLTAIC SYSTEM DESIGN FOR STRATEGIC INFRASTRUCTURE AND MOBILE COMMAND CENTRE


Jan Fabián*

Brno University of Technology
10 Technická, 616 00 Brno, Czech Republic, xfabia09@vutbr.cz
 <https://orcid.org/0000-0002-4761-0821>

Tomáš Binar

University of Defence
65 Kounicova, 662 10 Brno, Czech Republic, tomas.binar@unob.cz
 <https://orcid.org/0000-0003-4426-2857>

Pavel Šafl

Brno University of Technology
10 Technická, 616 00 Brno, Czech Republic, xsaf1p00@vut.cz
 <https://orcid.org/0000-0002-4430-3551>

Article history: Received 25 September 2022, Received in revised form 21 October 2022, Accepted 21 October 2022, Available online 21 October 2022

Highlight

This paper focuses on the design of photovoltaics systems for energy self-sufficiency of strategic infrastructure as well as mobile applications (e.g., command centres, first responders, refugee camps).

Abstract

With both the ecological and economical aspect of fossil fuels as a source of energy, the demand for renewable sources is rising. This paper aims to analyse two scenarios, which would benefit from the use of a photovoltaic system. In the first scenario, a strategically important warehouse is analysed, and a photovoltaic system is designed and simulated. In the second scenario, two designs of photovoltaic systems that could be used in mobile applications by first responders, military command centres, or during natural disasters are proposed. The results of the simulations are discussed and may serve as a basis for real-life system design and application.

Keywords

renewable energy; photovoltaics design; mobile PV applications; energy self-sufficiency.

Introduction

With the continuous development of renewable energy sources and the pursuit of clean energy, sources like photovoltaics, small wind turbines etc., have found great use in small-scale and stand-alone applications [1]. Based on this, the limitation of fossil fuels as a source of energy in remote areas, and the growing price of fossil fuels (tied to the economic crisis, the war in Ukraine etc.), designs for the replacement of fossil fuel sources by renewable energy sources are not only needed but also desired in many fields and applications [2]. Ranging from civil sector to military and first responders' applications, photovoltaic systems can present a reliable source of energy not only for strategically or otherwise important facilities (warehouses, hospitals, etc.) but also for mobile applications, such as command centres, refugee camps or the units of integrated rescue system for their operations in remote areas or disaster relief operations [3]. Mobile photovoltaic systems could present a reliable source of renewable energy in such operations and may also bring down the cost of such operations of the integrated rescue system. This paper aims to analyse two proposed scenarios that would benefit from the use of photovoltaic systems and to design and simulate those systems. For the use of photovoltaics for important infrastructure, the systems are mainly designed to increase energy self-sufficiency and can consist of multiple sources (i.e., photovoltaics and wind turbines). In mobile applications, the main goal is for the system to be easily transportable, modular, scalable, and not require specialized personnel to operate it. Currently, various versions of mobile photovoltaic and hybrid systems for use in stand-alone, remote applications as well as for military applications exist. Such examples can be the Alfons Mobile Energy Container [4], Energy Power Rack [5], and Multicon container [6] or various prototypes of hybrid systems for mobile applications [7] and other systems aimed at micro-grids for the use in applications such as refugee camps [8,9].

Methods

In order to appropriately evaluate the possible benefits and the negatives of the use of photovoltaics as a sustainable source of energy for important applications a two-step methodological approach – Analysis, Design & Simulation - was created. In the first step, we focused mainly on analysing the chosen scenarios. To design a system for important infrastructure, a central army warehouse was chosen based on its national and international strategic importance (from the viewpoint of NATO forces). On visits to this warehouse, we investigated the internal processes, the material stored there and the infrastructure of the army base.

A theoretical proposal of automated design for this warehouse was also considered. For the second scenario (mobile command centre), we discussed the importance of mobile command centres for fast response in the case of natural disasters such as tornadoes or floods. With the integrated rescue system needing a stable base of operation as well as a command centre, we focused especially on features such as mobility, modularity of the equipment and being energy self-sufficient [10]. A hypothetical situation based on historical floods in the town of Bohumin was used for this scenario. The second step consisted of creating a 3D model and a design of a practically applicable PV system for each scenario (Figure 1, Figure 2).



Figure 1. Warehouse PV system visualisation. *Source: Author.*

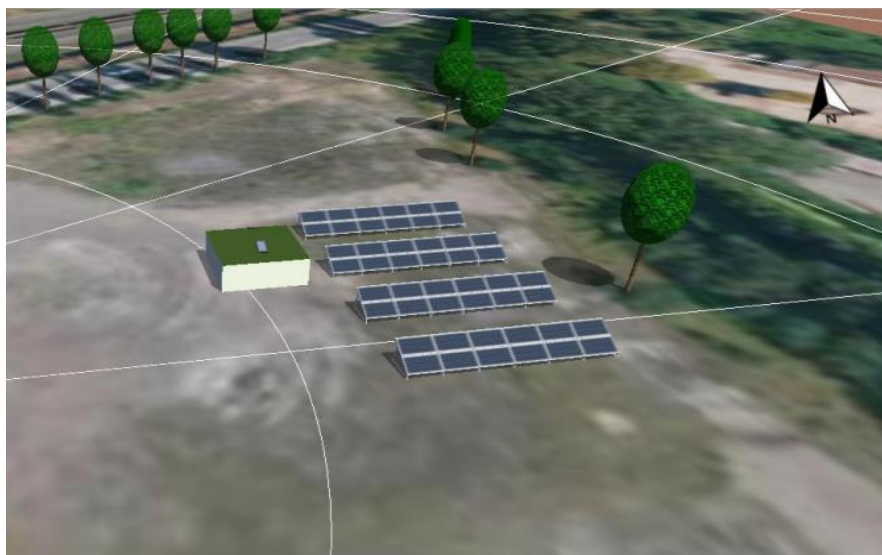


Figure 2. Mobile command centre PV system visualisation. *Source: Author.*

For the simulation of proposed solutions and their further optimization, PV*Sol software was used. Apart from the calculations, this system was also used for the creation of 3D models of the scenarios, which enabled us to account for external influences on the PV systems (e.g., shading). Based on the computed data, both systems were evaluated and optimized for better efficiency. Simulations for both scenarios were also run with the implementation of a backup generator into the system.

Automated warehouse scenario

The proposed automated design for a warehouse of 4 500 m² used for this scenario considers six automated ground vehicles (AGV) and a human staff of five employees. This means that there is no reduction in energy consumption due to safety standards needed for the human staff, however, the level of automatization promises increased efficiency in electric energy usage. Based on the analysis of the internal processes, case study on energy consumption in automated warehouses [11], other studies [12,13], and educated guess, the yearly energy consumption of the facility to be used in the design of the PV system was set as 415 000 kWh. Both the automatization and the importance of the facility to the Czech Armed Forces encourage the design of a solution for situations such as blackouts, which would also aim to increase the energy self-sufficiency of the facility. To guarantee energy self-sufficiency of important infrastructure even during blackouts, a practical solution used by GoodWe company was considered for the design (Figure 3) [14]. This solution uses regulated generators that are connected to the PV system, and are started in the case of grid failure, thus simulating grid parameters (voltage, FQ) needed for the operation of the inverters. They are also used to supply electricity into the system when the PV system is not operational (night, weather conditions).

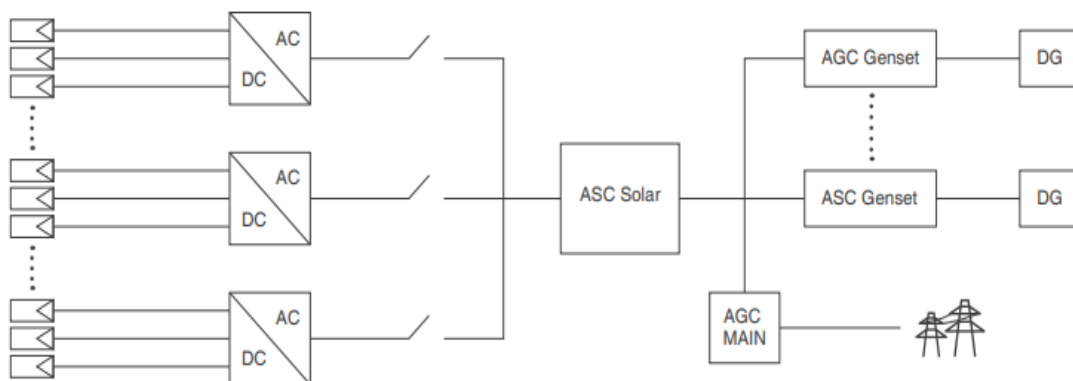


Figure 3. Backup generator scheme. Source: [14].

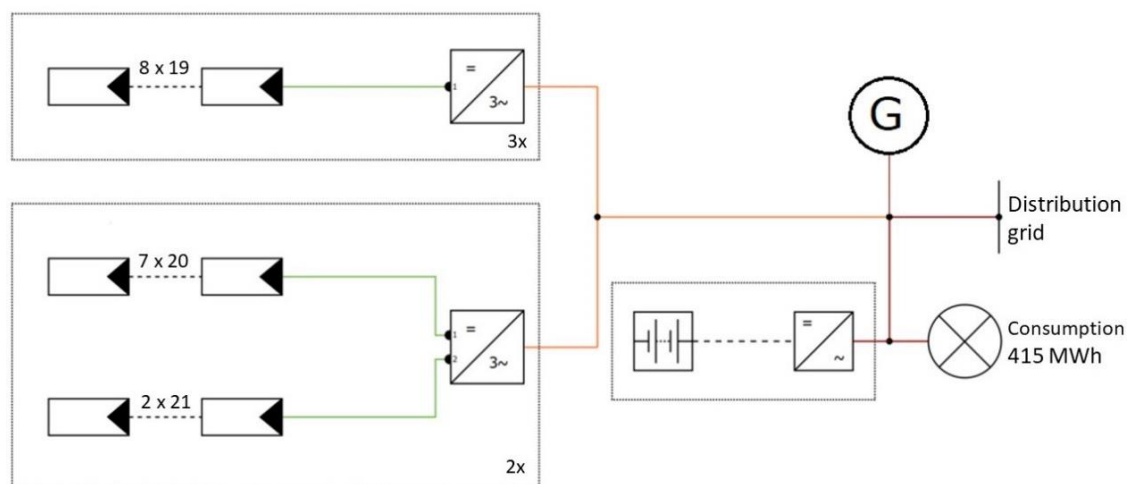


Figure 4. Schematic diagram of the proposed system. Source: Author

As the warehouse building by itself is not suitable for PV system installation, the roofs of surrounding buildings were chosen for the installation of the solar panels. Although the one inclined and six flat roofs offer ideal mounting surfaces, the SW (ca 220°) orientation reduces energy yield in the early mornings and creates slightly sub-optimal conditions for the system with energy being generated up to the late afternoon when the consumption is lower. This shows us the importance of batteries in the PV system as the available energy storage greatly increases the overall efficiency of the system.

The proposed PV system consists of 820 solar panels in total, with an installed power of 492 kWp. CanadianSolar HiKu7 CS7L-600 [15] panels were chosen for this system based on their 600 W peak output power and efficiency

of 21.2%. To convert the DC output to an AC output, five central inverters are used. These are GoodWe MT GW80KBF-MT [16] inverters with a nominal output of 80 kW. These inverters are able to work with very low starting voltages (200 V) and can work up to 150% of the nominal input voltage. From the wide range of generators used by the Czech Armed Forces, a three-phase, 60 kW 230/400V, diesel generator ČSAD-60-3-400 was used. Based on current trends in storage technologies, Lithium-iron-phosphate batteries made by Sonnen GmbH company were chosen.

To ensure enough capacity, a total of 540.6 kWh of battery capacity was used in the design. For the batteries to be able to be charged also by the grid or backup generator, they are connected in AC coupling. Although this type of connection introduces some losses of energy into the system, it is outweighed by the ability to be charged by sources other than solar power. A schematic diagram of the proposed system can be seen in Figure 4.

Mobile command centre scenario

The main goal of this scenario was to design and simulate a mobile photovoltaic system that would be able to provide electric energy for a command centre in a crisis, such as floods or other natural disasters. It was important for the proposed design to remain as mobile as possible and to supply enough energy. This was achieved with two designs, a fully off-grid photovoltaic system and an off-grid PV system with a backup generator. An interval of 6 months (April - September) was used for these simulations. This was due to the lesser probability of the need for mobile command centres during the rest of the year. Due to the lower availability of solar power during winter, completely self-sufficient system would not be optional. With regards to mobility, the design of a system with a backup generator would also be prioritised before other forms of hybrid systems. In the case of natural disasters or other situations, a command centre presents a strategically important part in the coordination of rescue teams and other forces. The design for this scenario was proposed with not only military applications in mind, but also the possibilities it presents for the integrated rescue system, who could utilize this system for assistance during natural disasters or in refugee camps [3,8,9]. Command centres should represent real control, communication, and coordination centres. To fulfil their tasks, conditions that are as suitable as possible for the planning and organization of activities need to be created. The organizational structure of the staff must also ensure and enable the issuing of tasks and cooperation with the state security forces in operation. For this, a constant and reliable supply of electrical power must be ensured [10]. Similar designs are also the goal of NATO initiative to reduce energy consumption of deployable camps [17]. For the design, optimization and simulation of the proposed PV system, a model of a command centre using a standard army tent was devised. Similar designs are also the goal of NATO initiative to reduce energy consumption of deployable camps. A list of electrical appliances for the needs of the command centre was created to simulate the load using PV*Sol database. The average total consumption of the mobile command centre per day was calculated as 55.73 kWh.

Table 1. Command centre electricity consumption per day. *Source: Author.*

Appliance	kWh/day
Electric kettle	0.56
Transmitters + chargers	10.98
Lights	1.10
Notebooks	36.43
Printer	5.23
Projector	1.43
Total	55.73

In total two designs were created for this scenario – with and without a backup generator. The solutions were designed with the aspect of mobility in mind. Thus, a solution using mobile trailers carrying the technology was used. A visualisation of a possible trailer design can be seen in Figure 5.

The first proposed system consists of one-phase inverters (GoodWe GW5048D-ES), AXITEC Li-ion batteries with a total capacity of 60.4 kWh and 18 pcs. of CanadianSolar HiKu7 CS7L-600 [15] 600 Wp solar panels. This is coupled with an army standard 4 kW/ 230 V generator that is operating when the energy produced from the sun is not enough to provide for the command centre. Visualisation of this design can be seen in Figure 6.

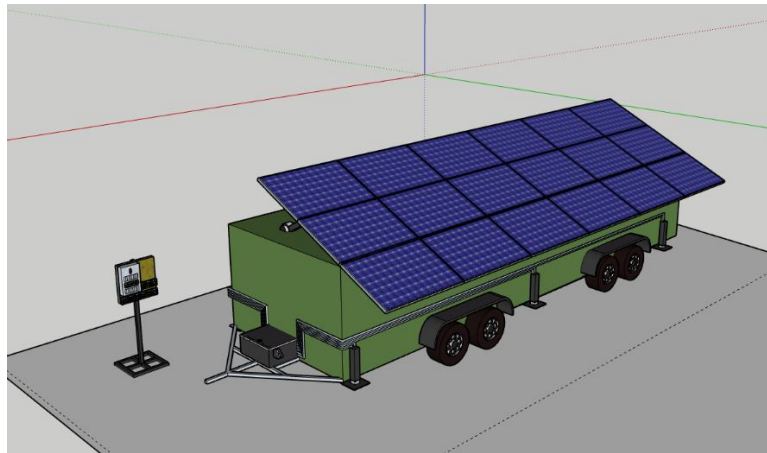


Figure 5. Visualisation of a mobile PV system trailer. *Source: Author.*



Figure 6. Visualisation of a PV system with a backup generator. *Source: Author.*

The main goal of the second design was to achieve full self-sufficiency of the command centre without the use of a generator. To achieve this, a total of 48 pcs. of PV panels needed to be used, along with a third inverter, and 16 batteries with a total capacity of 161 kWh. Due to the lack of a generator providing grid parameters, off-grid inverters (Fronius Simo 8) were used. This design eliminates the reliability of the command centre on fossil fuels, however, the space for the installation of such a system and the initial investment is much higher. The visualisation of the second proposed design can be seen in Figure 7.

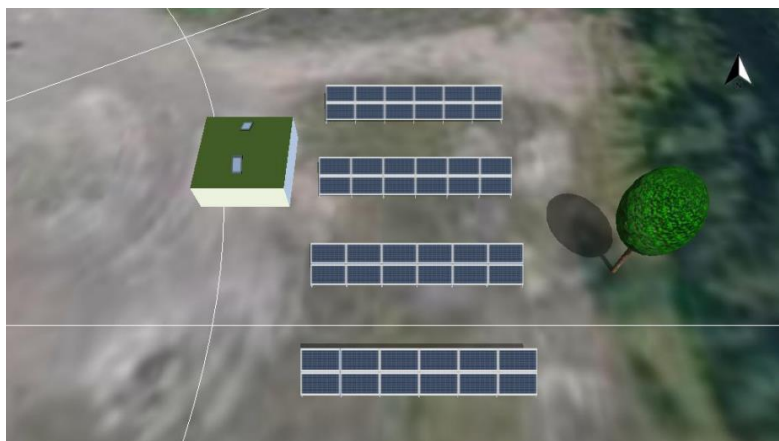


Figure 7. Visualisation of a fully photovoltaic system. *Source: Author.*

Results and discussion

Although the orientation and the tilt of PV panels have a significant effect on their efficiency and electricity production throughout the day [18], it may be easier sometimes to mount the panels in less favourable orientations (i.e. rooftop-mounted systems). Such systems then should be optimized through the technology used, battery capacity or consumption regulation, which may also assist in better solar energy utilization [19].

The main advantage of using simulation software is the amount of data that can be used to evaluate the benefits of the proposed designs beforehand. Based on the data from the simulations, the designs can be amended and optimized without any additional work. This also enables us to evaluate various conditions, such as the simulation of a blackout in the winter months. In mobile systems, we can use simplified calculation tools when placing the PV panels to ensure maximal efficiency based on the geographical place and time of year. Notable differences in the utilization of solar energy in different geographical locations can be observed in [20].

Automated warehouse scenario

Even though the used software lacks some simulation functions for a precise PV system with generator simulation, the created 3D design of a grid-tied system enabled us to account for losses and other influences on the system. The simulation was run as an on-grid system to simulate normal operations and then as an off-grid system to simulate power grid failure and get data about the backup generator usage in three days period with the lowest solar irradiation (21st-24th December) and the highest solar irradiation (22nd-25th June). The results of the simulation can be seen in Figure 8 below. Two parameters important for the design of a PV system are Own Power Consumption and Solar Fraction. The proposed PV system generates approximately 531 MWh/year. The Own Power Consumption parameter tells us that 58.4 % of it is used to power the facility and charge batteries, while the rest is sent to the grid. On the other hand, the Solar Fraction parameter is related to the consumption and, in our case, tells us that 72.7 % of the electric energy consumption was supplied by the PV system. The use of PV energy throughout the year is shown in Figure 9, where the generated energy surplus, especially in May-September, can be observed. This surplus occurs due to the amount of generated energy in days with lower consumption, as well as better irradiation conditions in the summer months in the Czech Republic. As this surplus of energy can be fed into the public grid and sold, it contributes to a faster return on the initial investment. We can also observe significant drop in the amount of generated power as the conditions during late autumn and winter are not satisfactory for PV systems. This, coupled with additional power consumption (e.g., heating), may in some situations prove the need of hybrid systems utilizing wind turbines, to be fully self-sufficient. Other methods of compensation for lower production and higher consumption, apart from the distribution grid, may be consumption regulations with the use of weather (and solar energy availability) forecasts [19].

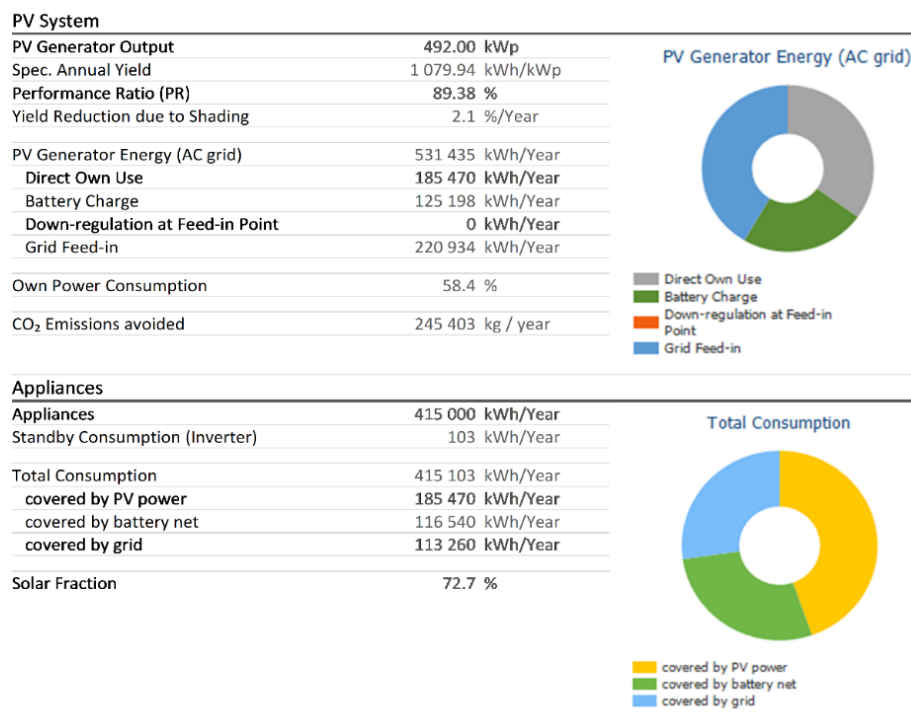


Figure 8. Simulation results (PV*Sol). Source: Author.

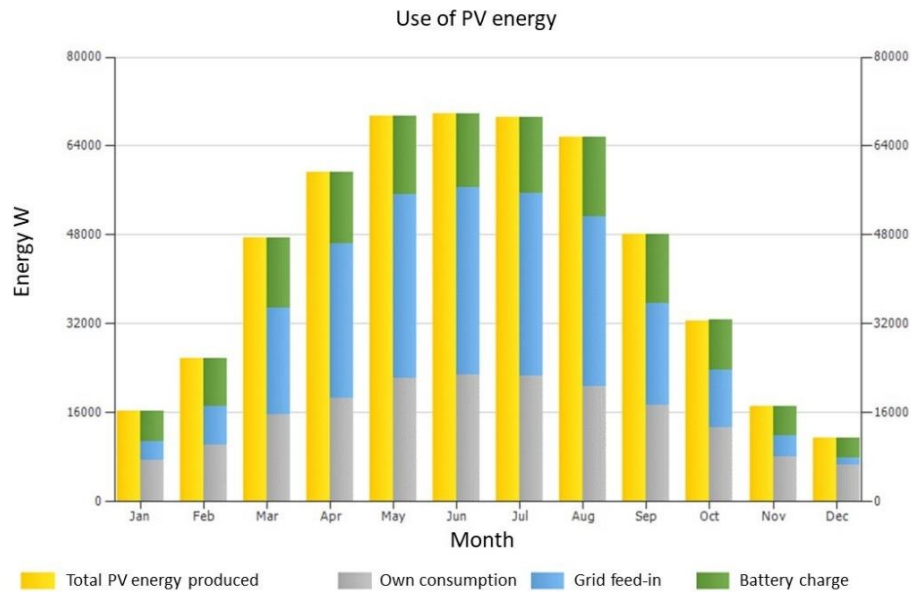


Figure 9. Graph of the use of PV energy in the warehouse (PV*Sol). *Source: Author.*

The use of backup generators, compared to solar energy, in simulated power grid failure on the days with the lowest irradiation is shown in Figure 10. We can observe a high utilization of the backup generator to cover the warehouse consumption, especially due to insufficient sunlight and short days. However, we can also see that the system is capable of covering part of the consumption with photovoltaic energy even at a relatively small intensity of irradiation around 270 W/m^2 . On the other hand, relatively low utilization of the backup generator is needed during days with high irradiation. In Figure 11, we can see a simulation of the system during June. With irradiation of around 850 W/m^2 , it is apparent that the generator is used only to upkeep the minimal state of charge (SOC) of the batteries and that the system is capable of supplying the warehouse with enough power to ensure its operation.

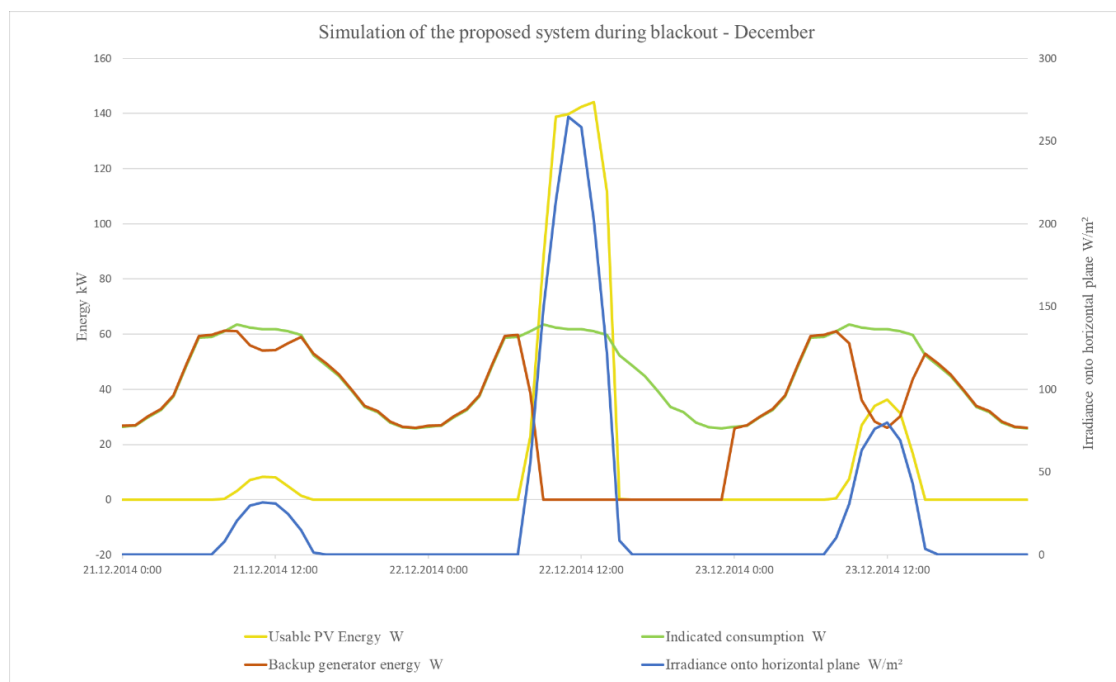


Figure 10. Use of backup generator during low-irradiation days (PV*Sol). *Source: Author.*

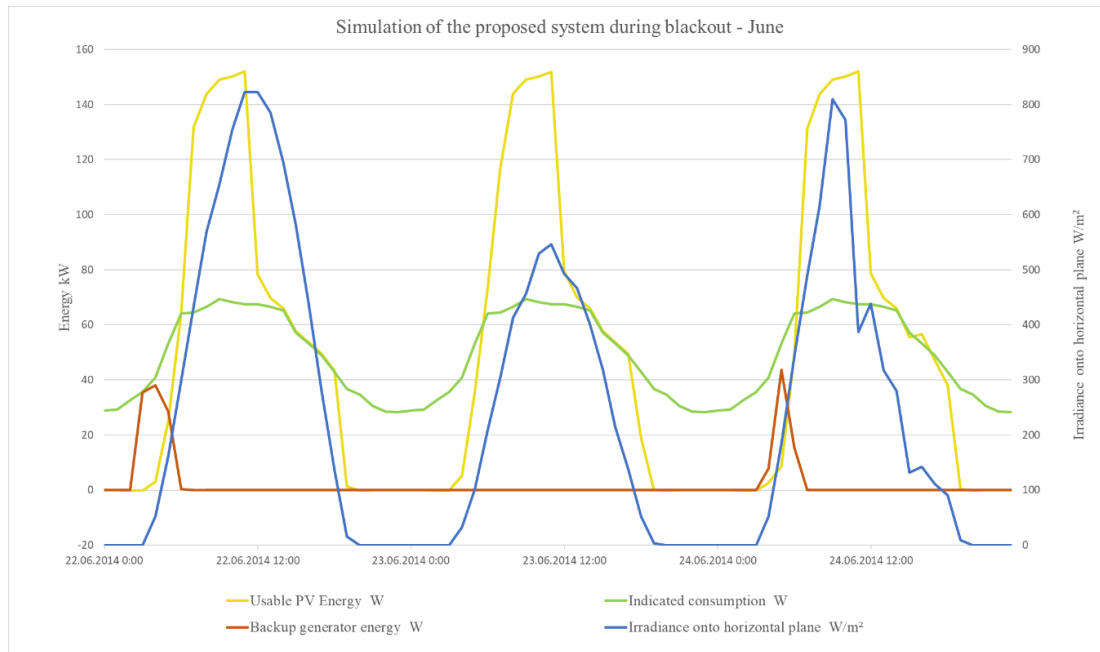


Figure 11. Use of backup generator during high-irradiation days (PV*Sol). *Source: Author.*

Mobile command centre scenario

As mentioned before, an interval of 6 months was used (April – September) for the simulation of the design for mobile command centre. Firstly, the simulation for the design with a backup generator was run. Based on the results of this simulation, the system was optimised and then we designed and simulated the PV-only system.

As we can observe from the results of the simulation below, the total consumption of the command centre over our interval would be 10 MWh. From this consumption, 68.3% would be covered using solar energy with the rest would be covered by the backup generator. This would mean estimated consumption of 2 235 L of fuel, or on average, 12.5 L / day.

Appliances

Consumption	10 078 kWh/Year
Consumption with Load Shedding	10 078 kWh/Year
Standby Consumption (Inverter)	3 kWh/Year
Cable Losses	0 kWh/Year
Total Consumption	10 081 kWh/Year
covered by PV power	4 029 kWh/Year
covered by battery	4 623 kWh/Year
covered by auxiliary generator	1 430 kWh/Year
Solar Fraction	69.0 %

Total Consumption



■ covered by PV power
■ covered by battery
■ covered by auxiliary generator

Figure 12. PV system with backup generator simulation results (PV*Sol). *Source: Author.*

Further optimization of this system would require additional batteries and a trade-off between their longer lifespan and set parameters of maximal discharge of the batteries, as the possibility to effectively use more of their stored energy (the simulated setting was max 80% SOD) would require less generator usage. Correct spacing between the construction, panel orientation and their tilt would also have to be adhered to during the system installation as this could create losses in power production due to shading. The fully photovoltaic solution for the mobile command centre design (Figure 13) had to be scaled to account for the need to supply enough

power even in inconvenient conditions. The simulation of the design showed us that the system would be around 32% efficient should the setup be used for the whole duration of the 6-month interval. On the other hand, it also proved that the system would be capable of energy self-sufficiency even in sustained adverse conditions (PV*Sol calculated 4.7 days of autonomy).

PV System

PV Generator Output	28.80 kWp
Spec. Annual Yield	1 079.07 kWh/kWp
Performance Ratio (PR)	87.98 %
Yield Reduction due to Shading	5.3 %/Year
Maximum possible PV Energy	31 116 kWh/Year
Usable PV Energy	11 502 kWh/Year
Coverage of Consumption	5 122 kWh/Year
Battery Charge	6 380 kWh/Year

Usable PV Energy



Appliances

Consumption	10 078 kWh/Year
Consumption with Load Shedding	10 078 kWh/Year
Standby Consumption (Inverter)	39 kWh/Year
Cable Losses	0 kWh/Year
Total Consumption	10 117 kWh/Year
covered by PV power	5 122 kWh/Year
covered by battery	4 994 kWh/Year
Solar Fraction	100.0 %

Total Consumption



Figure 13. Stand- alone PV system design simulation result (PV*Sol). *Source: Author.*

Impact

The presented paper deals with the design of photovoltaic systems as renewable energy sources and their use in specific applications to substitute fossil fuel energy sources (partially or fully). The presented designs are based on practical scenarios and lay the basis for future applications and development. The main impact is environmental, as we aimed to increase energy self-sufficiency in both presented scenarios. Not only do these designs reduce the dependability on fossil fuel use, but they also enable further development in the problematics, especially regarding mobile applications. Another environmental impact is the reduction of emissions due to using renewable energy sources. Based on the PV*Sol simulations, the utilization of the photovoltaic system for strategic warehouse would avoid generating approx. 245 t of CO₂ emissions per year. The mobile photovoltaic systems would avoid generating approx. 17 kg (backup generator design) and 22 kg of CO₂ emissions per day of operation. This would support the initiatives for renewable energy sources and declining trend of CO₂ emissions in Europe [21]. Although energy and resources are required to manufacture the technology for PV systems, their operation produces this energy back (without emissions) multiple times over the life cycle of the PV system [22,23]. The mobile applications have also the impact of lesser, or fully eliminated noise pollution as opposed to regular use of generators as a source of power. Lower dependability on fossil fuels and energy self-sufficiency also has an economic impact on both presented scenarios. For the designs used for critical infrastructure, the overall cost of energy for the general operations of the facilities is greatly reduced, especially in times of crisis, such as economic crisis or the current energy market crisis. For mobile applications, photovoltaic systems promise a reduction in the cost of fossil fuels that would be otherwise necessary for energy production. Exact economic impact would vary mainly with geographical location of the installed system. As the availability of solar energy and its effective usage reduces with the distance from the equator, countries closer to the equator would see larger energy output from the same system than e.g. Nordic countries [20]. Thus, the geographic location should be taken into

consideration during the design of the photovoltaic system as it impacts its overall efficiency and economic impact (return of investment, rentability). With the mobile photovoltaic system, this could be overcome by modularity of the system, i.e., scaling the system based on the specific locations and their availability of solar energy. Simulations of the designs in both scenarios brought results similar to other studies on the topic [3,7–9,19]. From a social point of view, the proposed designs aim at sustainable energy sources for the future. The designs present assurance in the form of reliable energy sources for critical infrastructure, as well as formobile command centres in both military and civil sectors. Especially the designs of photovoltaic systems for mobile applications are already impacting the integrated rescue system of the Czech Republic, as there is an effort aimed at practical applications of such systems. These could be used in medium to long-term operations during and following natural disasters (i.e., provisory shelters, energy source during the disaster clean-up and debris removal operations), for mobile hospitals (e.g., during COVID pandemic) or for refugee camps, where clean source of energy (i.e., without the noise pollution from generators) may be favoured. Specifically modular and scalable systems may impact such operations of the integrated rescue forces even during their assistance abroad.

Conclusions

To evaluate the possibility of the use of solar energy as a source of electricity in strategic applications and mobile applications, two scenarios were discussed and created. After this, many aspects of the scenarios (Automated warehouse, mobile command centre) were analysed to design an optimized photovoltaic system to ensure a reliable source of power as well as self-sufficiency in the events of blackout. For both scenarios, 3D models and visualisations were created. The proposed systems were optimised and simulated using PV*Sol software. The first scenario presented a central warehouse with significant strategic importance to Czech Army Forces and NATO forces. Due to the automatization of the facility and its importance as one of the few central warehouses of the Czech Armed Forces, a grid-tied PV system with an emergency backup generator was designed. The system was designed with a backup generator in mind to ensure the functioning of the system even in the case of power grid failure. PV*SOL software was used for the 3D design and simulations. The simulation showed us that the proposed system design fits the needs of the facility as it can cover approximately 71% of the warehouse energy consumption. However, due to the varying conditions of irradiation in winter and summer, approximately 40% of the generated energy would be sent to the grid. Although this energy could be sold, the system could be optimized by installing larger capacity energy storage. This would not be an issue as the system is easily scalable. Based on the simulations of blackout we found out that the system is fully able to function with the use of a 60 kW backup generator to ensure the functioning of the facility. In the second scenario, two designs of PV systems for mobile command centres were designed and simulated. Firstly, a system with the use of a backup generator was proposed. Such a system not only has a lower initial investment but is also significantly smaller and allows for easier transport than a fully PV system. The second design of a fully PV system proved to be able to support a mobile command centre using only solar energy, however, this comes with a few downsides. Namely the need for a larger system due to the need to supply enough power even in unfavourable conditions. With this comes not only transportation issues but also the higher initial cost of the system (even though the operating cost is lower). The analyses of the scenarios and simulations of the proposed systems showed us the possibilities of implementing renewable sources of energy not only in strategic applications but also in mobile applications. The results of the simulations are also comparable with results of similar researches [3,7–9,19]. A benefit for further research would be case studies, mainly aimed at the mobile command centre scenario, as this practical solution could be used in both military and civil sectors, especially with a focus on the integrated rescue system and its operations. Further research could also be aimed at the capabilities of such systems during winter months, when the energy output of solar system is notably reduced. Data measured this way (during real application) could also help with further optimising the proposed design and lead to the basis of fully modular designs that could be adjusted for specific needs and situations, such as operations of the integrated rescue system regarding a refugee crisis, refugee camps or natural disasters.

Conflict of interest

There are no conflicts to declare.

Acknowledgments

This work was supported by the specific graduate research of the Brno University of Technology No. FEKT-S-14-2293 and the Ministry of Defence of the Czech Republic project No. DZRO K-109, project. No. OFVVU20140001. This research work has been conducted in the Centre for Research and Utilization of Renewable Energy (CVVOZE). The authors gratefully acknowledge financial support from the Ministry of Education, Youth and Sports of the

Czech Republic under the NPU I Programme (project No. LO1210).

References

- [1] K.A. Makinde, O.B. Adewuyi, A.O. Amole, O.A. Adeaga, Design of Grid-connected and Stand-alone Photovoltaic Systems for Residential Energy Usage: A Technical Analysis, *J. Energy Res. Rev.* (2021) 34–50. <https://doi.org/10.9734/jenrr/2021/v8i130203>.
- [2] Renewable Energy Market Update, *Renew. Energy Mark. Updat.* (2022). <https://doi.org/10.1787/faf30e5a-en>.
- [3] S. Qazi, Mobile Photovoltaic Systems for Disaster Relief and Remote Areas, in: *Standalone Photovolt. Syst. Disaster Reli. Remote Areas*, Elsevier, 2017: pp. 83–112. <https://doi.org/10.1016/b978-0-12-803022-6.00003-4>.
- [4] Solarní Asociace, Mobilní Alfons dodává elektřinu ze slunce nejen armádě, (2015). <https://www.solarniasociace.cz/cs/aktualne/2838-mobilni-alfons-dodava-elektrinu-ze-slunce-nejen-armade>.
- [5] Multicon Solar container, (2022). <https://solarcontainer.info/home-2/energy-power-rack.html>.
- [6] J. Šiška, Solární proud (nejen) pro německou armádu.
- [7] K. Prompinit, B. Plangklang, S. Hiranvarodom, Design and construction of a mobile PV hybrid system prototype for isolated electrification, *Procedia Eng.* 8 (2011) 138–145. <https://doi.org/10.1016/j.proeng.2011.03.025>.
- [8] A. Borodinecs, D. Zajecs, K. Lebedeva, R. Bogdanovics, Mobile Off-Grid Energy Generation Unit for Temporary Energy Supply, *Appl. Sci.* 12 (2022) 673. <https://doi.org/10.3390/app12020673>.
- [9] J. Franceschi, J. Rothkop, G. Miller, Off-grid solar PV power for humanitarian action: From emergency communications to refugee camp micro-grids, *Procedia Eng.* 78 (2014) 229–235. <https://doi.org/10.1016/j.proeng.2014.07.061>.
- [10] J. Černý, Organizační a velitelské struktury a jejich vliv na organizaci velení a řízení vojsk u brigádního úkolového uskupení, *Econ. Manaement.* 02/2010 (2010).
- [11] K. Lewczuk, M. Kłodawski, P. Gepner, Energy consumption in a distributional warehouse: A practical case study for different warehouse technologies, *Energies.* 14 (2021) 2709. <https://doi.org/10.3390/en14092709>.
- [12] U.S. Energy Information Administration, Commercial buildings energy consumption survey (CBECS): Table PBA4. Electricity consumption totals and conditional intensities by building activity subcategories, (2012). <https://www.eia.gov/consumption/commercial/data/2012/c&e/cfm/pba4.php>.
- [13] Fenix Group, Elektrické vytápění při revitalizaci průmyslových objektů, (2012).
- [14] Solar+Diesel Generator Solution, (2022). <https://pl.goodwe.com/solar-diesel-generator-solution>.
- [15] CanadianSolar solar panel datasheet, (2022). https://static.csisolar.com/wp-content/uploads/2020/10/06153233/CS-Datasheet-HiKu7_CS7L-MS_v2.4_EN.pdf.
- [16] GoodWe MT series datasheet, (2022). https://en.goodwe.com/Ftp/EN/Downloads/Datasheet/GW_MT_Datasheet-EN.pdf.
- [17] Nato, New NATO scientific project to reduce energy consumption of deployable camps, (2018).
- [18] T.M. Yunus Khan, M.E.M. Soudagar, M. Kanchan, A. Afzal, N.R. Banapurmath, N. Akram, S.D. Mane, K. Shahapurkar, Optimum location and influence of tilt angle on performance of solar PV panels, *J. Therm. Anal. Calorim.* 141 (2020) 511–532. <https://doi.org/10.1007/s10973-019-09089-5>.
- [19] O. Shavolkin, I. Shvedchikova, J. Gerlici, K. Kravchenko, F. Pribilinec, Use of Hybrid Photovoltaic Systems with a Storage Battery for the Remote Objects of Railway Transport Infrastructure, *Energies.* 15 (2022) 4883. <https://doi.org/10.3390/en15134883>.
- [20] L. Zhang, Z. Chen, H. Zhang, Z. Ma, B. Cao, L. Song, Accurate study and evaluation of small PV power generation system based on specific geographical location, *Energy Eng. J. Assoc. Energy Eng.* 117 (2020) 453–470. <https://doi.org/10.32604/EE.2020.013276>.
- [21] M. Roser, H. Ritchie, CO₂ and Greenhouse Gas Emissions - Our World in Data, Our World Data. (2020). <https://ourworldindata.org/co2-and-other-greenhouse-gas-emissions#future-emissions>.
- [22] K. Komoto, H. Uchida, M. Ito, K. Kurokawa, A. Inaba, Estimation of energy payback time and CO₂ emission of various kinds of pv systems, in: *23rd Eur. Photovolt. Sol. Energy Conf. Exhib.*, 2008: pp. 3833–3835.
- [23] M. Simón-Martín, M. Díaz-Mediavilla, C. Alonso-Tristán, T. García-Calderón, M.C. Rodríguez-Amigo, Grid Connected PV Systems: Energy Payback Time Analysis, in: *5th Int. Conf. Sustain. Energy Environ. Prot.*, Dublin, 2012: pp. 174–179. <https://doi.org/10.13140/2.1.5180.6089>.

THE ROLE OF TiO₂ NPs CATALYST AND PACKING MATERIAL IN REMOVAL OF PHENOL FROM WASTEWATER USING AN OZONIZED BUBBLE COLUMN REACTOR

Saja A. Alattar

Department of Chemical Engineering, University of Technology, Iraq

che.20.24@grad.uotechnology.edu.iq

 <https://orcid.org/0000-0002-5227-1668>

Khalid A. Sukkar *

Department of Chemical Engineering, University of Technology, Iraq


khalid.a.sukkar@uotechnology.edu.iq

 <https://orcid.org/0000-0003-2024-2093>

May A. Alsaffar

Department of Chemical Engineering, University of Technology, Iraq

may.a.muslim@uotechnology.edu.iq

 <https://orcid.org/0000-0002-5658-6085>

Article history: Received 14 October 2022, Received in revised form 4 November 2022, Accepted 4 November 2022, Available online 4 November 2022

Highlight

This research aims to enhance mass transfer and reaction rate of phenol degradation from wastewater in ozonation process using packed bubble column reactor.

Abstract

Phenol is present as a highly toxic pollutant in wastewater, and it has a dangerous impact on the environment. In the present research, the phenol removal from wastewater has been achieved using four treatment methods in a bubble column reactor (treatment by ozone only, using packed bubble column reactor with ozone, utilizing ozone with TiO₂ NPs catalyst in the reactor without packing, and employing ozone with TiO₂ NPs in the presence of packing). The effects of phenol concentration, ozone dosage, TiO₂ NPs additions, and contact time on the phenol removal efficiency were determined. It was found that at a contact time of 30 min, the phenol removal was 60.4, 74.9, 86.0, and 100% for the first, second, third, and fourth methods, respectively. The results indicated that the phenol degradation method using catalytic ozonation in a packed bubble column with TiO₂ NPs is the best treatment method. This study demonstrated the advantages of using packing materials in a bubble column reactor to enhance the mass transfer process in an ozonation reaction and then increase the phenol removal efficiency. Also, the presence of TiO₂ NPs as a catalyst improves the ozonation process via the production of hydroxyl routes. Additionally, the reaction kinetics of ozonation reaction manifested that the first order model is more applicable for the reaction. Eventually, the packed bubble column reactor in the presence of TiO₂ NPs catalyst provided a high-performance removal of phenol with a high economic feasibility.

Keywords

petroleum refineries; phenol degradation; TiO₂ NPs; multiphase flow reactor; catalytic ozonation reaction.

Introduction

The demand for petroleum and other energy resources is increasing with the population increase and global economic development. The petroleum refinery requires huge quantities of water for an operating unit, and then large amounts of wastewater are produced [1–3]. Phenol regards one of the most harmful materials produced in wastewater effluent from petroleum refineries and results in environmental risks as well as hinders the normal operations of the ecosystems [4]. Phenol is a toxic and dangerous substance for all living organisms, as it causes many dangerous symptoms to humans, animals, and plants [5–8]. Therefore, efficient treatment methods are needed to ensure that phenol is completely removed from the water. According to the EPA classifications, phenol is selected as one of 129 priority contaminants that must be removed and controlled [5]. Many industrial methods are usually used for the removal of phenol from wastewater [9–14]. The advanced oxidation process (AOP) is considered one of the important methods used to treat polluted water [15–18]. Ozonation technology is one of the chief AOPs which increased the attention as a result of the finding of ozone's

potential to efficiently degrade various types of organic pollution, especially the phenol [17]. Multiphase reactors are widely used in ozonation process to remove organic compounds from industrial wastewater, such as trickle bed reactor, fluidized bed reactor, membrane reactor, and bubble column reactor [19–25]. The performance of these reactors is highly managed by the operation of the hydrodynamics parameters in the reactor [26]. Bubble column reactor is one of the main multiphase reactors that have an efficient contact among the gas, liquid, and solid phases [27–32]. Accordingly, bubble column reactor employed in ozonation process due to its ability to eliminate the contaminants in water in the presence of oxidation agents such as ozone [12,33]. Many authors have investigated the ozonation process to remove the phenol from wastewater using different nanomaterials in a bubble column reactor [34–36]. Sridar et al. [37] employed FeO and ZnO NPs to remove the phenol from synthetic and industrial wastewater. The authors noted that the removal of phenol effectiveness for FeO was 82%. Also, the efficiency of phenol removal from industrial wastewater using ZnO was found to be relatively low when compared to synthetic phenol solution. Iboukhoullef et al. [38] applied an ozonation reaction with BiFeO₃ nanocatalyst to treat the olive mill wastewater. It was observed that the degradation process caused by O₃/BiFeO₃/S₂O₈²⁻ under alkaline circumstances proved to be the most effective. This degradation achieved a reduction of phenolic compounds by ~83% and a reduction of COD by 98%. Wang et al. [39] studied the degradation of wastewater effluent from refineries via catalytic ozonation by using activated carbon-supported copper oxide (CuO/AC). It was observed that the (CuO/AC) was a suitable supported catalyst for enhancing the ozonation degradation of heavy oil from wastewater. Salcedo, et al. [40] investigated the phenol degradation process using a natural catalyst of Sand-coated-carbon in a batch reactor. It was noticed that about 65% of degradation occurred with an average of 16 phenols, and 41% of wastewater was mineralized. Also, the authors found that, with the reaction half-time values ranging between 0.01 and 3.6 h, the photocatalysis process was effective in degrading phenols. Al-Ghouti et al. [41] studied the removal of phenol from wastewater using graphene oxide NPs. It was indicated that the increase in operating temperature was caused by a clear reduction in the adsorption capacity. Zazouli et al. [42] tested the removal of pentachlorophenol from wastewater by photocatalytic ozonation process using graphene-dioxide titanium nanocomposite. It was seen that by increasing the dose of used nanocomposite material, the removal efficiency was enhanced. The highest removal efficiency was noted to be 98.82%. According to a literature survey, it was observed that the phenol oxidizes slowly during the ozonation process in the bubble column. Moreover, the low solubility of ozone in water leads to low ozone activity, as well as the production of intermediate products that cannot react with the ozone, resulting in low mineralization efficiency, which must be addressed [40–44]. Therefore, the main aims of the present work are to apply a packed bubble column to enhance the mass transfer and the reaction mechanism of phenol degradation from wastewater in the ozonation process, and to investigate the influence of TiO₂ NPs on the activity of ozone gas to increase the phenol degradation in the reactor.

Materials and Methods

Chemicals

In the present experimental work, many chemicals were used such as phenol (99.6% purity), and TiO₂ NPs (30 nm in size of 99.5% purity) were obtained from Sigma-Aldrich company. Iodide Potassium (99.6% purity), Sodium thiosulfate (99.6% purity), and Sulfuric acid (99.6% purity) were obtained from the Fluka company. Also, starch (99.6% purity) was used to determine the ozone concentration.

Experimental Setup and Procedure

In this investigation, a bubble column reactor was designed to carry out the experimental tests to remove the phenol from wastewater. Figure 1 shows the experimental system of packed bubble column reactor operated under a semi-batch mode, while Figure 2 illustrates a schematic diagram of the experimental apparatus. The reactor height was 150 cm, and its diameter was 8 cm. At a height of 100 cm, the reactor was packed with spherical glass beads of 1.5 cm in diameter. The gas phase was passed via the reactor bottom using a gas distribution that was constructed from stainless steel with 52 holes of 0.5 mm in diameter. Moreover, the ozone gas (gas phase) was generated using an ozone generator device of 20 mg/L. A calibrated gas flow meter was used to regulate the flow rate input into reactor. The reactor was equipped with a sampling valve that was supported at a height of 75 cm.

Simulated polluted wastewater was synthesized by dissolving phenol in distilled water. Four concentrations of phenol solutions were prepared (i.e., 3, 6, 9, 12, and 15 mg/L). The ozonation process of phenol treatment was achieved using input ozone gas at concentrations of 10, 15, and 20 mg/L. Each experiment was evaluated under total ozonation time (contact time) for 120 min with a 15 min period of time for drawing the samples.

Additionally, the concentration of ozone gas in the water was determined using the Indigo technique [18–20]. Actually, the experimental procedure was achieved using four different phenol treatment modes in bubble column reactors. The first one was carried out in a bubble column reactor with ozone gas only. The second mode of treatment was conducted using ozone in the presence of packing (O_3 /packing). The third treatment mode was achieved in the presence of ozone and TiO_2 NPs (O_3/TiO_2 NPs), while the final treatment mode was performed using ozone gas with packing and TiO_2 NPs (O_3 /packing/ TiO_2 NPs). Figure 3 summarizes the four stages of operating modes in the bubble column. At the end of each experiment, the phenol concentration was measured using a TOC analyzer (TOC-L-CSH E200).



Figure 1. The experimental apparatus of packed bubble column reactor. *Source: Author.*

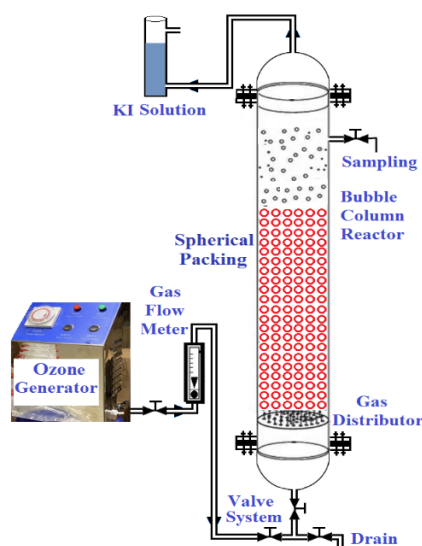


Figure 2. Schematic diagrams of experimental bubble column reactor apparatus. *Source: Author.*

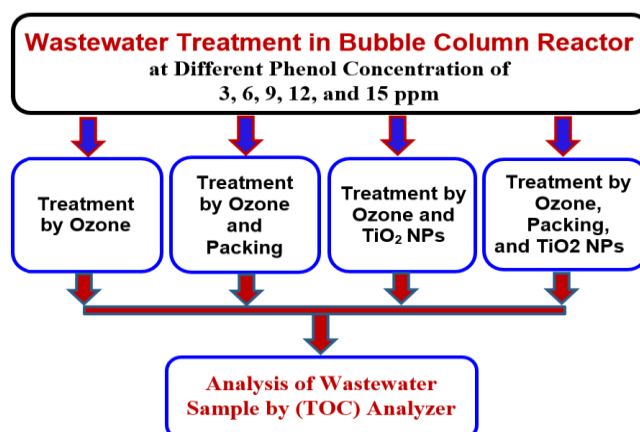


Figure 3. The four treatment stages of phenol removal in the bubble column reactor. *Source: Author.*

Results and Discussion

Evaluation of Phenol Removal Efficiency Using Ozone Only

In order to evaluate the influence of the concentration of phenol on the removal rates in all stages of treatment, four phenol concentrations of 3, 6, 9, 12, and 15 mg/L were investigated. The pH value was kept constants for all experiments at the value of 7. Also, the ozone concentration and the TiO_2 NPs dose were set at 50.3 mg/min and 0.1 g, respectively. Figure 4 displays the results of phenol degradation with contact time (treatment time) using ozone only in a bubble column reactor. The results evinced that at a contact time of 30 min, the phenol removal % recorded values were 60.42%, 52.19%, 43.09%, 38.33%, and 30.69% for phenol concentrations of 3, 6, 9, 12, and 15 mg/L, respectively. Also, the result elucidated that the best contact time was measured to be 75, 90, 105, and 120 min for phenol concentrations of 6, 9, 12, and 15 mg/L, respectively. Moreover, it was observed that a reaction time of 60 min is required to ensure the complete removal of phenol at an initial phenol concentration of 3 mg/L. Then, it was seen that as the initial phenol concentration was increased, the period of reaction time increased too. Accordingly, the contact time is regarded a major factor determining the removal efficiency of phenol. The same results were reported by Park et al. [21] and Nirmala et al. [23].

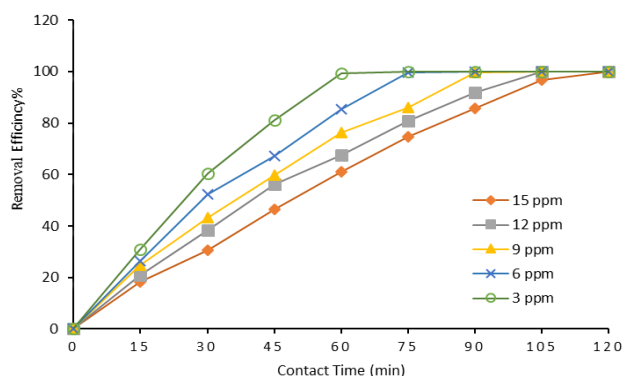


Figure 4. Effect of the initial phenol concentration on the removal rates using ozone only. *Source: Author.*

Influence of Packing on the Phenol Degradation Rate

Figure 5 illustrates the relationship between phenol removal efficiency and contact time using ozone and packing in a bubble column reactor. The results indicated that the phenol degradation rate increased with the decreasing of phenol dose. At a contact time of 30 min, the phenol removal efficiency was 74.98%, 52.97%, and 38.22% for phenol concentrations of 3, 9, and 5 mg/L, respectively. Also, at the time of 45 min, the removal efficiency was 100% at a phenol concentration of 3 mg/L. Moreover, at 15 mg/L of phenol concentration, the phenol removal was achieved 100% at a contact time of 105 min. Consequently, the addition of packing to the bubble column reactor enhances the removal of phenol efficiency significantly due to the improvement in the contact area between gas and liquid, and then a high mass transfer rate was obtained. Furthermore, the use of packing in bubble column reactor will work on lowering the ozone utilization efficiency, and then low mass transfer retardation will be achieved. Therefore, adding the packing material to the bubble column reactor is considered

an efficient method for enhancing the decomposition of ozone gas in an aqueous solution to improve the ozone utilization and increase the removal efficiency of phenol degradation [18–23]. Also, many investigators, such as Deshpande et al. [15], Xiong et al. [33], Sukkar et al. [36] indicated that the presence of packing inside different types of reactors enhances the mass transfer and the reaction rate dramatically.

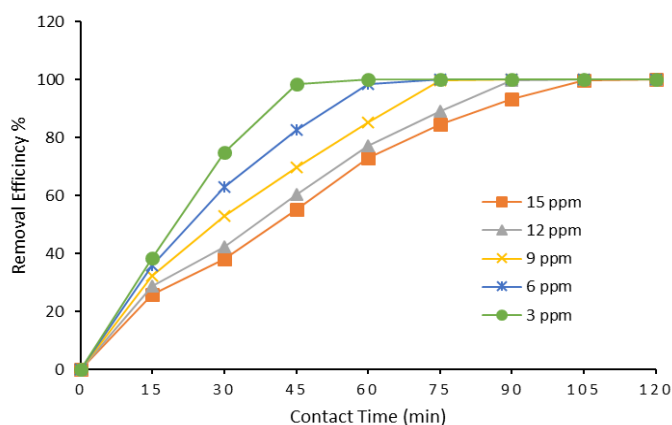


Figure 5. Effect of packing and ozone on the reactor performance to remove the phenol. *Source: Author.*

The use of a catalyst to initiate the reaction mechanism is considered an important task to improve the ozonation process and the high phenol degradation rate. Figure 6 clarifies the effect of the addition of TiO_2 NPs as a catalyst on the phenol removal efficiency with contact time. The catalyst addition was 0.1 g of TiO_2 NPs. The result in this figure exhibited that the TiO_2 NPs addition enhanced the phenol degradation rate in comparison with the treatment with ozone only (Figure 4). For a contact time of 30 min, the value of phenol removal % was 86.04%, 62.45%, and 48.16% for phenol concentrations of 3, 9, and 15 mg/L, respectively. Also, it was found that at a concentration of 3 mg/L, the complete removal of phenol (100%) was achieved at 45 min of contact time. On the other hand, for a phenol concentration of 15 mg/L, a contact time of 105 min is required for the complete removal of phenol from wastewater. A comparison between the results of phenol removal efficiency at 45 min of contact time depicted that a value of 100% and 81.22% was achieved for the presence and absence of TiO_2 NPs catalyst, respectively. Actually, when the ozone gas was used in the reactor without TiO_2 NPs, the phenol ozonation process was found to be rather limited, due to the slow reaction of ozone with phenol (degradation reaction). These results were clearly noted in Figure 6 mainly due to the enhancement and high conversion of phenol accomplished in the catalytic ozonation process owing to the action of free radicals generated by the self-decomposition of ozone on the active site of the TiO_2 NPs, thus an increase in the removal rate of phenol by catalytic ozonation at the gas-liquid interface [6,12,33]. The same results were obtained by Parvin and Ali [24] in their work; they found that after 30 min, the change of TOC for ozone/ ZnO NPs and ozone alone was 54.9% and 27.4%, respectively. This result indicates the rapidly mineralized pollutants by the heterogeneous catalytic ozonation using the ZnO NPs than ozone alone.

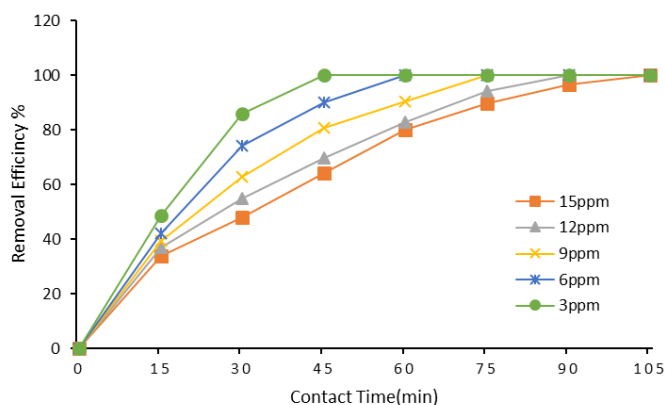


Figure 6. Effect TiO_2 NPs addition as a catalyst with ozone on the phenol removal rates. *Source: Author.*

Influence of TiO₂ NPs and Packing on the Phenol Degradation Rate

The results of the fourth stage of phenol treatment were achieved using TiO₂ NPs in presence of packing in a bubble column reactor. Figure 7 demonstrates the influence of contact time on the removal efficiency of phenol in the presence of TiO₂ NPs and packing in the reactor. The results revealed that at a contact time of 30 min and a phenol concentration of 3 mg/L, a percentage of 100% of phenol removal was observed. Also, it was found that the removal efficiency of phenol at 9 and 15 mg/L was 79.32% and 64.11%, respectively. Then, it was noted that the presence of TiO₂ NPs in a packed bubble column reactor improved the reaction mechanism of phenol degradation significantly. As an example, at a phenol concentration of 15 mg/L, 90 min of treatment time was needed to achieve the phenol removal of 100%. These results mainly evinced that the use of TiO₂ NPs in a packed bubble column reactor is higher than that of the other previous three treatment methods. At a contact time of 30 min and a phenol concentration of 3 mg/L, the treatment results for O₃ gas only, O₃/packing, O₃/TiO₂ NPs, and O₃/packing/TiO₂ NPs were 60.42%, 74.98%, 86.04%, and 100%, respectively.

These results indicated that the use of a packed bubble column is considered to provide an increased interfacial contact area, lower ozone gas rising velocity, longer ozone gas stagnation time, increased contact time, and higher mass transfer coefficient. All these factors enable the ozonation process to increase the phenol removal efficiency.

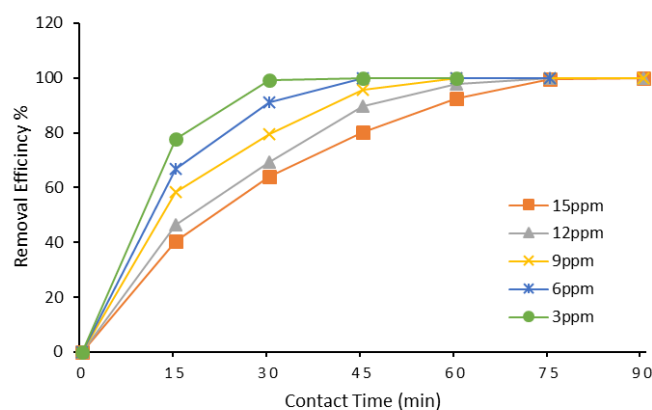


Figure 7. Effect of TiO₂ NPs and packing on the phenol removal rates in the reactor. *Source: Author.*

Effect of Ozone Concentration

The influence of ozone gas concentration on the phenol degradation process was evaluated in the present study. Three levels of ozone were tested (i.e., 10, 15, and 20 mg/L), while the concentration of phenol was kept constant at 3 mg/L. Figure 8 reveals the effects of the ozone dose on the phenol removal rate. From this figure, it was noted that at the treatment time of 30 min, the ozone dose of 10, 15, and 20 mg/L provided a phenol removal efficiency of 73.34, 88.95, and 99.43%, respectively. Then, the results in this figure indicated that as the ozone dose increased in the bubble column reactor, faster phenol degradation was achieved. Actually, when the system operated with high concentrations of ozone, the degradation ability of organic materials increased dramatically with a short treatment time. The same finding was noted by Mohsen et al. [28] via their investigation on the catalytic ozonation of caffeine. It was found that with the increasing of ozone concentration, the pollutants removal rate increased too. Furthermore, it was observed that the phenol degradation efficiency arrived at 100% when the reaction was carried out at an ozone concentration of 2.5 mg/L and 5 mg/L at treatment times of 80 min and 60 min, respectively. Then, it was seen that as the ozone concentration was increased, the treatment time required lower contact time to achieve 100% removal of phenol. Accordingly, many authors have also noted that the increase in ozone concentration will provide better phenol removal efficiency [12,29,40]. Then, the experimental results in figure 8 clearly portrayed the importance of increasing the ozone concentration in the aqueous phase to get a significant impact on the rate of organic materials oxidation.

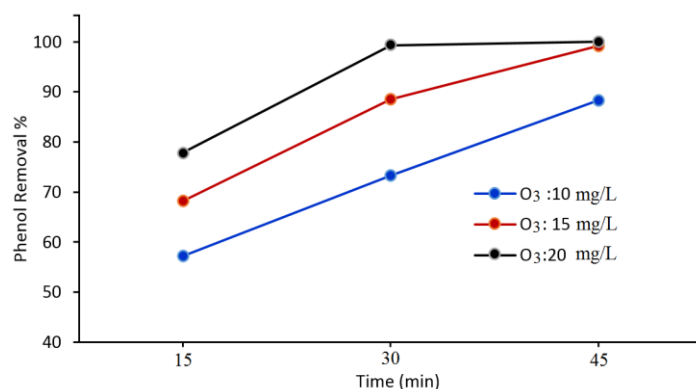


Figure 8. Effect of ozone concentration on phenol removal efficiency at different contact times (phenol dose of 3 mg/L and TiO₂ NPs catalyst of 0.1 g). *Source: Author.*

Effect of TiO₂ NPs Catalyst Dosage

In this section, the TiO₂ NPs were used as a catalytic material to improve the reaction of phenol degradation. Accordingly, from an economic point of view, determining the optimal dosage of nanocatalyst is regarded the most important criterion for a high reaction performance. Four dosages of TiO₂ NPs catalyst were tested (0.025, 0.05, 0.1, and 0.2 g/L) at an ozone concentration of 20 mg/L in the presence of packing material. The phenol concentration was 3 mg/L for all sets of experiments. Figure 9 elucidates the effect of catalyst dose on the degradation of phenol at different treatment times. The results indicated that the dose of TiO₂ NPs catalyst plays a significant impact on the rate of phenol degradation. Accordingly, it was noted that at 30 min of reaction time using ozonation treatment in the presence of packing material, the use of TiO₂ NPs catalyst of 0.025, 0.05, and 0.1 g/L provided a phenol removal of 80.45 and 92.62, and 99.35%, respectively. Actually, the increasing of TiO₂ NPs catalyst will initiate the formation of more active sites on the catalyst surface, and then more (OH) radicals will be generated in the reaction system. Such operation leads to a significant improvement in the phenol degradation mechanism with a high mass transfer rate. Moreover, at a contact time of 30 min, it was found that when the TiO₂ NPs catalyst concentration was 0.1 and 0.2 g, the phenol removal efficiency was 99.35%, and 95.25% respectively. It is important to mention here that the best TiO₂ NPs catalyst dose was 0.1 g which provides the highest phenol degradation (100%) within the shorter time of 30 min. Moreover, it was noted that the increase of TiO₂ NPs catalyst amount was not influenced by the reaction mechanism for further phenol degradation. In fact, increasing the dose of the catalyst can lead to the accumulation and precipitation of the catalyst causing inactivation of some TiO₂ NPs surface active sites and a reduction of free radicals generated. Also, one can demonstrate that the catalyst dose had a positive effect on the conversion of phenol in the catalytic ozone process under a high dosage of TiO₂ NPs. These results the pollutant removal efficiency decreased. Also, the same result was noted by Jose et al. [30].

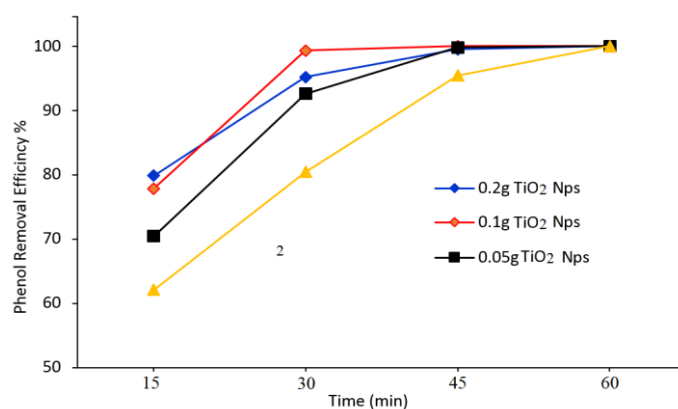


Figure 9. Effect of TiO₂ NPs dose on the removal rates of phenol at different dosages of TiO₂ NPs catalyst in the presence of packing material. *Source: Author.*

Evaluation of Phenol Degradation Kinetics

In the present study, the kinetics of phenol degradation by the ozonation process was studied. A mole balance was achieved in the reaction system to provide a clear description for the phenol degradation reaction. Two reaction orders were assumed for the present kinetics study (first order and second order). The reaction rate constants were determined depending on the different concentrations of the phenol in the reaction system [35]. Equations 1 and 2 illustrate the mole balance for the first and second order assumption, respectively.

- (1) $\ln C_t/C_0 = -k_1 t$ First order assumption
- (2) $C_t = C_0 / (1 + C_0 k_2 t)$ Second order assumption

Figures 10 and 11 view the theoretical and experimental results. Applying the validity of the first and second models was done by using equations (1) and (2), which were evaluated using the values of determining the coefficient (R^2). However, the kinetic reaction rate factor (k_a) of the first-order model was calculated by the slope of the best fit line of the $\ln (C_t/C_0)$ vs. the time (t), and the second-order model was calculated by the slope of the best fit line plot of $(1/C_t)$ vs. the time (t) [36]. The results of these measurements can be seen in Table 1 and Table 2, respectively. As a result of the high well of (R^2) values that were achieved (>0.9), it is evident that the first-order model provided a good fit for the kinetic data, as shown in Figure 10. In addition, the use of the packed ozonation technique resulted in a considerable rise in the reaction rate value. These results are in accordance with the results of Fadhil and Nada [29], and Melahat et al. [37].

Additionally, four lines appear in Figure 10 with four colors as indications for the four phenol treatment stages in the bubble column reactor at the assumption of a first-order reaction kinetics. The blue one refers to the ozonation process with ozone gas only. The gray color refers to using of TiO_2 NPs catalyst (O_3/TiO_2). While the red color refers to the treatment stage in presence of packing ($\text{O}_3/\text{packing}$). Finally, the orange color refers to the treatment stage in presence of TiO_2 NPs catalyst and packing material ($\text{O}_3/\text{TiO}_2/\text{packing}$) in the reactor. On the other, Figure 11 shows the reaction kinetics of the second-order assumption. The red color refers to the ozonation process, the orange color refers to the (O_3/TiO_2) treatment, the gray color refers to the ($\text{O}_3/\text{packing}$) treatment level, and the blue color refers to ($\text{O}_3/\text{TiO}_2/\text{packing}$) stage.

Table 1. Experimental kinetic data of phenol reaction using first order equation assumption. *Source: Author.*

Type of Treatment	$Y = \ln(C_0/C_t)$, and $x = t$	k_1 (1/min)	R^2 (1/min)
O_3 only	$y = 0.0386x - 0.1133$	0.07469	0.9726
$\text{O}_3/\text{packing}$	$y = 0.0511x - 0.1177$	0.08911	0.9844
O_3/TiO_2 NPs	$y = 0.0752x - 0.1051$	0.13624	0.9893
$\text{O}_3/\text{packing}/\text{TiO}_2$ NPs	$y = 0.1112x + 0.0521$	0.1681	0.9971

Table 2. Experimental kinetic data of phenol reaction using second order equation assumption. *Source: Author*

Type of Treatment	$Y = \ln(C_0/C_t)$, and $x = t$	k_2 (l/mg. min)	R^2 (l/mg. min)
O_3 only	$y = 0.0298x + 0.1405$	0.02978	0.905
$\text{O}_3/\text{packing}$	$y = 0.0458x + 0.0675$	0.04575	0.9154
O_3/TiO_2 NPs	$y = 0.0632x + 0.1554$	0.06081	0.9285
$\text{O}_3/\text{packing}/\text{TiO}_2$ NPs	$y = 0.074x + 0.4699$	0.07397	0.9395

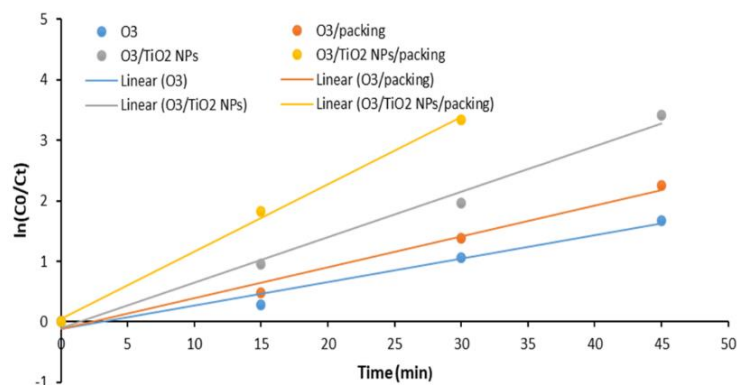


Figure 10. Assumption of first-order reaction kinetics of phenol degradation. *Source: Author.*

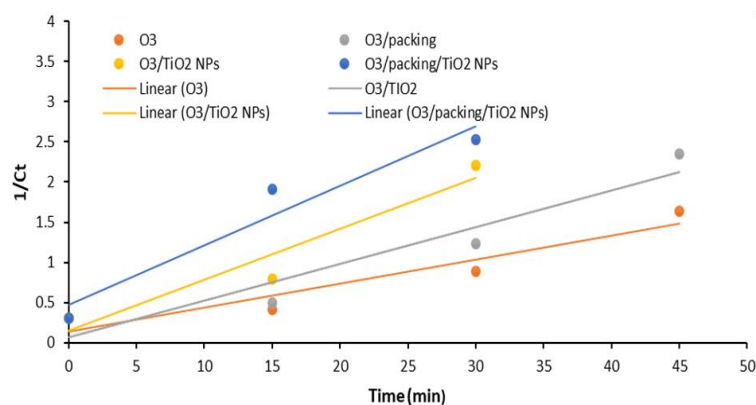


Figure 11. Assumption of second-order reaction kinetic of phenol degradation. *Source: Author.*

Impact

Effluents from petroleum refineries contain many hazardous materials, which have contributed to the presence of dangerous environmental impacts. The use of TiO_2 NPs catalyst in a packed bubble column reactor will have a high economic impact at the industrial scale by providing clean water with zero phenol. From an environmental point of view, wastewater pollution with organic compounds especially phenol is considered a major environmental problem. The treatment of wastewater in the present work regards will contribute to reusing water in operating units in petroleum refineries efficiently. Such a challenge to reduce the pollution of wastewater is highly desirable and has an enormous impact on industrial, economic, and environmental impacts. Moreover, a bubble column reactor is characterized by simple operation and no need to move or agitate parts. The agitations processes are usually achieved due to the rising of gas bubbles (ozone gas). Accordingly, the consumed energy in such reactor type is very low in comparison with other types of industrial multiphase reactors such as fluidized bed reactors or moving bed reactors. Furthermore, the use of TiO_2 NPs as a heterogeneous catalyst with packing material contributes to improving phenol removal from wastewater significantly by enhancing the ozonation process. Also, the presence of packing material in the bubble column reactor solves the problem of the low solubility of ozone gas in water. Then, the packing material contributes to obtaining a higher concentration of ozone with higher solubility in water. Such contribution will enhance economic savings by using all generated amounts of ozone gas to increase the performance of the treatment system. The highest phenol removal of 100% was achieved at a contact time of 30 min. As a result, by increasing the contact surface area between the gas and liquid phases, the mass transfer process in the reactor will increase. Accordingly, the phenol degradation reaction was enhanced dramatically within a shorter time and then with low operational costs. Finally, the process of wastewater treatment using ozonation technology in a packed bubble column reactor allows for the promotion of sustainability by providing high-quality water with simple operation and low economic cost. It is also worth noting that the using catalytic ozonation process is eco-friendly practices where phenol decomposes into CO_2 and H_2O without any secondary pollutants that harm the environment and reduce negative factors.

Conclusions

In the present work, it was found that the use of TiO_2 NPs catalyst in a packed bubble column reactor provided

a significant removal efficiency of phenol from wastewater effluent from petroleum refineries. Actually, the ozonation process was enhanced due to the effect of TiO₂ NPs as a catalyst and the presence of packing with a removal rate of 100% at a shorter contact time. Moreover, the results manifested that the presence of packing in the reactor improved the mass transfer process with a high contact area between gas and solid, and a low resistance to mass transfer was achieved. At a phenol concentration of 3 mg/L, the ozone dose of 3 g/h, pH = 7, and TiO₂ NPs of 0.1 g/l, the phenol removal efficiency provided the best contact increased, the mass transfer rate of the ozone gas increased, and then the removal of phenol increased. Additionally, the TiO₂ NPs catalytic improved the ozonation process via increasing the reaction of ozone in the active site of the catalytic led to the generation of hydroxyl routs which is considered better oxidation than ozone, so better removal of efficiency was got. Finally, the use of TiO₂ NPs in a packed bubble column reactor in the degradation of phenol is regarded an efficient process with low economic cost compared to other methods.

Conflict of interest

There are no conflicts to declare.

Funding information

There is no fund involved in this work.

Acknowledgments

The authors are grateful to the team of the Design and Industrial Production Research Unit at the Chemical Engineering Department/University of Technology-Iraq for their scientific support of this work.

References

- [1] S. Varjani, R. Joshi, V.K. Srivastava, H.H. Ngo, W. Guo, Treatment of wastewater from petroleum industry: current practices and perspectives, *Environ. Sci. Pollut. Res.* 27 (2020) 27172–27180. <https://doi.org/10.1007/s11356-019-04725-x>.
- [2] M.H. El-Naas, M.A. Alhaija, S. Al-Zuhair, Evaluation of a three-step process for the treatment of petroleum refinery wastewater, *J. Environ. Chem. Eng.* 2 (2014) 56–62. <https://doi.org/10.1016/j.jece.2013.11.024>.
- [3] Treatment of petroleum wastewater by conventional and new technologies A review, *Glob. NEST J.* 19 (2017) 439–452. <https://doi.org/10.30955/gnj.002239>.
- [4] A. Prasetyaningrum, W. Widayat, B. Jos, Y. Dharmawan, R. Ratnawati, UV irradiation and ozone treatment of k-carrageenan: kinetics and products characteristics, *Bull. Chem. React. Eng. Catal.* 15 (2020) 319–330. <https://doi.org/10.9767/bcrec.15.2.7047.319-330>.
- [5] K.A. Mohamad Said, A.F. Ismail, Z. Abdul Karim, M.S. Abdullah, A. Hafeez, A review of technologies for the phenolic compounds recovery and phenol removal from wastewater, *Process Saf. Environ. Prot.* 151 (2021) 257–289. <https://doi.org/10.1016/j.psep.2021.05.015>.
- [6] W. Duan, F. Meng, H. Cui, Y. Lin, G. Wang, J. Wu, Ecotoxicity of phenol and cresols to aquatic organisms: A review, *Ecotoxicol. Environ. Saf.* 157 (2018) 441–456. <https://doi.org/10.1016/j.ecoenv.2018.03.089>.
- [7] W.F. Elmobarak, B.H. Hameed, F. Almomani, A.Z. Abdullah, A review on the treatment of petroleum refinery wastewater using advanced oxidation processes, *Catalysts.* 11 (2021) 782. <https://doi.org/10.3390/catal11070782>.
- [8] M. Cheng, G. Zeng, D. Huang, C. Lai, P. Xu, C. Zhang, Y. Liu, Hydroxyl radicals based advanced oxidation processes (AOPs) for remediation of soils contaminated with organic compounds: A review, *Chem. Eng. J.* 284 (2016) 582–598. <https://doi.org/10.1016/j.cej.2015.09.001>.
- [9] R. Ratnawati, E. Enjarlis, Y.A. Husnil, M. Christwardana, S. Slamet, Degradation of phenol in pharmaceutical wastewater using TiO₂/Pumice and O₃/active carbon, *Bull. Chem. React. Eng. Catal.* 15 (2020) 146–154. <https://doi.org/10.9767/bcrec.15.1.4432.146-154>.
- [10] Z.Y. Shanian, M.F. Abid, K. Suker, Photodegradation of mefenamic acid from wastewater in a continuous flow solar falling film reactor, *Desalin. WATER Treat.* 210 (2021) 22–30. <https://doi.org/10.5004/dwt.2021.26581>.
- [11] V.N. Lima, C.S.D. Rodrigues, R.A.C. Borges, L.M. Madeira, Gaseous and liquid effluents treatment in bubble column reactors by advanced oxidation processes: A review, *Crit. Rev. Environ. Sci. Technol.* 48 (2018) 949–996. <https://doi.org/10.1080/10643389.2018.1493335>.
- [12] Y.. Chen, X. Duan, X. Zhou, R. Wang, S. Wang, N. Ren, S.H. Ho, Advanced oxidation processes for water disinfection: Features, mechanisms and prospects, *Chem. Eng. J.* 409 (2021) 128207. <https://doi.org/10.1016/j.cej.2020.128207>.
- [13] A.D. Thamir, K.A. Sukkar, A. A. Ati, Improve the process of enhancing oil recovery (EOR) by applying

- nanomagnetic cobalt ferrite nanoparticles, *Eng. Technol. J.* 35 (2017) 872–877. <https://doi.org/10.30684/etj.35.9A.1>.
- [14] C.V. Rekhate, J.K. Srivastava, Recent advances in ozone-based advanced oxidation processes for treatment of wastewater- A review, *Chem. Eng. J. Adv.* 3 (2020) 100031. <https://doi.org/10.1016/j.cej.2020.100031>.
- [15] S.S. Deshpande, J. Walker, J. Pressler, D. Hickman, Effect of packing size on packed bubble column hydrodynamics, *Chem. Eng. Sci.* 186 (2018) 199–208. <https://doi.org/10.1016/j.ces.2018.04.045>.
- [16] K. A. Sukkar, S.A. Duha, A. A. Hussein, R.M. Mohammad, Synthesis and characterization hybrid materials (TiO₂ /MWCNTS) by chemical method and evaluating antibacterial activity against common microbial pathogens, *Acta Phys. Pol. A.* 135 (2019) 588–592. <https://doi.org/10.12693/APhysPolA.135.588>.
- [17] Y. Tang, G. Luo, Z. Cheng, Packing size effects on the liquid circulation property in an external-loop packed bubble column, *AIChE J.* 68 (2022). <https://doi.org/10.1002/aic.17851>.
- [18] H. Bader, Determination of ozone in water by the indigo method: A submitted standard method, *Ozone Sci. Eng.* 4 (1982) 169–176. <https://doi.org/10.1080/01919518208550955>.
- [19] H. Bader, J. Hoigné, Determination of ozone in water by the indigo method, *Water Res.* 15 (1981) 449–456. [https://doi.org/10.1016/0043-1354\(81\)90054-3](https://doi.org/10.1016/0043-1354(81)90054-3).
- [20] Z. Honarmandrad, N. Javid, M. Malakootian, Removal efficiency of phenol by ozonation process with calcium peroxide from aqueous solutions, *Appl. Water Sci.* 11 (2021) 14. <https://doi.org/10.1007/s13201-020-01344-7>.
- [21] J.M. Park, C.M. Kim, S.H. Jhung, Melamine/polyaniline-derived carbons with record-high adsorption capacities for effective removal of phenolic compounds from water, *Chem. Eng. J.* 420 (2021) 127627. <https://doi.org/10.1016/j.cej.2020.127627>.
- [22] R. Zhao, Y. Li, J. Ji, Q. Wang, G. Li, T. Wu, B. Zhang, Efficient removal of phenol and p-nitrophenol using nitrogen-doped reduced graphene oxide, *Colloids Surfaces A Physicochem. Eng. Asp.* 611 (2021) 125866. <https://doi.org/10.1016/j.colsurfa.2020.125866>.
- [23] G. Nirmala, T. Murugesan, K. Rambabu, K. Sathiyarayanan, P.L. Show, Adsorptive removal of phenol using banyan root activated carbon, *Chem. Eng. Commun.* 208 (2021) 831–842. <https://doi.org/10.1080/00986445.2019.1674839>.
- [24] P. Gharbani, A. Mehrizad, Heterogeneous catalytic ozonation process for removal of 4-chloro-2-nitrophenol from aqueous solutions, *J. Saudi Chem. Soc.* 18 (2014) 601–605. <https://doi.org/10.1016/j.jscs.2012.07.013>.
- [25] E.M. Lakhdissi, A. Fallahi, C. Guy, J. Chaouki, Effect of solid particles on the volumetric gas liquid mass transfer coefficient in slurry bubble column reactors, *Chem. Eng. Sci.* 227 (2020) 115912. <https://doi.org/10.1016/j.ces.2020.115912>.
- [26] J. Wang, H. Chen, Catalytic ozonation for water and wastewater treatment: Recent advances and perspective, *Sci. Total Environ.* 704 (2020) 135249. <https://doi.org/10.1016/j.scitotenv.2019.135249>.
- [27] S.J. Wang, J. Ma, Y.X. Yang, J. Zhang, T. Liang, Degradation and transformation of organic compounds in songhua river water by catalytic ozonation in the presence of TiO₂ /Zeolite, *Ozone Sci. Eng.* 33 (2011) 236–242. <https://doi.org/10.1080/01919512.2011.560561>.
- [28] Z.M. Shakor, A.A. AbdulRazak, K.A. Sukkar, A detailed reaction kinetic model of heavy naphtha reforming, *Arab. J. Sci. Eng.* 45 (2020) 7361–7370. <https://doi.org/10.1007/s13369-020-04376-y>.
- [29] F.K. Dawood, N.N. Abdulrazzaq, Direct oxidation of antibiotics from aqueous solution by ozonation with microbubbles, *J. Phys. Conf. Ser.* 1973 (2021) 012157. <https://doi.org/10.1088/1742-6596/1973/1/012157>.
- [30] M.K. Mohsin, A.A. Mohammed, Catalytic ozonation for removal of antibiotic oxy-tetracycline using zinc oxide nanoparticles, *Appl. Water Sci.* 11 (2021) 9. <https://doi.org/10.1007/s13201-020-01333-w>.
- [31] R. Shahbazi, A. Payan, M. Fattahi, Preparation, evaluations and operating conditions optimization of nano TiO₂ over graphene based materials as the photocatalyst for degradation of phenol, *J. Photochem. Photobiol. A Chem.* 364 (2018) 564–576. <https://doi.org/10.1016/j.jphotochem.2018.05.032>.
- [32] I.I.N. Etim, P.C. Okafor, R.A. Etiuma, C.O. Obadimu, Solar photocatalytic degradation of phenol using cocos nucifera (coconut) shells as adsorbent, *J. Chem. Biochem.* 3 (2015). <https://doi.org/10.15640/jcb.v3n1a3>.
- [33] W. Xiong, W. Cui, R. Li, C. Feng, Y. Liu, N. Ma, J. Deng, L. Xing, Y. Gao, N. Chen, Mineralization of phenol by ozone combined with activated carbon: Performance and mechanism under different pH levels, *Environ. Sci. Ecotechnology.* 1 (2020) 100005. <https://doi.org/10.1016/j.ese.2019.100005>.
- [34] S. T. Alnasrawy, G. Y. Alkindi, T. M. Albayati, Removal of high concentration phenol from aqueous

- solutions by electrochemical technique, *Eng. Technol. J.* 39 (2021) 189–195. <https://doi.org/10.30684/etj.v39i2A.1705>.
- [35] P. Yang, S. Luo, H. Liu, W. Jiao, Y. Liu, Aqueous ozone decomposition kinetics in a rotating packed bed, *J. Taiwan Inst. Chem. Eng.* 96 (2019) 11–17. <https://doi.org/10.1016/j.jtice.2018.10.027>.
- [36] K.A. Sukkar, F. K. Al-Zuhairi, E.A. Dawood, Evaluating the influence of temperature and flow rate on biogas production from wood waste via a packed-bed bioreactor, *Arab. J. Sci. Eng.* 46 (2021) 6167–6175. <https://doi.org/10.1007/s13369-020-04900-0>.
- [37] R. Sridar, U.U. Ramanane, M. Rajasimman, ZnO nanoparticles – synthesis, characterization and its application for phenol removal from synthetic and pharmaceutical industry wastewater, *Environ. Nanotechnology, Monit. Manag.* 10 (2018) 388–393. <https://doi.org/10.1016/j.enmm.2018.09.003>.
- [38] H. Iboukhoullef, R. Douani, A. Amrane, A. Chaouchi, A. Elias, Heterogeneous fenton like degradation of olive mill wastewater using ozone in the presence of BiFeO₃ photocatalyst, *J. Photochem. Photobiol. A Chem.* 383 (2019) 112012. <https://doi.org/10.1016/j.jphotochem.2019.112012>.
- [39] W. Wang, H. Yao, L. Yue, Supported-catalyst CuO/AC with reduced cost and enhanced activity for the degradation of heavy oil refinery wastewater by catalytic ozonation process, *Environ. Sci. Pollut. Res.* 27 (2020) 7199–7210. <https://doi.org/10.1007/s11356-019-07410-1>.
- [40] G.M. Salcedo, L. Kupski, J.L. de Oliveira Arias, S.C. Barbosa, E.G. Primel, Bojuru sand as a novel catalyst for refinery wastewater treatment and phenol degradation by heterogeneous photo catalysis, *J. Photochem. Photobiol. A Chem.* 402 (2020) 112796. <https://doi.org/10.1016/j.jphotochem.2020.112796>.
- [41] M.R. El-Aassar, O.M. Ibrahim, F.S. Hashem, A.S.M. Ali, A.A. Elzain, F.M. Mohamed, Fabrication of Polyaniline@ β -cyclodextrin Nanocomposite for Adsorption of Carcinogenic Phenol from Wastewater, *ACS Appl. Bio Mater.* (2022). <https://doi.org/10.1021/acsabm.2c00581>.
- [42] M.A. Zazouli, M. Yousefi, F. Ghanbari, E. Babanezhad, Performance of photocatalytic ozonation process for pentachlorophenol (PCP) removal in aqueous solution using graphene-TiO₂ nanocomposite (UV/G-TiO₂/O₃), *J. Environ. Heal. Sci. Eng.* 18 (2020) 1083–1097. <https://doi.org/10.1007/s40201-020-00529-1>.
- [43] M. Al-Nuaim, A.A. Al-Wasiti, Z.Y. Shnain, A.K. Al-Shalal, The combined effect of bubble and photo catalysis technology in BTEX removal from produced water, *Bull. Chem. React. Eng. Catal.* 17 (2022) 577–589. <https://doi.org/10.9767/bcrec.17.3.15367.577-589>.
- [44] M.H. Mahdi, T.J. Mohammed, J.A. Al-Najar, Removal of tetracycline antibiotic from wastewater by fenton oxidation process, *Eng. Technol. J.* 39 (2021) 260–267. <https://doi.org/10.30684/etj.v39i2A.1915>.